THE UNIVERSITY OF ASTON IN BIRMINGHAM

SUMMARY

"THE STUDY OF THE SULPHATION OF α-OLEFINS"

MEHMET RIZA ALTIOKKA Ph.D October 1983

The sulphation of hexadecene, in concentrated sulphuric acid (98% w/w) has been investigated in a votator scraped-surface heat exchanger reactor with "no-leak". The reactor flow pattern (tangential and axial) has been investigated and the theoretical tangential flow velocity profile determined when it was found that, at the annulus width d/3, the flow direction is always reversed and each side exhibits a parabolic velocity profile. Therefore a model was developed which showed that the reactor consisted of two series of C.S.T.R. approximations in parallel having the volumes of $\left(\frac{1}{3} V_{total}\right)$ and $\left(\frac{2}{3} V_{total}\right)$.

The scaling-up of a pilot plant reactor for industrial purposes has been based on the power consumption and a semi-empirical equation representing the power consummation has been derived from the experimental results.

The conversion of hexadecene to the reaction products, namely monoalkyl sulphuric acid, dialkyl sulphate and polymer, was examined at the different reaction parameters (the speed of rotation of the inner cylinder, residence time and molar ratio of the reactants) and it was shown that, although the reactants are immiscible initially, the heterogeneous reactions become homogeneous in a very short time (less than a second). So that the reaction kinetics can be analysed by an homogeneous model and the best conditions to achieve the highest yield was found experimentally.

Key Words: Sulphation
Monoalkyl Sulphuric Acid
Dialkyl Sulphate
Polymer
"no-leak" Votator

ACKNOWLEDGEMENTS

I wish to express my gratitude to Professor G. V. Jeffreys for the supervision of this thesis and for his continuous encouragement during the course of the work.

I thank Mr. P. T. Cartwright for his assistance in operating the reactor.

Thanks are also due to Dr. A. F. Gaines for many fruitful discussions.

Help received from Dr. C. S. Fairclough of Uniliver Research, with regard to analytical techniques, is gratefully acknowledged.

I thank Mrs. H. A. Smart for her meticulous typing of this thesis.

Finally, my thanks go to the Turkish Government for providing me with a grant, and also to the Turkish people, whose hard work makes the creation of such grants possible.

CONTENTS

Cont. ...

LIST OF FIGURES

LIST OF TABLES

CHAPTER 1

1.0 INTRODUCTION

Carboxylate soaps have been used for domestic and industrial laundrying for many centuries but during the twentieth century fat shortages and their relatively poor solubility in dilute acids and hard water led to the development of "synthetic" detergents.

Secondary-alkyl sulphates (SALS) have been known for many years as types of synthetic detergents but they have achieved only limited commercial success. This is because they have never matched alkyl-benzene sulphonate (ABS) and linear-alkyl-benzene sulphonate (LAS) in terms of quality or price. However, the need for ecologically biodegradable (soft) surfactants which remain on the surface of the water for a short period only has prompted a renewed interest in (SALS).

SALS are prepared to-day by either sulphation of long chain (C_{12}-C_{20}) α-olefins or esterification of alcohols with the same range of carbon chain. The sulphation of α-olefins using concentrated sulphuric acid can be made in an inert solvent or in the absence of a solvent. The solvent process (40/60 petroleum ether or pentane) is inherently more hazardous than the non-solvent process because the reactions are extremely exothermic. Also SALS made by the solvent processes are likely to be more expensive (27). Therefore, in this study, the possibility of achieving a high percentage olefin conversion to SALS in a non-solvent system has been investigated.

The olefin utilized was high quality hexadecene-1 which is within the range of olefin chain length of particular interest to the detergent industry and is readily available from petroleum

companies. Ninety eight (98) percent (w/w) sulphuric acid was chosen as sulphating agent on the grounds of availability and cost.

The reactor used was the votator, a form of scraped surface heat exchanger with "no-leak", designed by Dykes (2) in a previous study.

The objectives of this study were therefore defined as follows:-

i) To investigate the flow patterns, power consumption characteristics and residence time distribution function in the scraped surface heat exchanger with "no-leak" reactor.

ii) To investigate the effect of various reactor and reaction parameters on the conversion and product yields in order to further the understanding of the reaction mechanism.

iii) To investigate and establish scale-up criteria for the process with a view to commercial manufacture.

CHAPTER 2

TYPE OF REACTOR

2.1 INTRODUCTION

The sulphation of α-olefins using concentrated sulphuric acid is a very fast and extremely exothermic reaction. The heat of reaction in the literature is given about 30 kcals per g-mole Olefin (1). In order to achieve a high percentage of olefin conversion to monoalkyl sulphuric acid, the reaction has to take place in a reactor which is capable of providing good heat transfer and vigorous mixing. It is also desirable that all segments of the fluid undergo the same reaction history and so plug-flow in the axial direction is preferred.

There are many types of reactors which could be considered for the study of fast exothermic immiscible liquid/liquid reactions. They can be classified as follows (1):-

i) Jet-cum-static mixer reactor

ii) Continuous flow stirred tank reactors in series

iii) Loop reactor

iv) Votator type reactor

2.2 CHOICE OF A REACTOR

For research purposes the reactor, apart from the features mentioned in Section (2.1) should also:

i) Be capable of working under a wide range of operating conditions

ii) Be capable of scale-up

iii) Be available, if required, on the market as a standard unit

iv) Be mechanically simple to avoid problems usually associated with complex design

Malhotra and Jeffreys (1) have examined the alternative reactors mentioned in Section (2.1) and they concluded that the votator type reactor possessed the greatest potential for satisfying the requirements, especially if its design was modified to incorporate "no-leak" blades.

On this premise a "no-leak" votator type reactor was designed by Dykes (2) in a previous study and was the unit used for this research.

2.3 CONSTRUCTION OF THE REACTOR

The reactor consisted of two concentric cylinders sealed at both ends. The inner cylinder was connected to a variable speed unit and had three blades with a rubber end attached to the outer rim. As the inner cylinder rotated the blades scraped the inner surface of the outer cylinder thereby providing good heat transfer. Without the scraping action of the blades a thick viscous liquid layer would build up on the inner surface of the outer cylinder causing poor heat transfer from the reactor contents to the refrigerant. The outer cylinder was cooled by Freon-12 refrigerant. Details of the cylinders and blades are illustrated in figure (2.1).

Sulphuric acid and olefin were fed into the top of the reactor through separate pipes and the rates were monitored by rotameters. A pressure release pipe was attached to the acid feeding pipe so that it was possible to fill the reactor with the reactants. The chemical reactions occurred in the annulus and products were withdrawn from the bottom of the reactor when they were neutralized with 20% (w/w) NaOH in the neutralization system. Reactor temperature was measured by means of thermocouples fixed to the outer surface of the outer cylinder. The reactor is illustrated in figure (2.2).

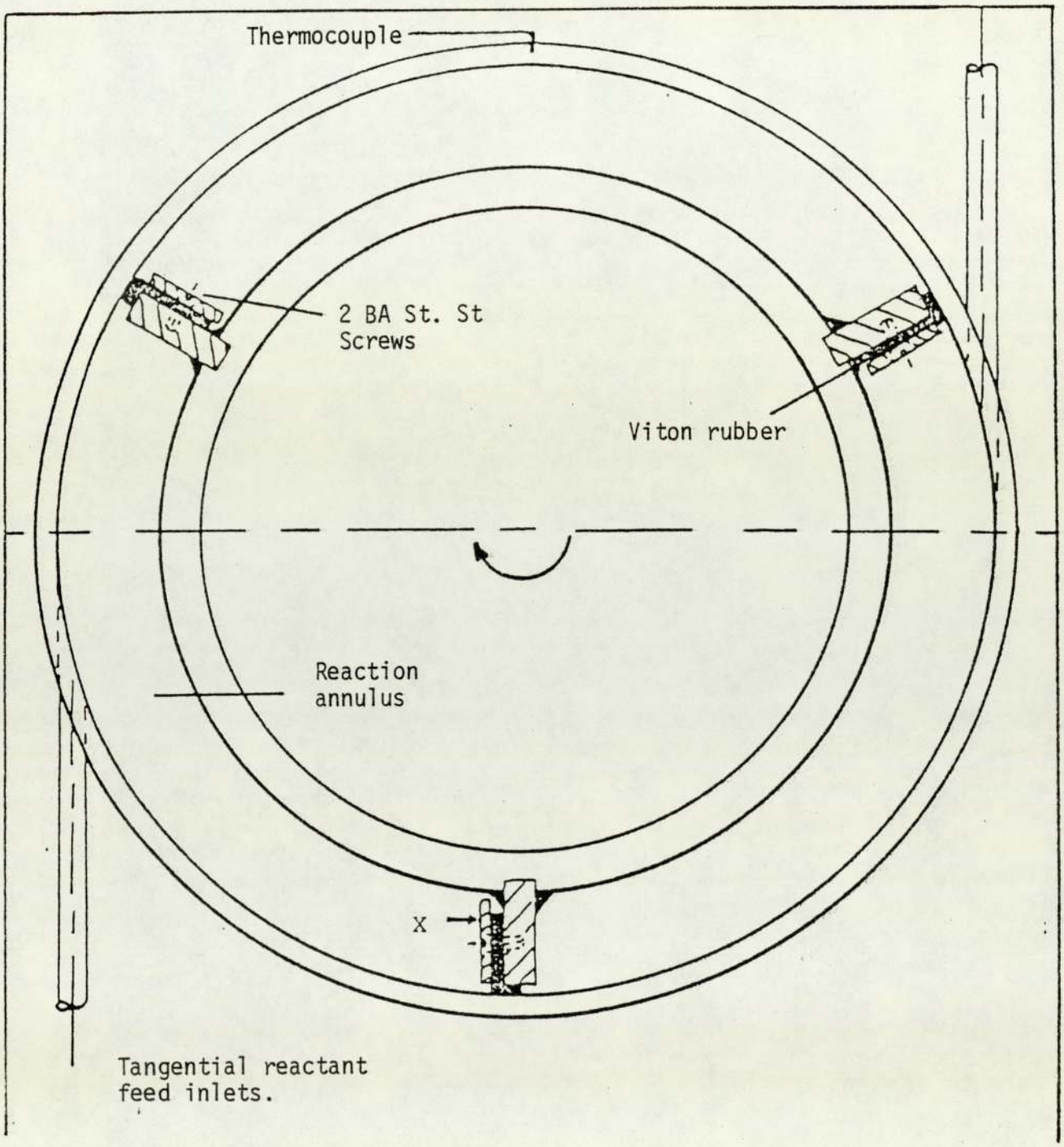

Figure 2.1 Scraper Blades.

The following changes have been made before starting to do experiments.

i) The hollow shaft passing through the inner cylinder was replaced by a solid shaft.

ii) The rubber pads on the blades were renewed by viton rubber which is more durable against acid attack under the working conditions.

iii) The liquid ammonia refrigerant system was replaced by a Freon-12 refrigerant system on the grounds that ammonia is more hazardous.

The overall flow diagram is illustrated in figure (2.3).

2.4 DIMENSIONS OF THE REACTOR

The original reactor was designed by Dykes (2) for the following range of operating conditions:-

Residence time	$\leq$ 3 min.
Acid/olefin mole ratio	3:1 to 1:1
Acid strength	97% (w/w)
Olefin chain length	C_{12} to C_{18}
Reaction temperature	5°C
Heat of reaction (based on olefin)	up to 125 kJ $(g\text{-mole})^{-1}$
Viscosities	up to 0.3 Nsm^{-2}
Density	930 $kg\ m^{-3}$

The dimensions of the modified reactor are:-

Diameter of outer cylinder	0.1429 m
Diameter of inner cylinder	0.1111 m
Width of annulus	0.0159 m
Length of the reactor	0.4572 m
Heat transfer surface	0.205 m^2
Volume of the reactor	2.9×10^{-3} m^3

The reactor and its auxiliary equipment are presented in photographs (1) and (2).

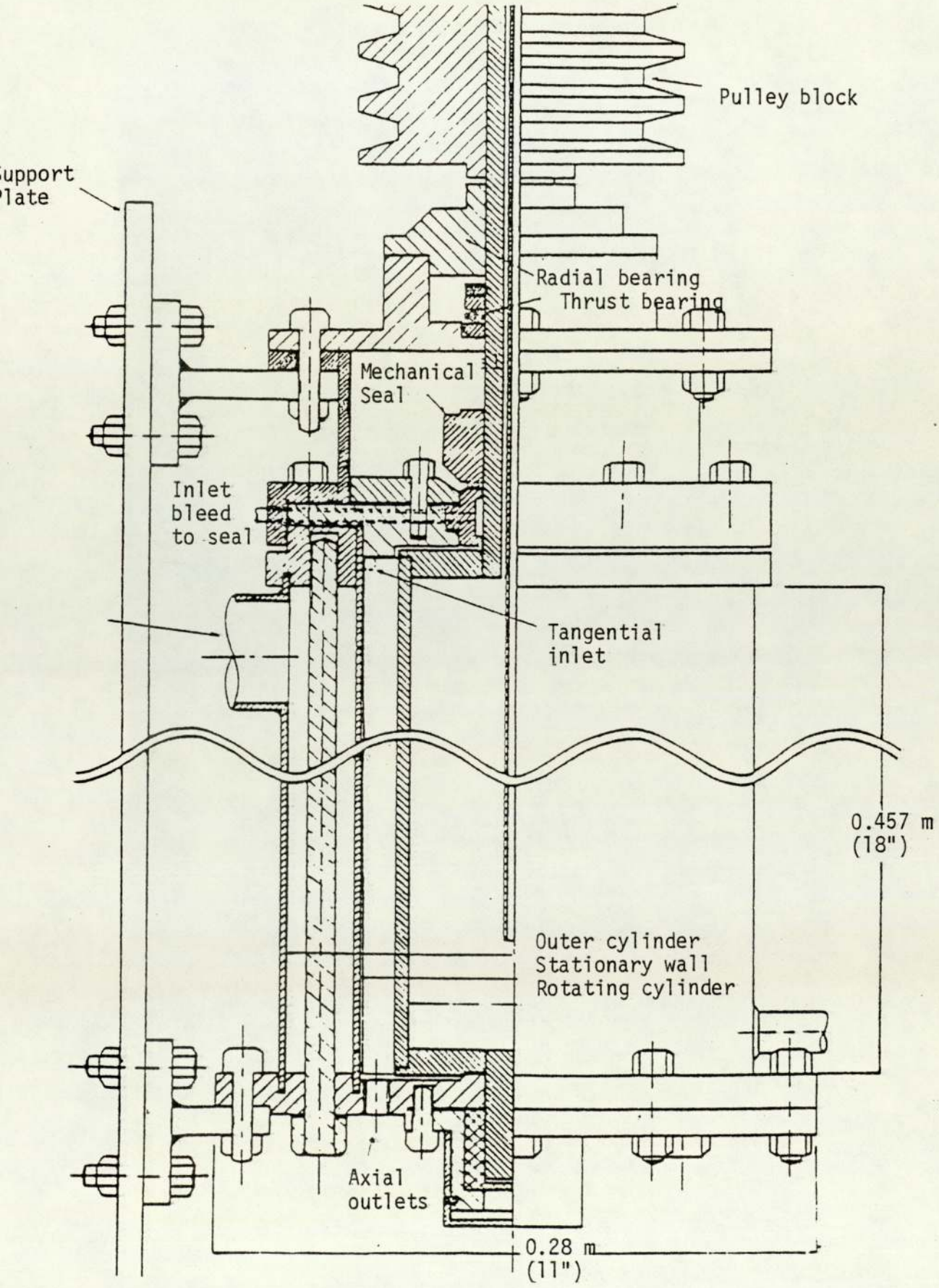

Figure 2.2 Reactor Construction

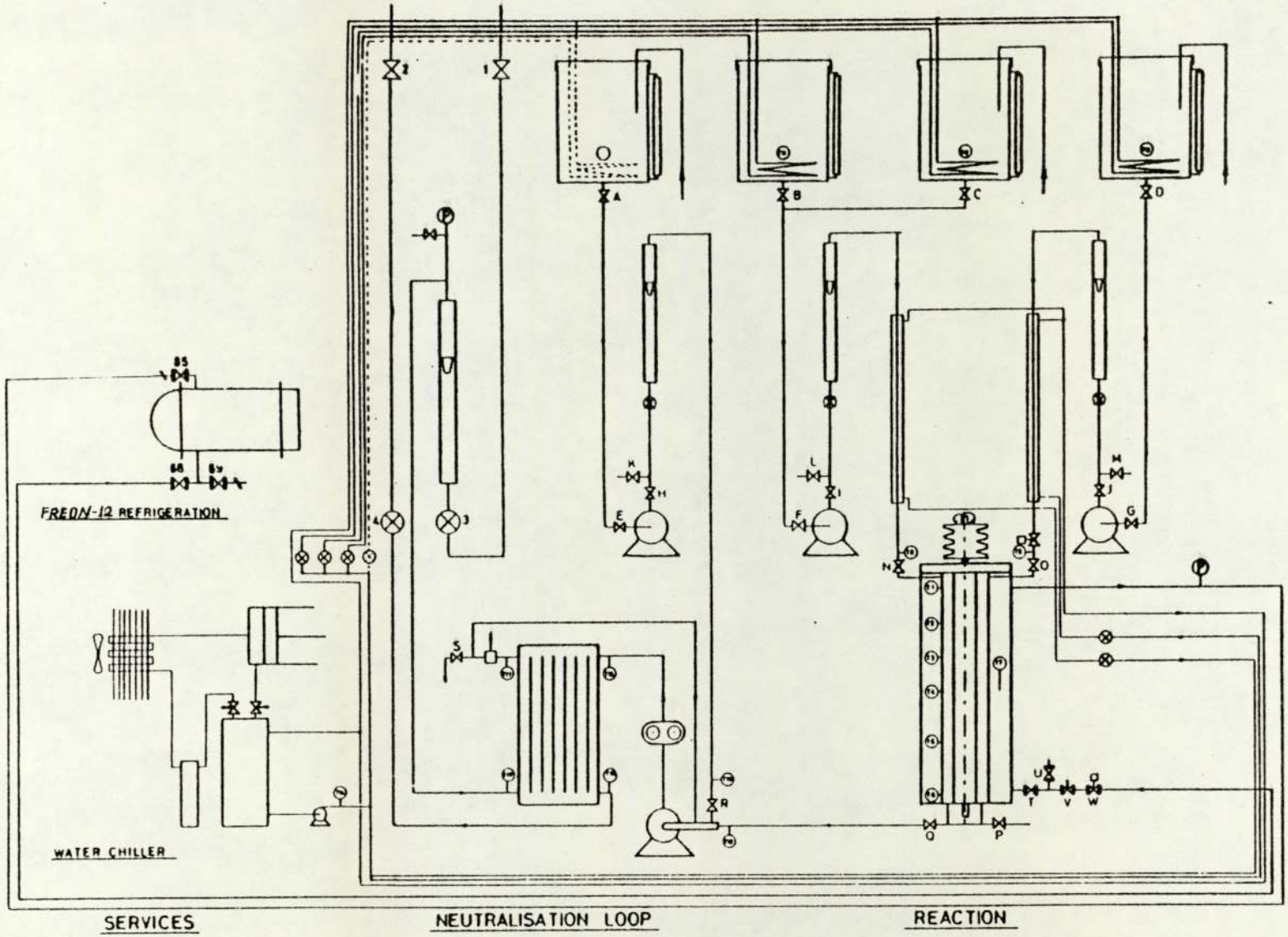

Figure 2.3 Overall Flow Diagram

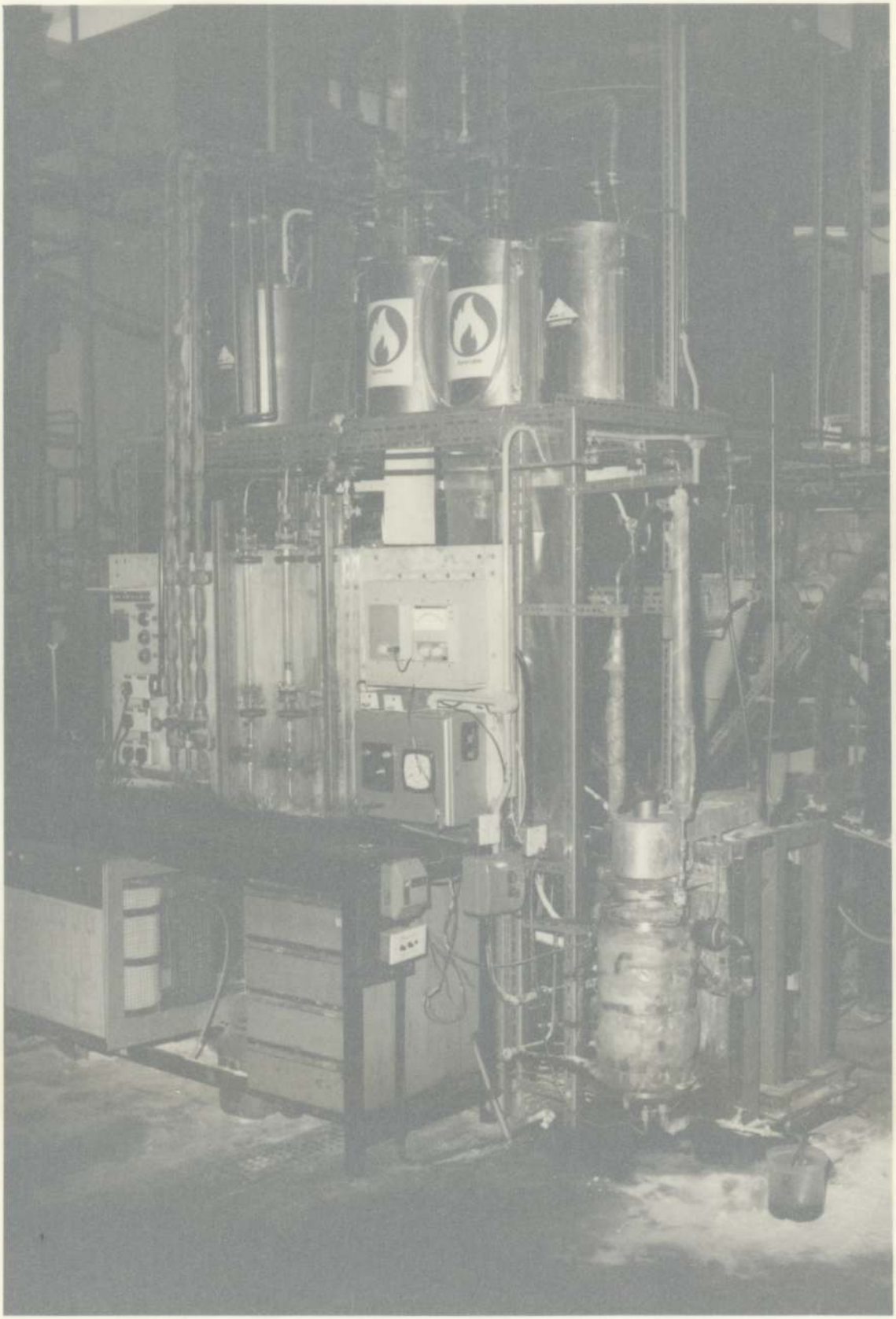

Photograph 1 Reactor with auxiliary equipment used in this research.

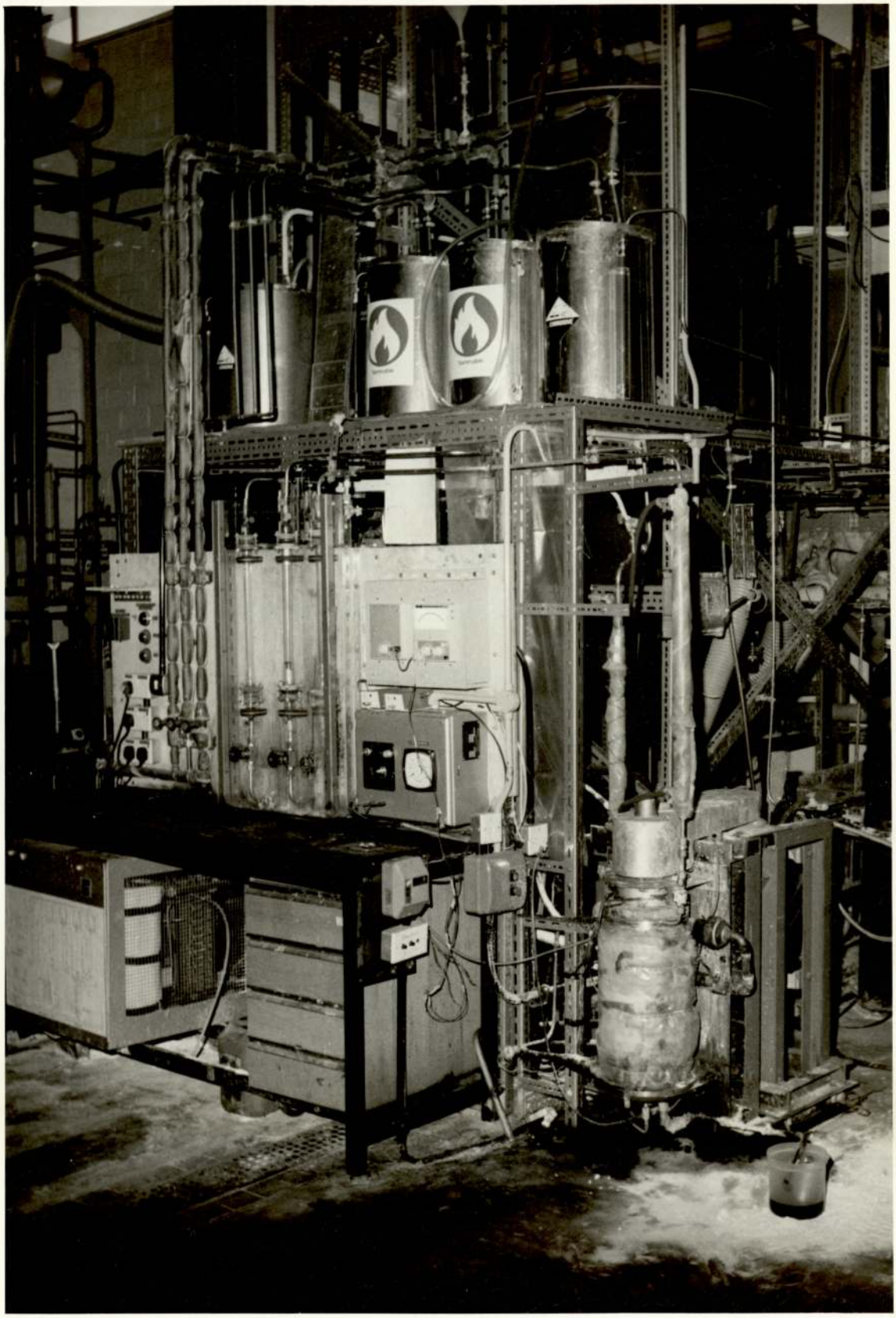

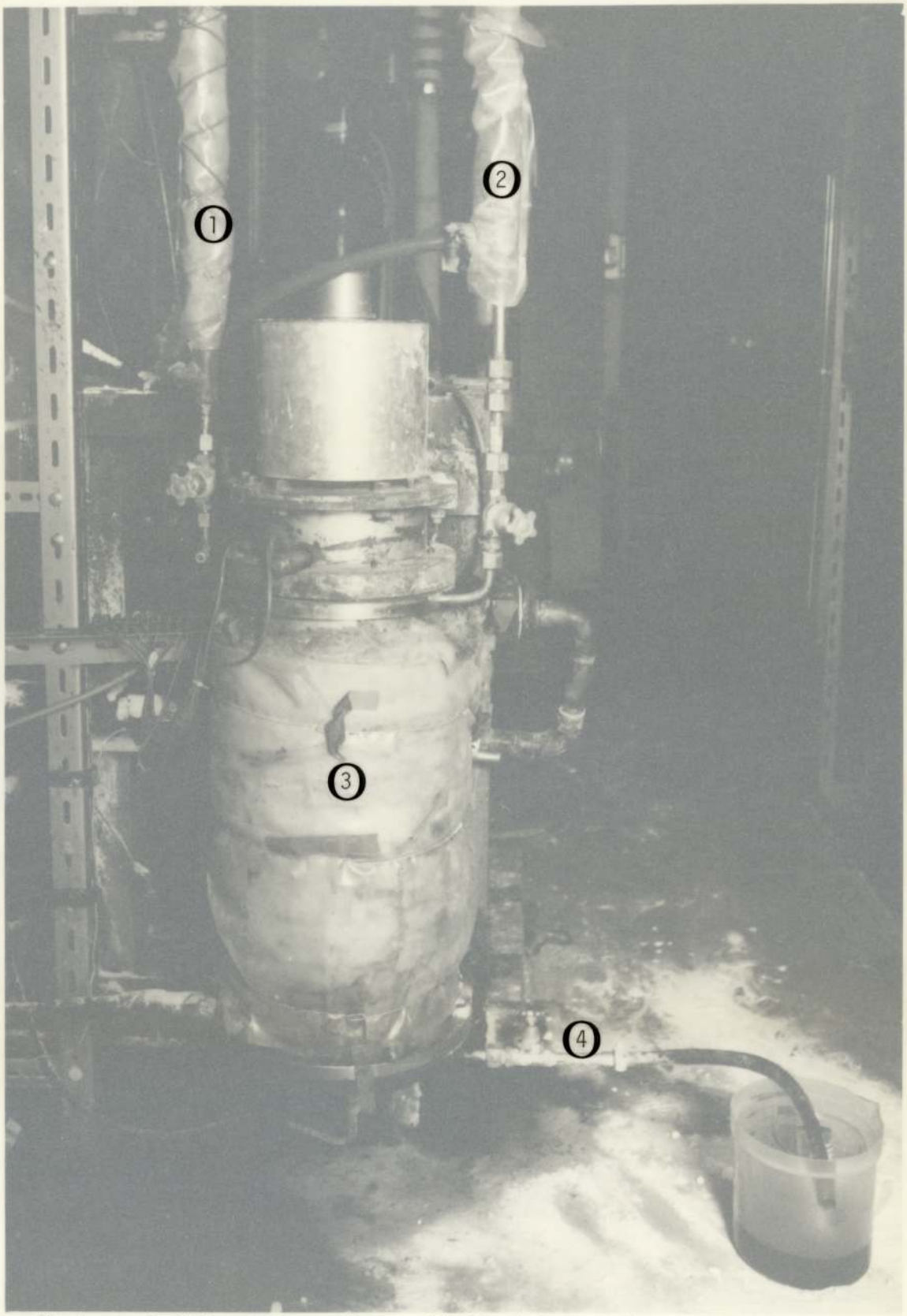

Photograph 2 Reactor

1 - Olefin inlet
2 - Acid inlet
3 - Reactor
4 - Product outlet

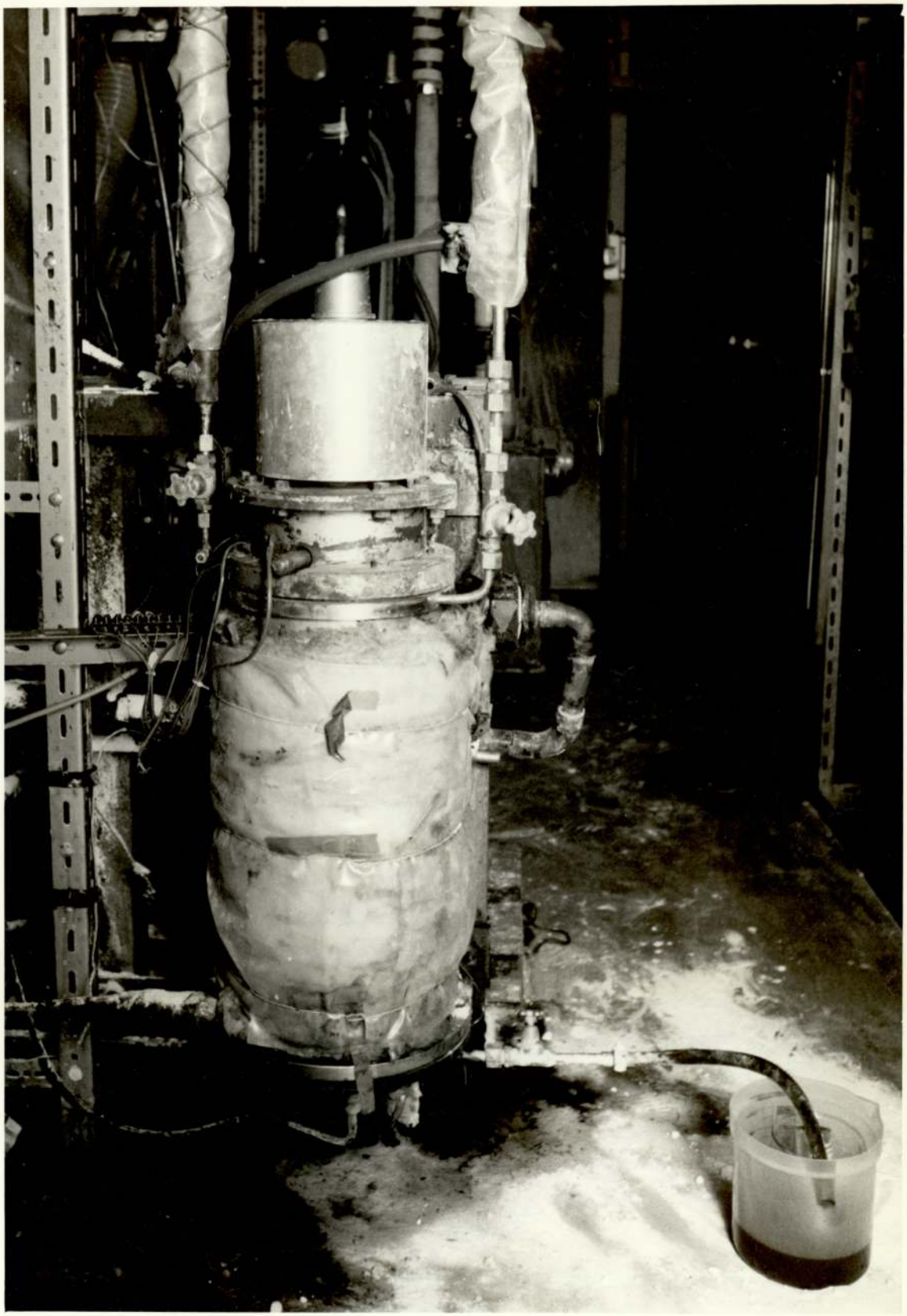

CHAPTER 3

REACTOR FLOW CHARACTERISTICS

3.1 INTRODUCTION

In this chapter various aspects of the flow within the annulus will be discussed. The importance of the flow patterns can be summarized as follows:-

i) In order to achieve a good heat transfer the liquid layer removed from the outer wall must be distributed within the bulk fluid. The efficiency of this distribution is determined by the tangential flow pattern.

ii) The flow pattern determines the shear stresses in the liquid and therefore the mixing and the power dissipation.

iii) In the case of the chemical reaction between sulphuric acid and α-olefins the size of the olefin droplets and their distribution within the continuous phase (sulphuric acid) is also determined by the flow pattern.

iv) The residence time distribution can only be determined by the volumetric flow pattern.

In this chapter tangential and axial flow patterns have been studied. Tangential flow phenomena has been investigated theoretically because it was not possible to observe the flow pattern in the reactor and residence time distributions were determined experimentally under various operating conditions using a tracer analysis.

3.2 TANGENTIAL VELOCITY PROFILE

To develop a mathematical expression for tangential velocity profiles the following assumptions have been made:-

i) The fluid is Newtonian and of constant density and viscosity

ii) Parallel flow (radial and axial velocity are negligible.

iii) There is a constant tangential pressure gradient.

iv) Steady flow.

Both cylindrical and rectangular coordinate systems were used to find an equation for tangential velocity profiles.

3.2.1 Cylindrical Coordinate Systems

Tangential fluid motions within the annulus are illustrated in figure (3.1).

Taking assumptions made in Section (3.2) into account and using the equations of motion (3) the θ-component of velocity can be written as:-

$$0 = -\frac{1}{r}\frac{\partial P}{d\theta} + \mu \frac{1}{r}\frac{\partial}{\partial r}\left(rV_\theta\right) \qquad (3.1)$$

The solution of equation (3.1) gives

$$V_\theta = \frac{1}{2\mu}\frac{dP}{d\theta} r \ln r + \left(\frac{C_1}{2} - \frac{1}{4\mu}\frac{dP}{d\theta}\right) + \frac{C_2}{r} \qquad (3.2)$$

Since $dP/d\theta$ is constant, equation (3.2) can be expressed in the general form

$$V_\theta = Ar \ln r + Br + Cr^{-1} \qquad (3.3)$$

To find the constants in equation (3.3) three boundary conditions are needed. These are:-

i) At $r = r_i$, $V_\theta = V_i$

ii) At $r = r_o$, $V_\theta = 0$

iii) $\int_{r_i}^{r_o} V_\theta dr = 0$ (Between concentric cylinders with complete reversed flow, the net flow is zero (4).)

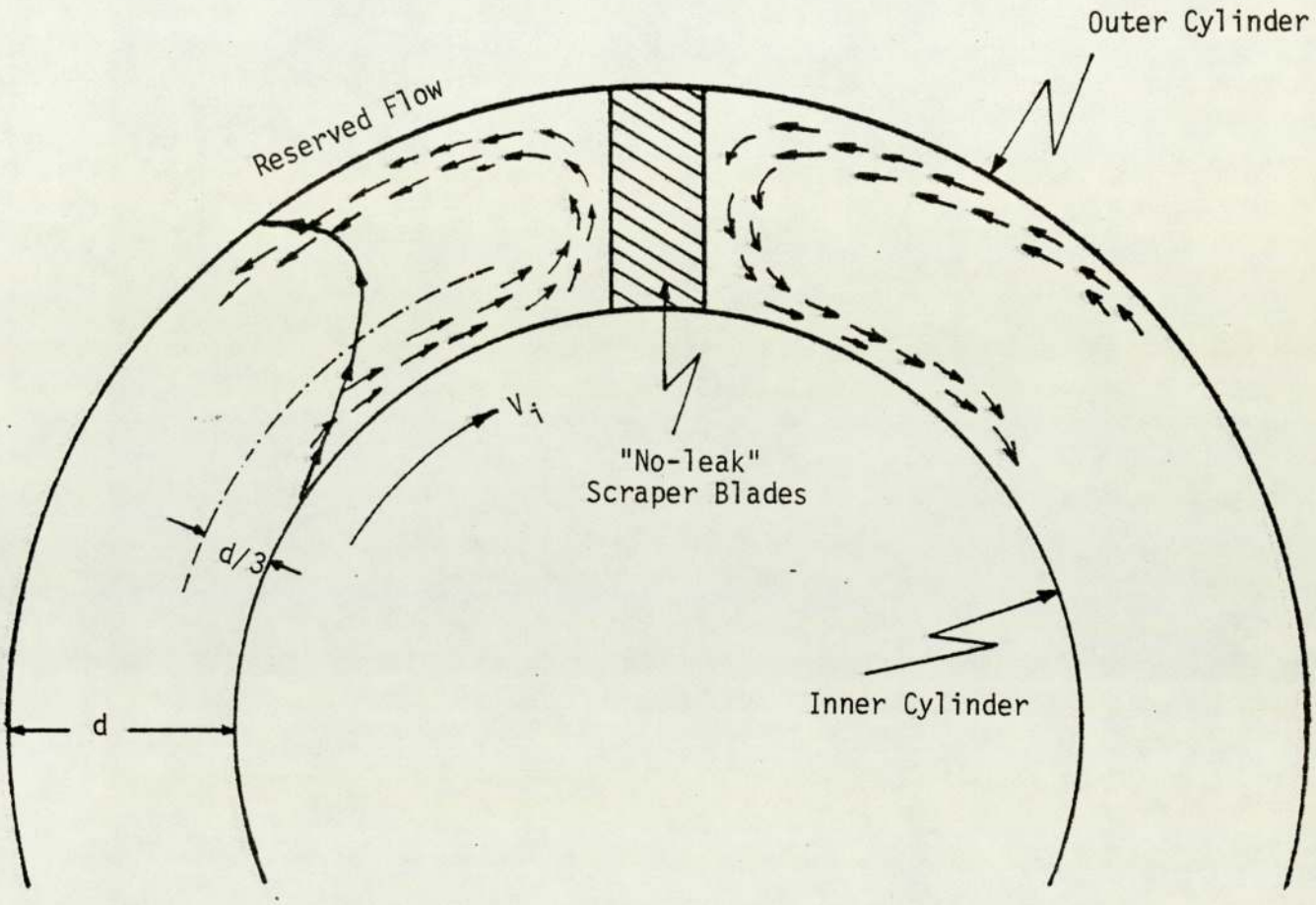

Figure 3.1 Tangential Flow Patterns in the Annulus

Using these boundary conditions and the reactor dimensions equation (3.3) becomes

$$\frac{V_\theta}{V_i} = 715.34\ r\ \ell n\ r + 1584.91r + \frac{1.545}{r} \qquad (3.4)$$

3.2.2 Rectangular Coordinate Systems

The annular space is small with respect to the circumference of the inner cylinder and it can be compared to the space between two vertical planes at a distance $d = (r_0 - r_i)$ one of which is moving at a speed V_i with respect to the other (5).

Let x indicate the direction of motion of the inner cylinder, y and z be the horizontal and vertical directions respectively. Using the equation of motion (3) the x-component of velocity can be written as:-

$$0 = -\frac{\partial P}{\partial x} + \mu \frac{\partial^2 V_x}{\partial y^2} \qquad (3.5)$$

where dP/dx is constant.

The solution of equation (3.5) gives

$$V_x = \frac{1}{2\mu} \frac{dP}{dx} y^2 + Ay + B \qquad (3.6)$$

The boundary conditions are:-

i) At $y = 0$, $V_x = V_i$

ii) At $y = d$, $V_x = 0$

iii) $\int_0^d V_x dx = 0$ ("No-leak" votator)

From (i) $B = V_i$

From (ii) $$A = -\left(\frac{V_i}{d} + \frac{1}{2\mu}\frac{dP}{dx}d\right)$$

and equation (3.6) becomes

$$V_x = \left(\frac{d-y}{d}\right)V_i - \frac{y(d-y)}{2\mu}\frac{dP}{dx} \tag{3.7}$$

From equation (3.7) and the third boundary condition it can be shown that

$$\frac{dP}{dx} = \frac{6\mu}{d^2}V_i \tag{3.8}$$

Therefore the final form of equation (3.6) becomes

$$\frac{V_x}{V_i} = \frac{d-y}{d} - \frac{3(d-y)y}{d^2} \tag{3.9}$$

Using the pilot plant reactor dimensions (d = 0.0159m) equation (3.9) becomes

$$\frac{V_x}{V_i} = 1 - 251.6y + 11867y^2 \tag{3.10}$$

It can be seen from equation (3.9) that at the point y = d/3 the fluid motion changes directions. The velocity profile presented by equations (3.3) and (3.9) was verified experimentally by A. M. Trommelen (6).

The equations (3.4) and (3.10) are plotted in figure (3.2). There it can be seen that there is only a small difference between the two curves and therefore equation (3.9) will be used in the further analysis. This simplifies the calculations.

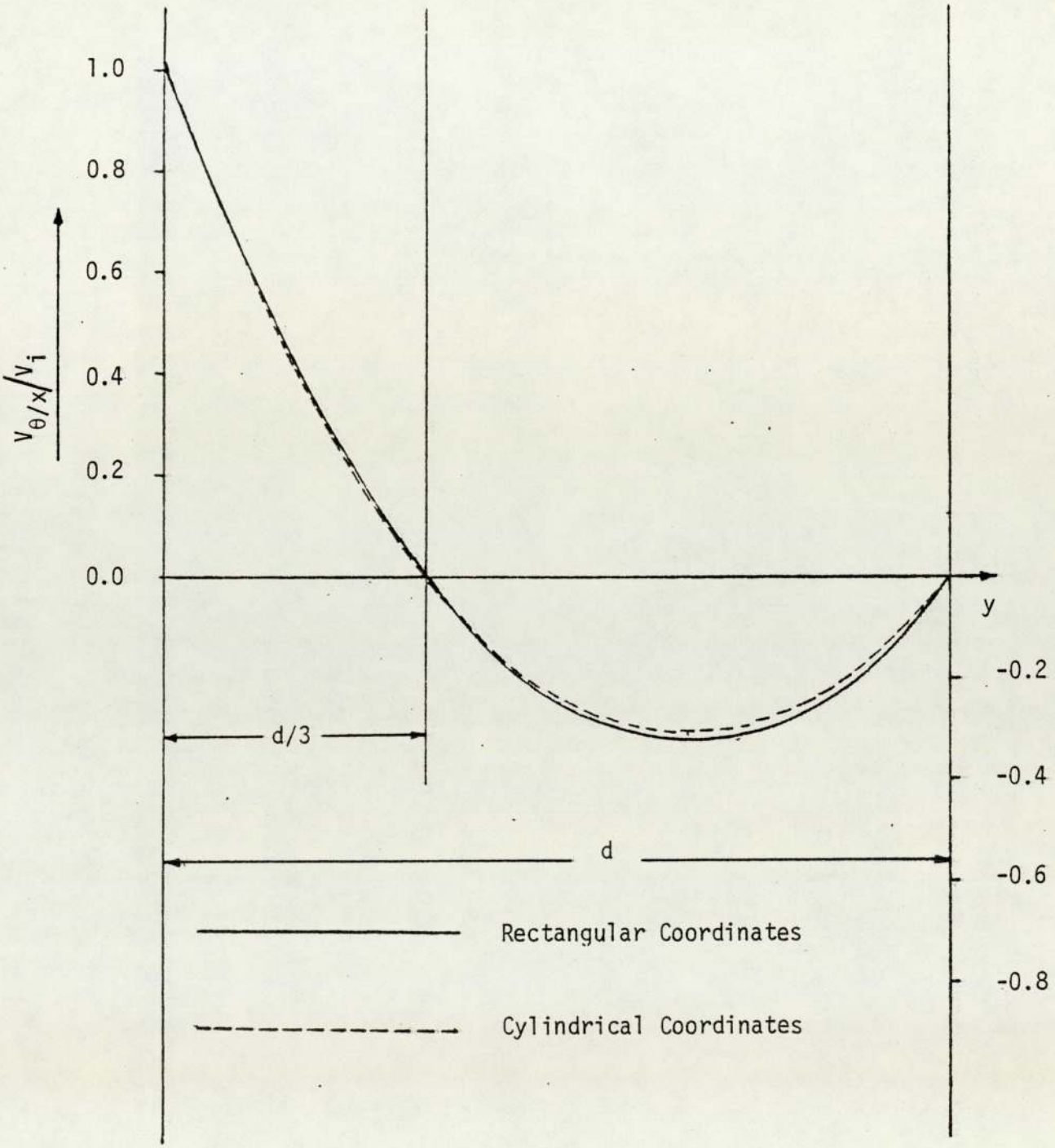

Figure 3.2 Tangential Velocity Profile of the reactor

3.2.3 Onset of Flow Instability

The stability of laminar flow between rotating concentric cylinders has been studied by many workers. G. I. Taylor (7) was the first to show analytically and experimentally that for cylinders of given radii and a liquid of a specified viscosity there were definite angular velocities of the outer and inner cylinders at which instability would occur. He further showed that the motion resulting from instability was three dimensional and consisted of pairs of toroidal vortices, the rotation within each being in the opposite direction to its neighbour. The spacing of these toroids along the axis of the cylinders is constant for a particular apparatus and speed of rotation of the cylinders. The diameter of a vortex is approximately that of the annular width. These vortices are illustrated in figure (3.3).

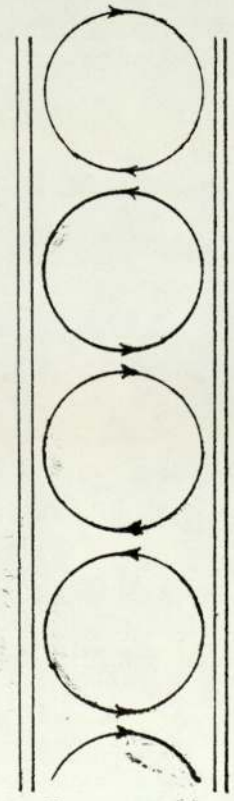

Figure 3.3 Taylor Vortices

Taylor showed that when only the inner cylinder was rotating the critical angular velocity for instability is given by

$$\frac{\Omega_c^2 \, r_i^2 \, d^3}{\frac{1}{2}(r_i+r_o)\nu^2} = \frac{\pi^2 f}{0.0571 + 0.00059} \qquad (3.11)$$

where $f = 1 - 0.0652(d/r_i)$.

Lewis (8) confirmed Taylor's work experimentally and showed that the approximation $(d/r_i) < r_i$ used by Taylor in his theoretical analysis held for values of (d/r_i) as high as 0.7. In the present reactor $(d/r_i) = 0.1$. Therefore the Taylor criteria can be used without any error.

For negligible (d/r_i), equation (3.11) can be re-arranged in terms of the Taylor number (T_a)

$$T_a = \frac{V_c d}{\nu} \sqrt{\frac{d}{r_i}} \geq 41.3 \qquad (3.12)$$

Later Dean (9) has shown theoretically that disturbances of the same type as those described by Taylor for Coutte flow can exist for a parabolic velocity distribution in curved pipes. He showed that the critical velocity for instability can be expressed with the aid of a characteristic number known as the Dean number (D_a).

$$D_a = \frac{V_c d}{\nu} \sqrt{\frac{d}{r_i}} \geq 36 \qquad (3.13)$$

The zone at which fluid flow changes its direction allows the inner and outer sections of the profile to be analysed separately.

3.2.3.1 Inner Section

Assuming that Taylor's criterion holds for the inner section r_i to (r_i+d_0) and that the section behaves like an inner cylinder of radius r_i rotating in a stationary outer cylinder of radius (r_i+d_0), then the critical velocity for instability can be calculated from either equation (3.11) or (3.12). Then using the pilot plant reactor dimensions, it was found that

$$\left.\begin{aligned} V_c &= 2.66 \times 10^4 \nu \\ N_c &= 7.60 \times 10^4 \nu \end{aligned}\right\} \text{ from equation (3.11)}$$

$$\left.\begin{aligned} V_c &= 2.52 \times 10^4 \nu \\ N_c &= 7.22 \times 10^4 \nu \end{aligned}\right\} \text{ from equation (3.12)}$$

Use of equation (3.12) causes a 5% error therefore the use of equation (3.11) is preferable.

Later Brewster and Nissan (4) found that Taylor's criterion is not applicable to accurate prediction of the critical velocity, because it appears more reasonable to assume that the liquid flowing between (r_i+d_0) and r_0 has an effect on the stability of the inner section, since the flow between (r_i+d_0) and r_0 has no Coutte velocity distribution but a parabolic distribution. They assumed that the flow was similar to that of the liquid in the section (r_i+d_0) to r_0 between cylinders rotating in opposite directions at such a value that $(d_0/d) = 1/3$. Using the parameter S proposed by Di Prima (10) Brewster and Nissan successfully derived a relationship between S and the critical velocity. S is defined as follows:-

$$S = \frac{8\Omega_c^2 \, d_0^3 r_i}{\nu^2\left[4+8(d_0/r_i)+5(d_0/r_i)^2+(d_0/r_i)^3\right]} \qquad (3.14)$$

Di Prima himself using the results of experiments carried out by Taylor (7) has plotted values of S against d_0/d, see figure (3.4). It can be seen from figure (3.4) that S has a constant value of about 1000 up to a value of 0.6 for (d_0/d). In the present flow $(d_0/d) = 0.33$ therefore the value of S is 1000. Using equation (3.14) and reactor dimensions $V_c = \Omega_c r_i$ can be calculated

$$\left.\begin{aligned} V_c &= 1.5 \times 10^4 \nu \\ N_c &= 4.3 \times 10^4 \nu \end{aligned}\right\} \text{ from equation (3.14)}$$

It is clear that the critical velocity found using the S parameter is $\sqrt{\frac{1000}{3400}} = 0.54$ times smaller than the critical velocity found using the Taylor criterion, since the value of S is 3400 at $(d_0/d) = 1$.

3.2.3.2 Outer Section

The outer section is bounded by two curved planes, both of which are at rest. The radius of the inner plane is (r_i+d_0) whilst the outer radius is r_0. This Section has a parabolic velocity distribution, so Dean's criteria (9) for instability can be applied. That is, from equation (3.13), instability sets in when

$$\overline{V}_c = 36\sqrt{\frac{r_r+d_0}{d-d_0}}\ \frac{\nu}{d-d_0} \qquad (3.15)$$

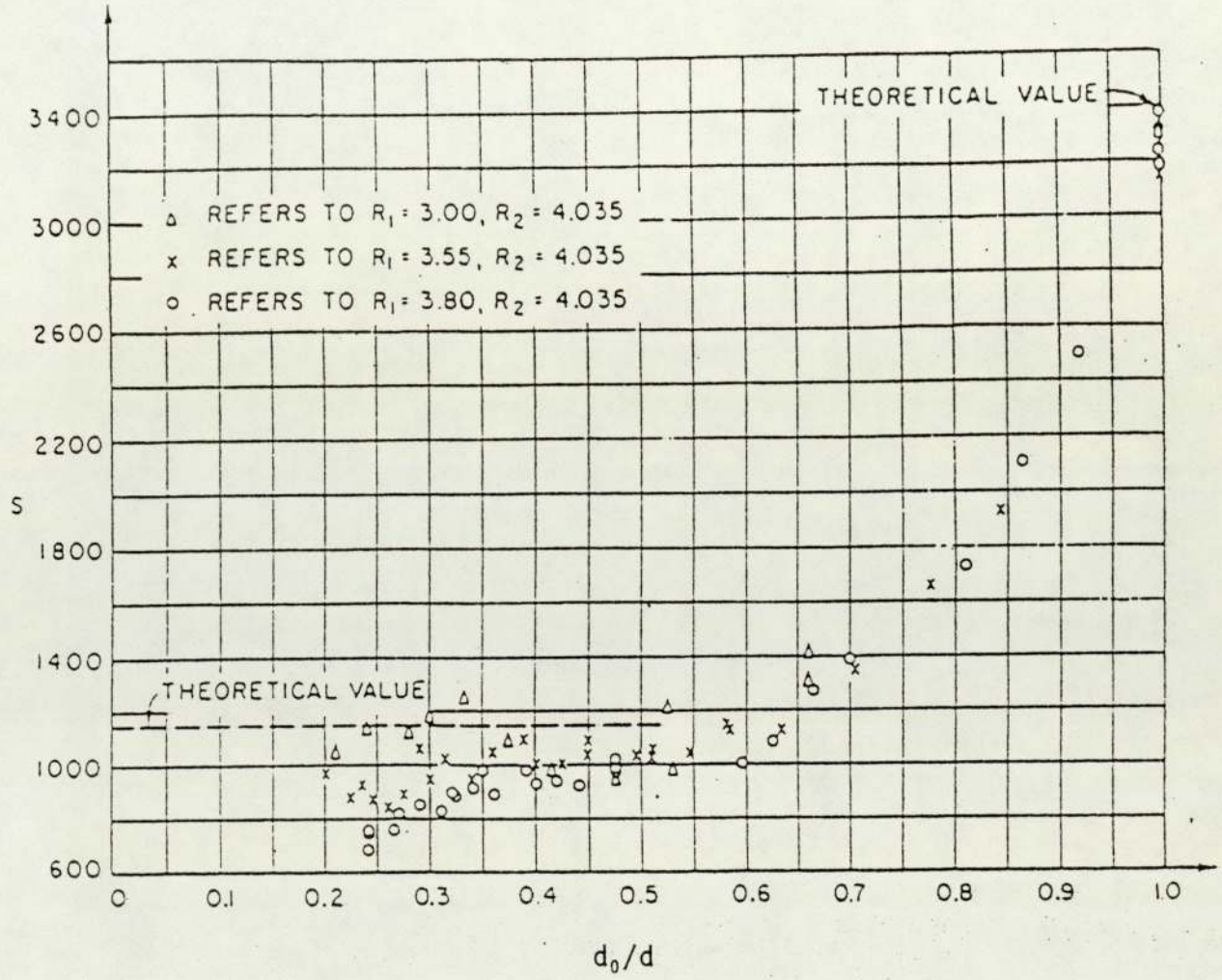

Figure 3.4 S(Experimental) vs d_0/d

The average velocity in this section may be calculated from equation (3.9); this average can be expressed as follows:-

$$\overline{V} = \frac{3}{2d} \int_{d/3}^{d} \left[\frac{d-y}{d} - \frac{3y(d-y)}{d^2} \right] V_i \, dy$$

and $$\overline{V} = -\frac{2}{9} V_i \text{ or } \overline{V}_c = -\frac{2}{9} V_c \qquad (3.16)$$

The minus sign shows that the flow is a reverse flow and for calculation of the absolute value of the critical velocity the sign can be ignored. Thus from equations (3.15) and (3.16) V_c can be calculated. Inserting the pilot plant reactor dimensions the calculated value of V_c and the corresponding value of N_c are as follows:-

$$V_c = 3.66 \times 10^4 \nu$$

$$N_c = 10.5 \times 10^4 \nu$$

Comparison of critical velocities shows that as N increases instability will first occur in the inner section.

3.3 AXIAL FLOW

3.3.1 Introduction

The residence time distribution of flow between concentric cylinders with the inner cylinder rotating has been studied by Van Lookeren Campagne (11). He showed that it can be described with the "plug-flow with dispersion model". However, for the scrape surface heat exchange Trommelen (6) proved that the plug-flow with dispersion model does not fully represent the residence time distribution. For a low shaft speed and high viscosity the residence time distribution function is much wider than for a high shaft speed and low viscosity. This is caused partly by the differences

in velocity and in the length of different streamlines and partly by dispersion due to vortices and a pumping effect caused by the scraper blades.

The residence time distribution for the scraped surface heat exchanger has also been studied by other workers. Azoory et al. (12) showed that the residence time distributions for the scraped surface heat exchanger approach plug-flow. Finally Jeffreys and Malhotra (1) suggested that for "no-leak" votators intense mixing in the radial direction is highly likely to flatten the parabolic velocity profile in the annulus in the axial direction thus helping to create plug-flow.

3.3.2 Experimental Methods

It has already been shown in Section (3.2.3) that at speeds of rotation of the inner cylinder greater than $10.5 \times 10^4 \nu$ (M.K.S. unit) instabilities occur in both inner and outer sections. The first instability is also known to occur at the speed of rotation $4.3 \times 10^4 \nu$ (M.K.S. unit) in the inner section. Below these speeds of rotation stable flow exists. Additionally, the theoretical analysis by Goldstein (13) and experimental studies by Cornish (14) indicate that the axial and rotational flow characteristics are independent of each other. Therefore, it might be expected that the axial flow, even in the presence of the Taylor vortices, is laminar.

Experiments to study residence time distribution were carried out in both the stable and instable flow regimes. Five points at which residence time distribution data were obtained are tabulated in the table (3.1).

Measurement of the residence time distribution of a reactor at various viscosities and speed of rotation requires the monitoring

of the outlet response to either a step change or pulse input. A pulse input was applied in this study because this was most convenient and produced the minimum amount of contaminated waste stream.

Run	Speed of rotation (r.p.s)	Kinematic viscosity ($\times 10^4$ m^2s^{-1})	Flow rate ($lit.min^{-1}$)
1	4.17	0.45	1.50
2	8.33	0.45	1.67
3	4.17	1.30	1.40
4	8.33	1.30	1.40
5	16.67	0.01	2.30

Table 3.1 Five points at which the residence time distribution data were obtained.

The working fluid was glycerol which was diluted to the required viscosities. 0.1% (w/w) methyl violet 2B was employed as the dye as this has an absorbance peak detected by Ultra Violet Spectrophotometry at 584 nm which was very close to the wavelength of the sodium lamp (589 nm) which was used in the Atomic Absorption Spectrophotometer. See figure (3.5).

10.0 mls the dye solution were injected into the inlet stream through a rubber septum incorporated in the pipe work. Simultaneously the camera, which was focussed on to a circular perspex cell in the outlet pipe, was set in motion. The film speed was arranged at two frames per second and the camera was made to film for twice the nominal residence time. It was expected that most of the dye would have passed through the reactor within this period. A check on the flow rate was made by measuring the volume of fluid collected at regular time intervals and the viscosity was measured

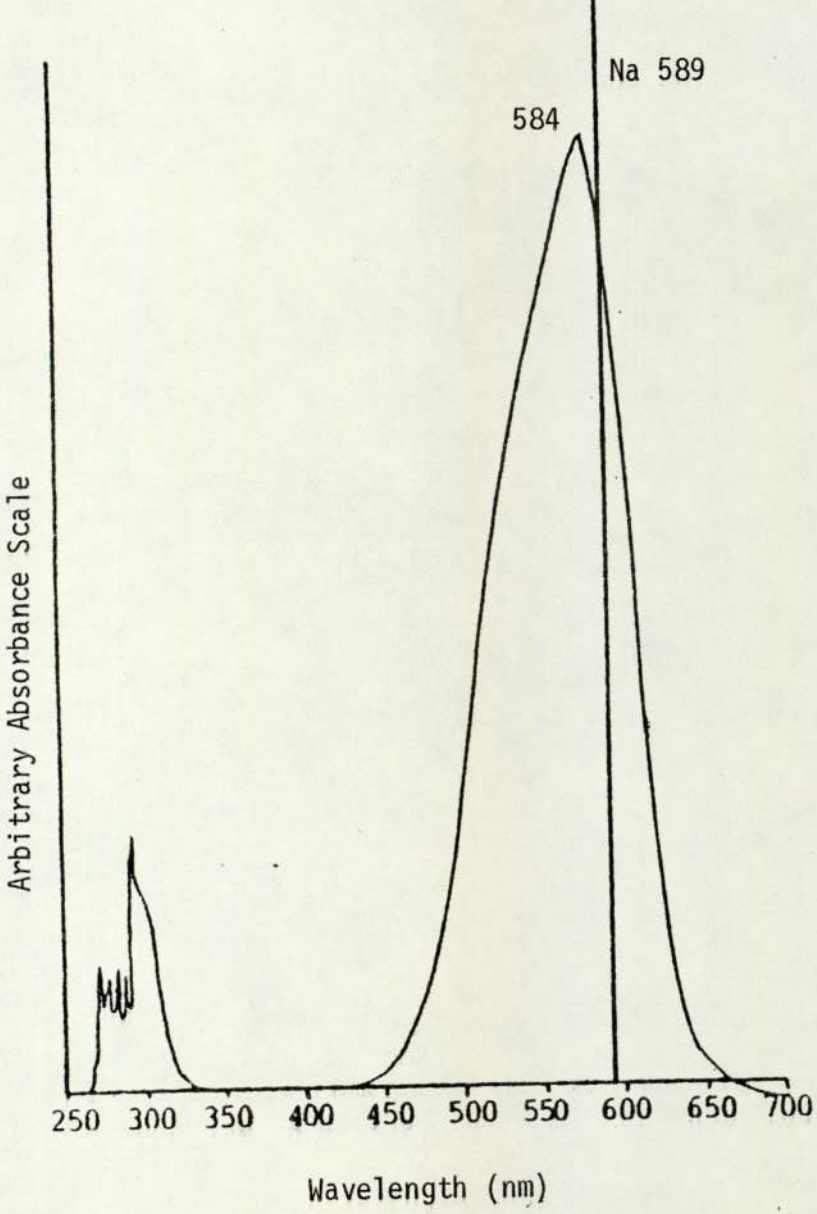

Figure 3.5 Methyl Violet Absorbance and Sodium Lamp Wavelength

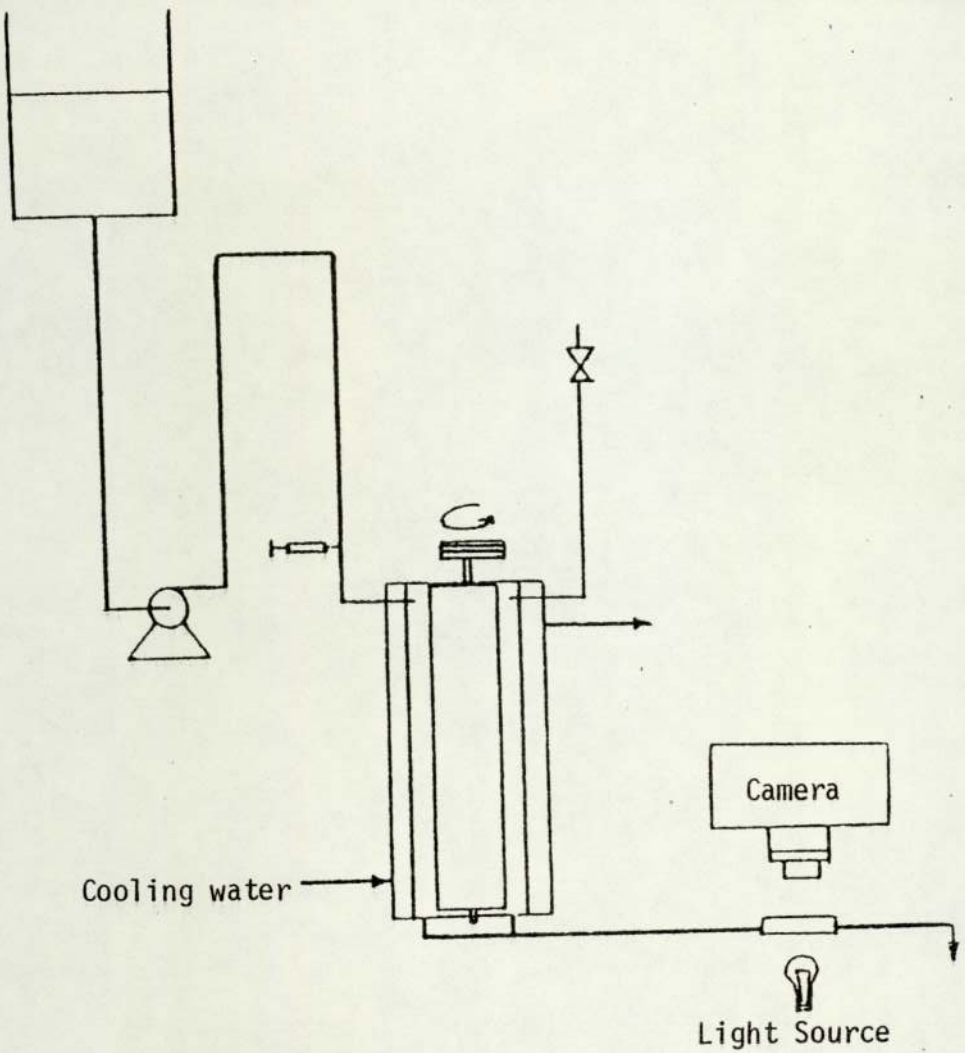

Figure 3.6 R.T.D. Study Diagram

as described in Section (4.3.1).

The developed colour film was analysed using the Atom Absorption Spectrophotometer and a Photo-Optical Data Analyser Projector. The beam from the sodium lamp passed through the central coloured portion of the film. The projector was set in motion and the change in colour intensity was detected and recorded on a Pen-Chart Recorder. The speed of the projector was 8 frames per second and chart speed was 6 seconds per cm.

The experimental procedure is illustrated in figure (3.6).

3.3.3 Residence Time Distribution Curve Analysis

To represent the residence time distribution several types of curves are available (15). Among these E and F curves are widely used to analyse residence time distribution. The E curve is generally applied to a pulse input while the F curve is more suitable for a step change. Therefore, in this study, the chosen function was the E curve. It is also known that the F curve can be obtained from the E curve in accordance with the following expression:-

$$F(t) = \int_0^t E(t)dt \qquad (3.17)$$

In treating models, it is often convenient to use the dimensionless time unit and its corresponding function. The dimensionless time unit is defined as follows:-

$$\theta = \frac{t}{\bar{t}} \qquad (3.18)$$

where $\bar{t}$ is the mean residence time (Volume of Reactor/flow rate). The correspondence E function becomes:-

$$E(\theta) = \bar{t}E(t) \qquad (3.19)$$

From the speed of the chart recorder, projector and film and also the mean residence time, the dimensionless unit scale can be calculated. For example, in Run-1

The speed of chart recorder	6 sec/cm
Projector speed	8 frames/sec
Film speed	2 frames/sec
Flow rate	1.5 lit/min
Volume of the Reactor	3.0 lit
Mean residence time ($\bar{t}$)	3.0/1.5 = 2 min = 120 sec.

Therefore, 1 cm on the chart recorder output equals

$$\frac{8}{2} \times 6 = 24 \text{ seconds real time}$$

when $t = \bar{t} = 120$ seconds, $\theta = t/\bar{t} = 1$

Therefore, at the distance 120/24 = 5 cm from the starting point θ is equal to 1. Using the rule "equal distance corresponds to equal time" any desired scale can be obtained and it is also known that

$$\int_0^\infty E(\theta)d\theta = 1 \qquad (3.20)$$

Therefore, dividing the total area under the curve by the length at which $\theta = 1$, the distance at which $E(\theta) = 1$ can be obtained. In this example, the total area under the curve was calculated using the Simpson Rule and it was found to be 49.2 cm^2. Thus, at the distance 49.2/5 = 9.8 cm from the origin, $E(\theta) = 1$. Any desired scale can also be obtained for $E(\theta)$, using the same method by which the θ-scale was obtained.

The results of this example were illustrated in figure (3.7) and also the corresponding values of $E(\theta)$ and $E(\theta)$ were tabulated in table (3.2).

θ	$E(\theta)$	$\int_{\theta_1}^{\theta_2} E(\theta)d\theta$	$F(\theta)$
0.0	0.00		0.000
		0.013	
0.2	0.13		0.013
		0.097	
0.4	0.84		0.110
		0.189	
0.6	1.05		0.299
		0.189	
0.8	0.84		0.488
		0.144	
1.0	0.60		0.632
		0.102	
1.2	0.42		0.734
		0.073	
1.4	0.31		0.807
		0.054	
1.6	0.23		0.861
		0.040	
1.8	0.17		0.901
		0.030	
2.0	0.13		0.931
		0.021	
2.2	0.08		0.952
		0.014	
2.4	0.06		0.966
		0.010	
2.6	0.04		0.976
		0.006	
2.8	0.02		0.982
		0.003	
3.0	0.01		0.985

Table 3.2 The values of $E(\theta)$ and $F(\theta)$ for Run-1

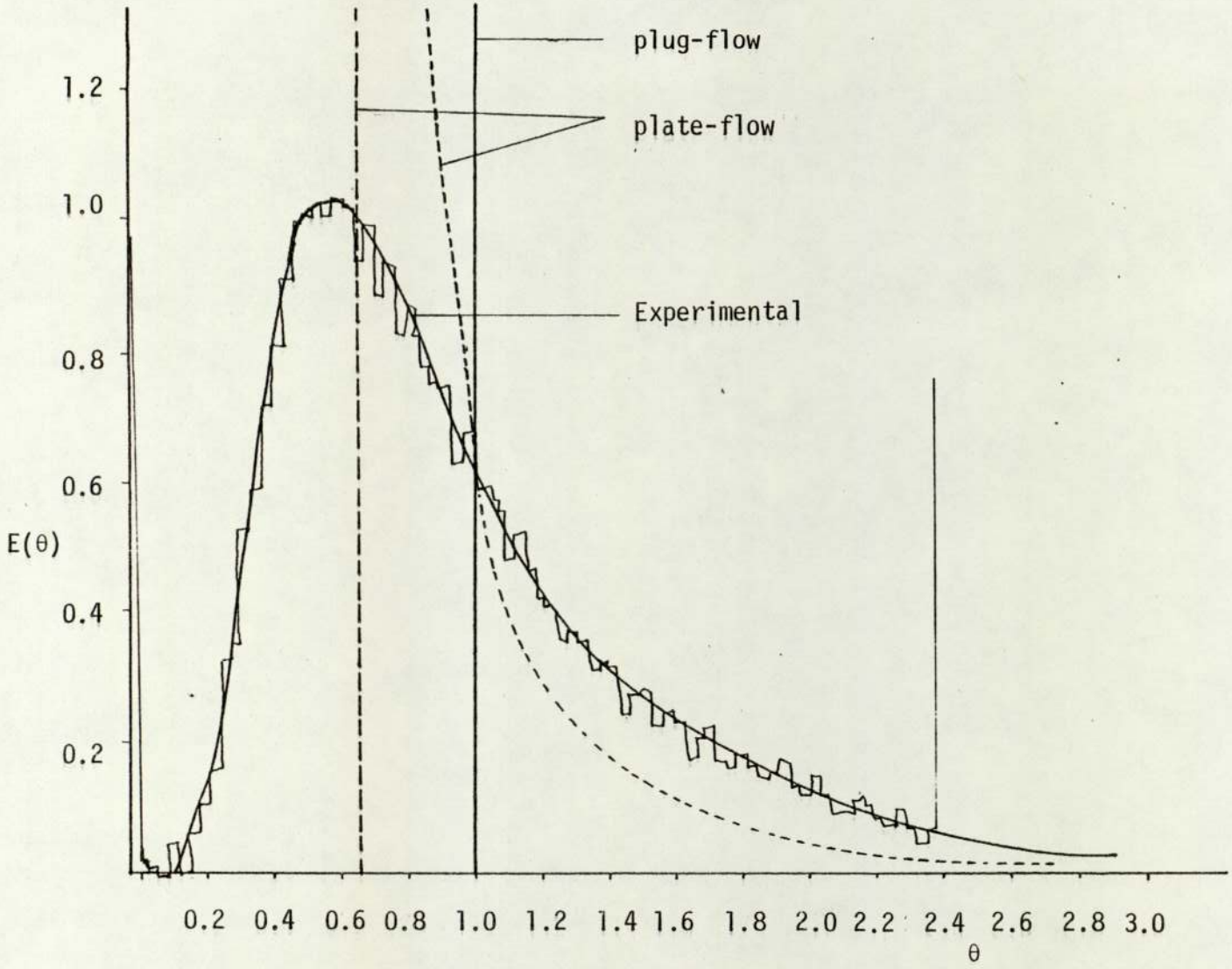

Figure 3.7 R.T.D. Curves for Run-1

3.3.4 Model for Residence Time Distribution

First the residence time distribution caused by the axial velocity profile was considered. The flow in an annulus is similar to flow between two flat plates if the annular space is small with respect to the outer diameter. The laminar flow profile for this flow results in a residence time distribution function given by

$$\left.\begin{aligned} E(\theta) &= 0 && \text{for } 0 < \theta < 2/3 \\ E(\theta) &= \frac{1}{3\theta^3}\,\frac{1}{\left(1 - \frac{2}{3\theta}\right)^{\frac{1}{2}}} && \text{for } \theta > 2/3 \end{aligned}\right\} \qquad (3.21)$$

Derivation of equation (3.21) is given in Appendix (A1).
For an annulus that is not infinitely narrow, the breakthrough point will be lower than $\theta = 2/3$.

Trommelen (6) showed that a high viscosity (1.0 Nsm^{-2}) and low speed of rotation ($4S^{-1}$) and with 10^{-2}m annulus width, the residence time distribution curve approaches the curve represented by equation (3.21). The residence time distribution curves obtained in this study are not in good agreement with equation (3.21). However, it can be seen that when the viscosity is high and the speed of rotation is low the curves became closer to the model represented by equation (3.21). Also it is believed that dispersion in the annulus due to vortices and pumping effects of the blades cause deviation from the ideal flow as postulated above.

The second type of model tested was the "tank-in-series" model. From the tangential flow analysis it is known that the annulus consists of two sections (inner and outer sections) and their volumes are approximately 1 and 2 litres respectively. At the Taylor vortices present each vortice acts as a perfect mixing tank and

because of the two sections it forms a set of two parallel "tank-in-series" with probably by-pass between them. This model is illustrated in figure (3.8).

A mathematical model for the system represented by figure (3.8) has been developed. A mass balance can be set up as follows:-

$$\left.\begin{aligned} RC_{exist} &= f_1 RC_n + f_2 RC_m + (1-f_1-f_2)RC_0 \\ C_{exist} &= f_1 C_n + f_2 C_m + (1-f_1-f_2)C_0 \end{aligned}\right\} \qquad (3.22)$$

From the definition of F(t) and mass balance

$$F(t) = \frac{C_{exit}}{C_0}$$

and it follows that:-

$$F(t) = f_1\left\{1-\exp(-nf_1Rt/V_n)\left[1 + \frac{nf_1Rt}{V_n} + \frac{1}{2!}\left(\frac{nf_1Rt}{V_n}\right)^2 + \ldots + \frac{1}{(n-1)!}\left(\frac{nf_1Rt}{V_n}\right)^{n-1}\right]\right\}$$

$$+ f_2\left\{1-\exp(mf_2Rt/V_m)\left[1 + \frac{mf_2Rt}{V_m} + \frac{1}{2!}\left(\frac{mf_2Rt}{V_m}\right)^2 + \ldots + \frac{1}{(m-1)!}\left(\frac{mf_2Rt}{V_m}\right)^{m-1}\right]\right\}$$

$$+ (1-f_1-f_2) \qquad (3.23)$$

and from equation (3.17)

$$E(t) = \frac{dF(t)}{dt} = f_1 \frac{n^n}{(n-1)!}\left(\frac{f_1R}{V_n}\right)^n t^{n-1} \exp(-nf_1Rt/V_n)$$

$$+ f_2 \frac{m^m}{(m-1)!}\left(\frac{f_2R}{V_m}\right)^m t^{m-1} \exp(-mf_2Rt/V_m) \qquad (3.24)$$

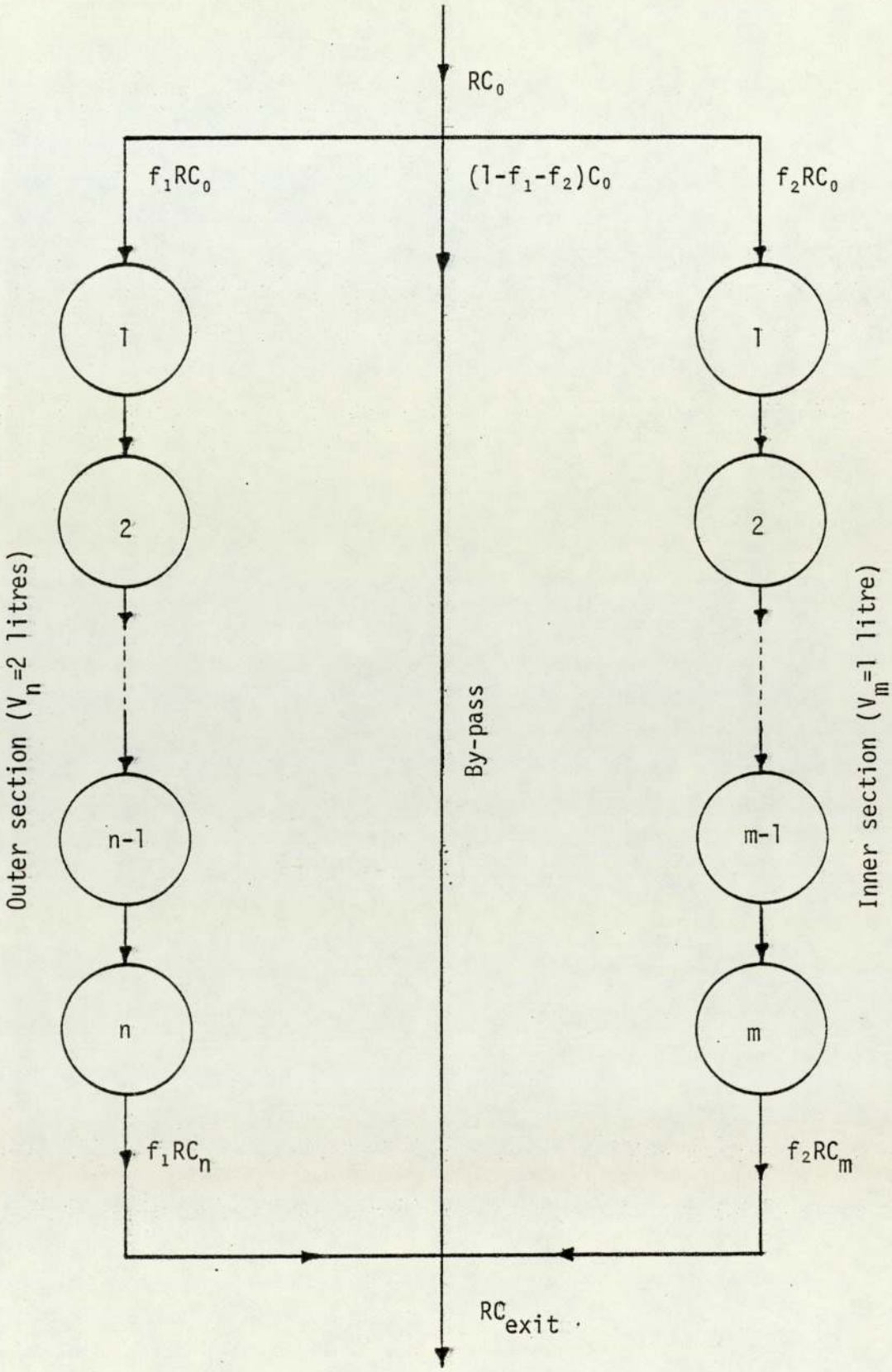

Figure 3.8 Two Parallel Tanks-in-Series with By-pass

to find $E(\theta)$ the following definition can be held:-

$$\bar{t} = f_1 \bar{t}_1 + f_2 \bar{t}_2 \tag{3.25a}$$

$$\theta = \frac{t}{\bar{t}} \tag{3.25b}$$

$$\alpha = \frac{\bar{t}_2}{\bar{t}_1} \tag{3.25c}$$

$$\beta = f_1 + f_2 \alpha \tag{3.25d}$$

it follows that:-

$$\bar{t}_1 = \frac{\bar{t}}{\beta} \tag{3.26a}$$

$$\bar{t}_2 = \frac{\alpha}{\beta} \bar{t} \tag{3.26b}$$

and it was also assumed that V_n = 2 litres, V_m = 1 litre.

Therefore:-

$$f_2 = \frac{f_1}{\alpha} \tag{3.27a}$$

$$\beta = 1.5 f_1 \tag{3.27b}$$

where $\bar{t}_1 = V_n/f_1 R$, $\bar{t}_2 = V_m/f_2 R$ and R is flow rate.

From expressions (3.19), (3.24), (3.26) and (3.27) $E(\theta)$ function can be obtained as follows:-

$$E(\theta) = \bar{t}E(t) = f_1 \frac{n^n}{(n-1)!} \beta^n \theta^{n-1} \exp(-n\beta\theta) + \frac{f_1}{2\alpha} \frac{m^m}{(m-1)!} \left(\frac{\beta}{\alpha}\right)^m \theta^{m-1} \exp(-m\beta\theta/\alpha) \tag{3.28}$$

There are four parameters in equation (3.28)

$$f_1, \alpha, n, m \quad \text{since } \beta = 1.5 f_1$$

These parameters were evaluated by trial-error. The closest curve to the experimental curve has been chosen as the best. It was obtained by adjusting the parameters and the curves obtained are

presented at the end of this chapter. It was found that the by-pass was negligible and the number of "tanks-in-series" increased with low speed of rotation and high viscosity. Because of high viscosities (3×10^{-4} - 3.5×10^{-4} m^2s^{-1}) reaction conditions are closer to that of Run-3 in table (3.1) in which the number of "tanks-in-series" in the inner and outer branch are 6 and 9 respectively. "Tanks-in-series" greater than 5 can be approximated to the plug-flow reactor (50) and therefore it was concluded that the reactor consists of two parallel plug-flow reactors with different volumes (inner branch is 1 litre while the outer is 2 litres). It was also found that 50% of the flow rate passed through each branch.

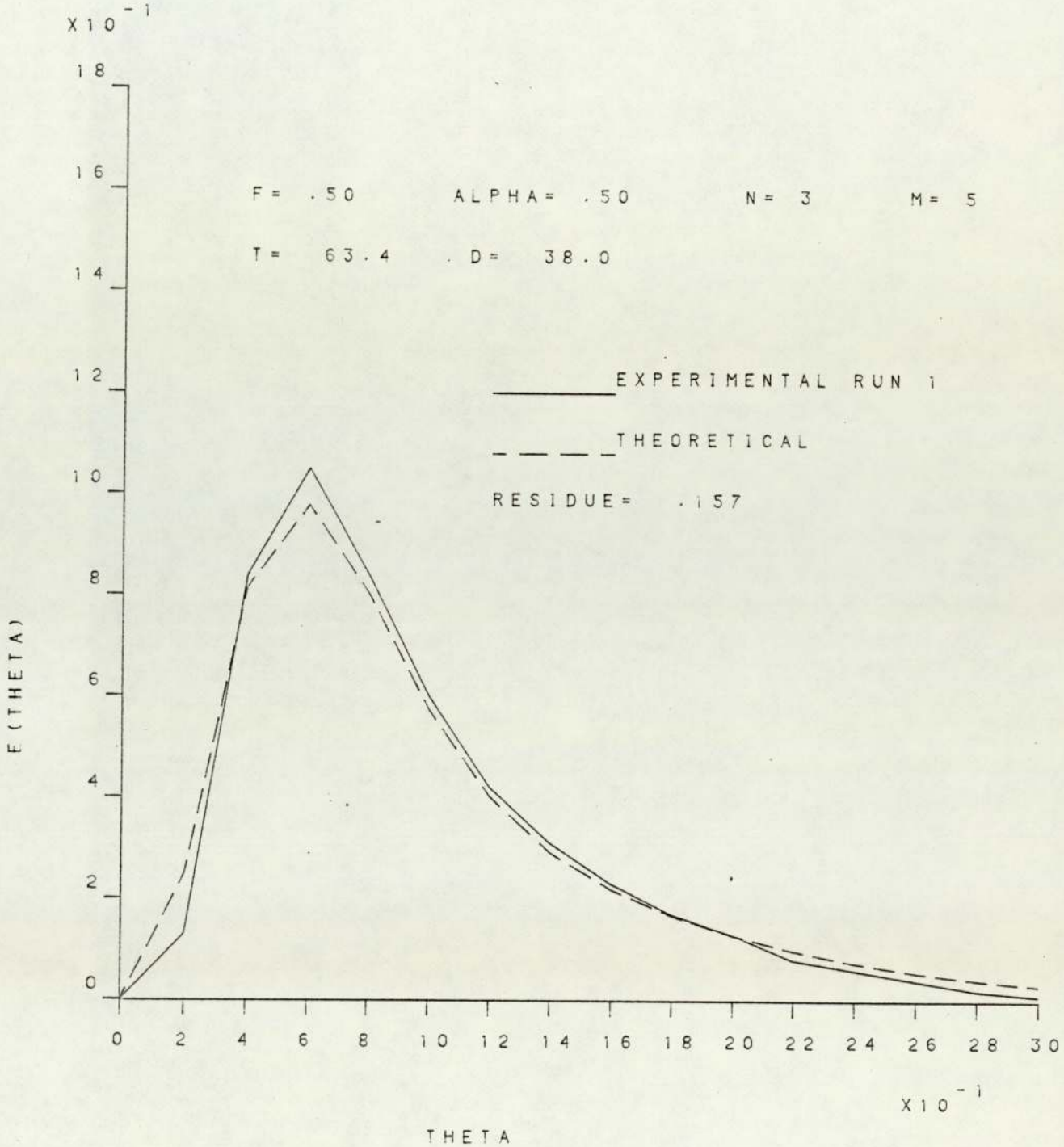

Figure 3.9 R.T.D. Curve for Run-1

(N = 4.17 r.p.s; ν = 45cS; R = 1.50 lit.min^{-1})

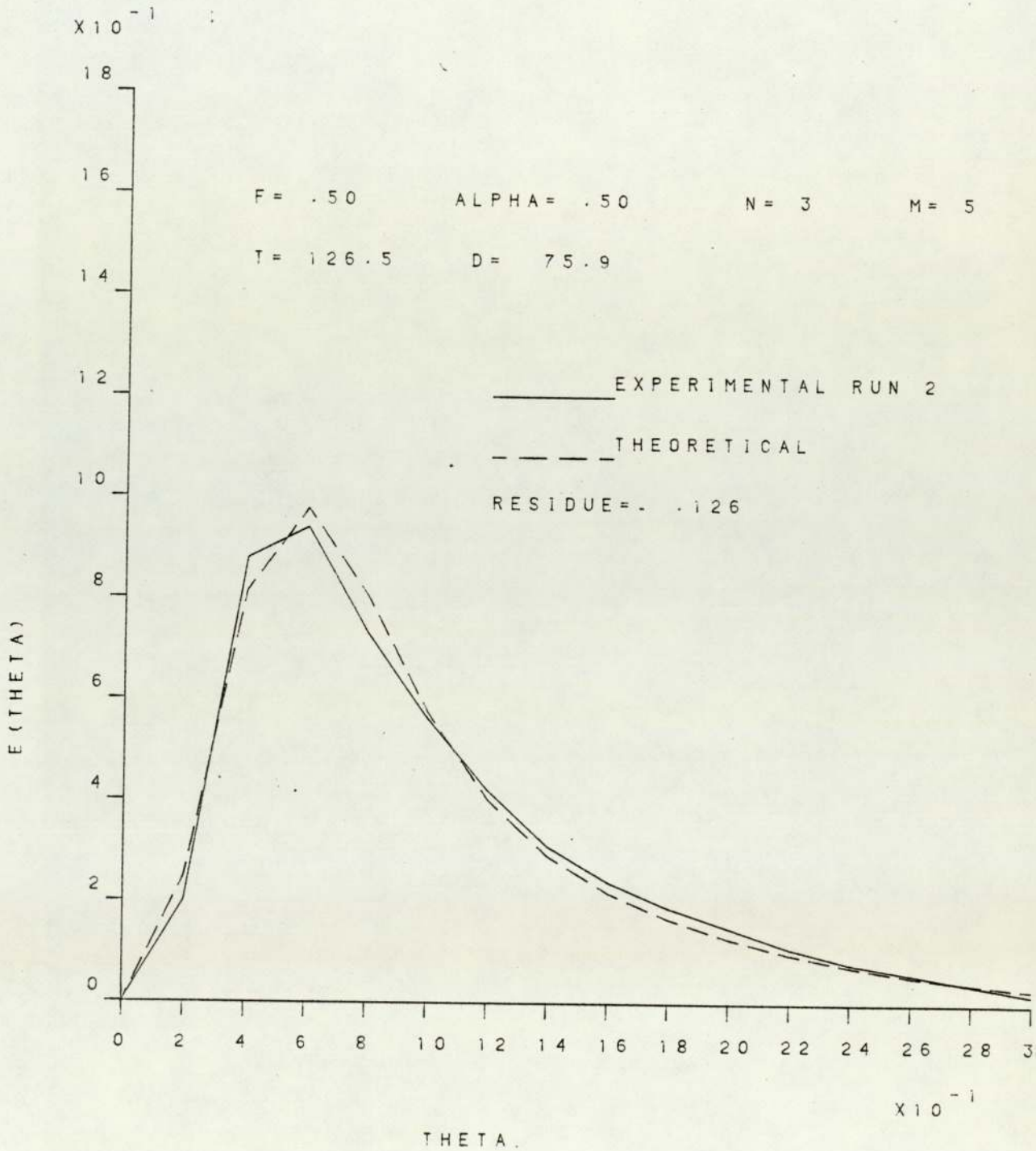

Figure 3.10 R.T.D. Curve for Run-2

(N = 8.33 r.p.s; ν = 45cS; R = 1.67 lit.min^{-1})

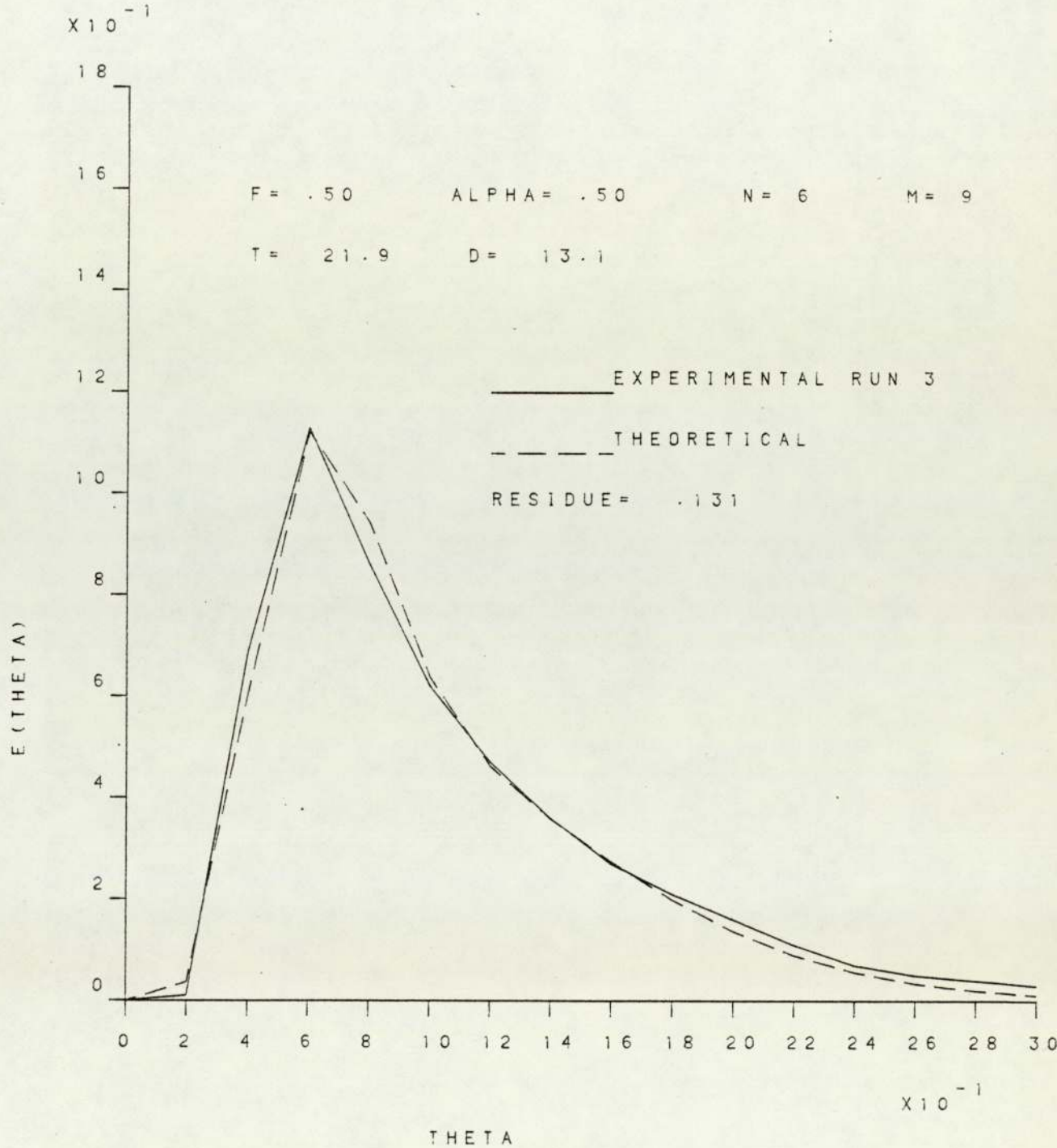

Figure 3.11 R.T.D. Curve for Run-3

(N = 4.17 r.p.s; ν = 130cS; R = 1.40 lit.min^{-1})

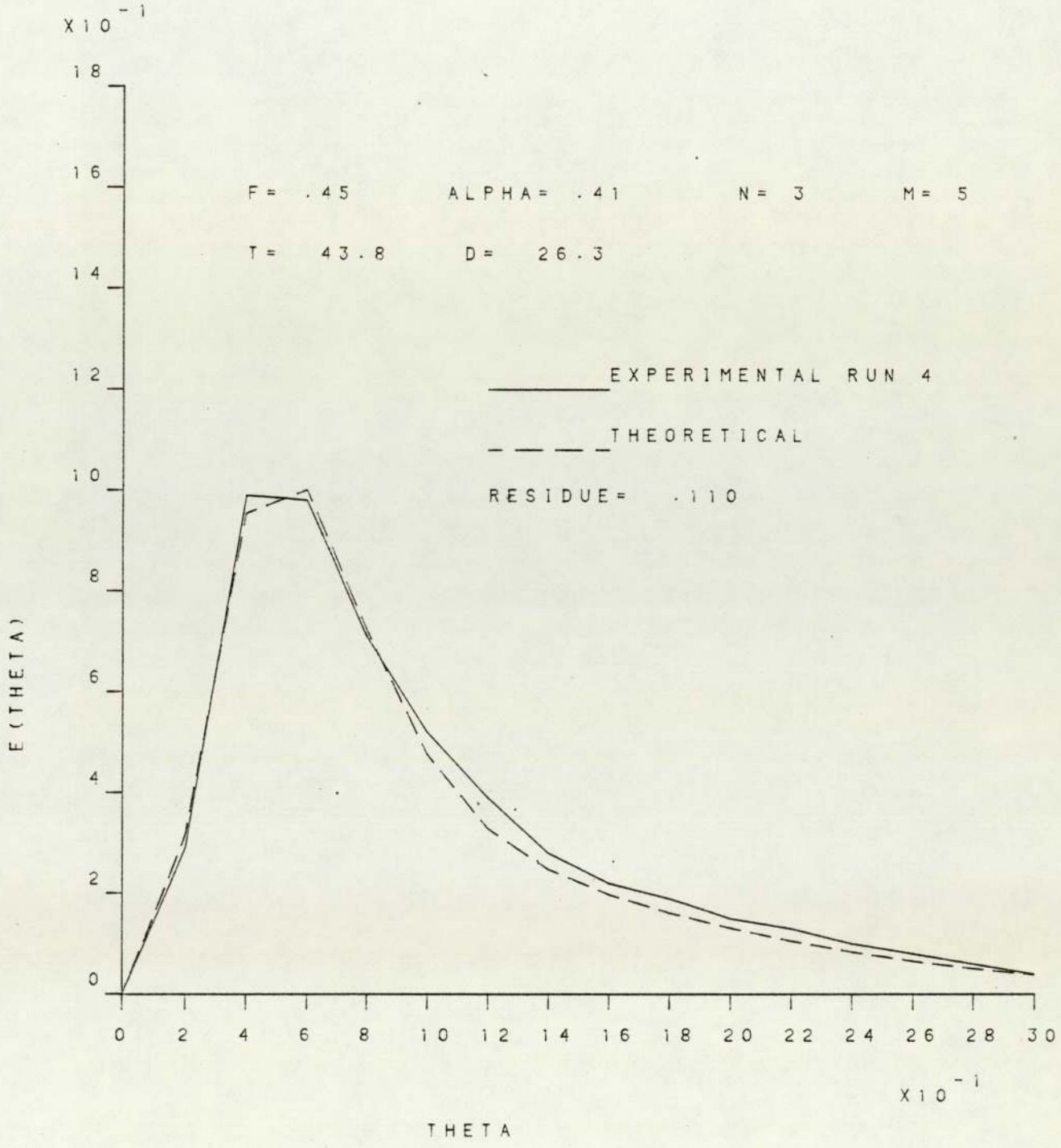

Figure 3.12 R.T.D. Curve for Run-4

(N = 8.33 r.p.s; ν = 130cS; R = 1.40 lit.min^{-1})

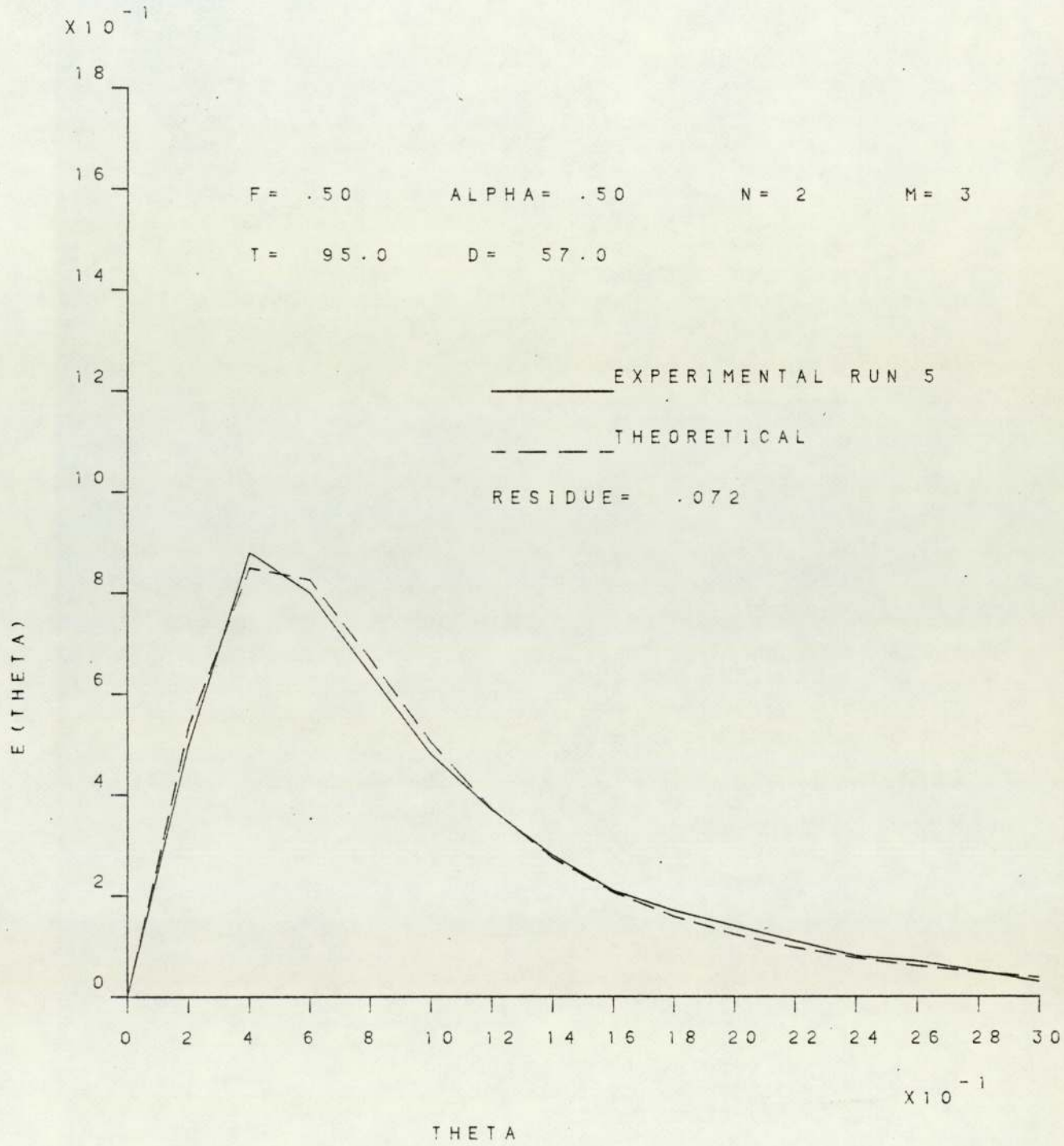

Figure 3.13 R.T.D. Curve for Run-5

(N = 16.67 r.p.s; ν = 1.0cS; R = 2.30 lit.min^{-1})

CHAPTER 4

POWER REQUIREMENT

4.1 INTRODUCTION

In Scaling-up a pilot plant reactor for industrial use, the power consumption of the impeller and other mechanisms is amongst the more important considerations (i.e. cost, achieving good conversion, controlability etc.). Although this power requirement cannot be estimated theoretically, even in the simplest agitated system, many research workers concluded that the Power number (P_0) can be directly related to the Reynolds number of rotation $\left(N_{Re_R}\right)$. This criteria is widely used for the scale-up of agitated reactors. However, Trommelen and Boerama (5) showed that this is not true for scraped surface heat exchanger; the Power number (P_0) increases at constant Reynolds number as the viscosity of the working liquid decreases. This deviation from normal agitators is attributed to the decrease of the fluid viscosity between the wall and blade, due to a rise in temperature through viscous dissipation and through frictional forces by the scraping action of the blades against the wall.

The type of the scraped surface heat exchanger used previously to determine the power requirement is different from the reactor under consideration ("no-leak" votator). Therefore it is necessary to find an expression to predict the power requirement conditions for "no-leak" and to generalize the relations.

4.2 POWER CONSUMPTION THEORY

The power consumption in a votator (or scraped surface heat exchanger) reactor is made up as follows:-

a) Power dissipated in the liquid contained in the annulus space due to shear stresses created by the fluid.

b) Power lost by the scraping action of the blades against the wall.

c) Power required to overcome friction in the bearings.

d) Power required to rotate the mass of the inner cylinder and blades themselves.

Only the power consumption due to (a) can be calculated theoretically when the reactor is operated within the laminar flow regime since then the velocity profile is known. Therefore, generally the total power consumption can only be expressed in the form of a semi-empirical equation.

4.2.1 Proportion of Power Dissipated in the Fluid Due to Internal Friction.

This part of the power consumption can be calculated using the velocity profile equations derived in Sections (3.2.1) and (3.2.2). The assumptions made in Section (3.2) hold for the calculation of the power consumption. For these purposes rectangular and cylindrical coordinate systems can be used.

4.2.1.1 Rectangular Coordinate Systems

In the rectangular coordinate systems the shear stress is given by (3):-

$$\tau_{xy} = \tau_{yx} = - \mu \left| \frac{\partial V_x}{\partial y} + \frac{\partial V_y}{dx} \right| \qquad (4.1)$$

where $V_y = 0$, therefore $\partial V_y / \partial V_x = 0$ (from assumption (ii) in Section 3.2) $\partial V_x / \partial y$ can be obtained by differentiating equation (3.9)

$$\frac{\partial V_x}{\partial y} = V_i \left(\frac{6y^2}{d^2} - \frac{4}{d} \right) \qquad (4.2)$$

The shear stress becomes

$$\tau_{xy} = - \mu V_i \left(\frac{6y}{d^2} - \frac{4}{d} \right) \qquad (4.3)$$

and

$$\text{Torque} = \tau_{xy}\Big|_{y=0} \times r_i \times 2\pi r_i L = \frac{8\pi r_i^2 L V_i \mu}{d} \qquad (4.4)$$

It is also known that

$$\text{Power} = \text{Torque} \times 2\pi N \qquad (4.5)$$

From equation (4.4) and (4.5) and replacing V_i by $2\pi N r_i$ the power consumption becomes

$$P = \frac{32\pi^3 L}{d} r_i^3 N^2 \mu \qquad (4.6)$$

Equation (4.6) can be arranged in terms of Power and Reynolds numbers. Thus:-

$$P_0 = \frac{32\pi^3 L}{d} N_{Re_R}^{-1} \qquad (4.7)$$

where $P_0 = \dfrac{P}{N^3 r_i^5 \rho}$ (Power number)

$N_{Re_R} = \dfrac{N r_i^2 \rho}{\mu}$ (Reynolds number)

Inserting the pilot plant reactor dimensions into equation (4.6) the power utilized in the liquid contained within the annulus becomes

$$P = 4.90\ N^2 \mu \qquad (4.8)$$

4.2.1.2 Cylindrical Coordinate Systems

The equation of the velocity profile in cylindrical coordinate systems is given by the expression (3.4). That is:-

$$\frac{V_\theta}{V_i} = 715.34r \ln r + 1584.91r + \frac{1.545}{r} \qquad (3.4)$$

and the shear stress (3)

$$\tau_{r\theta} = -\mu r \left[\frac{\partial}{\partial r}\left(\frac{V_\theta}{r}\right)\right] \qquad (4.9)$$

Therefore

$$\tau_{r\theta} = -\mu r V_i \left(\frac{715.34}{r} - \frac{3.090}{r^3}\right) \qquad (4.10)$$

$$\text{Torque} = \tau_{r\theta}\Big|_{r=r_i} \times r_i \times 2\pi r_i L = 2\pi \times 286 \times V_i r_i^2 L\mu \qquad (4.11)$$

It is also known that:-

$$P = \text{Torque} \times 2\pi N \text{ and } V_i = 2\pi N r_i \qquad (4.12)$$

From expressions (4.11) and (4.12) the power consumption becomes

$$P = 8 \times 286 \times \pi^3 r_i^3 L N^2 \mu \qquad (4.13)$$

For the dimensions of the reactor under consideration

$$P = 5.56\ N^2\mu \qquad (4.14)$$

Comparison of equations (4.8) and (4.14) reveals that a 12% error is incurred using simple rectangular coordinates. Trommelen and Boerama (5) showed that even in the laminar flow regime there is no reliable agreement between equations (4.6) or (4.13) and the experimental results. Experimental results are far greater than those calculated from equations (4.6) and (4.13). Therefore the power consumption has to be estimated using empirical equations based on experimental results.

For the Taylor instability regime it is impossible to develop a theoretical expression. However, it has been shown (6) that the Power number (P_0) can be given by:-

$$P_0 = K N_{Re_{R_{cr}}}^{-0.5} \; N_{Re_R}^{-0.5} \tag{4.15}$$

where $N_{Re_{R_{cr}}}$ is the rotational Reynolds number at the critical speed of the inner cylinder, while N_{Re_R} is Reynolds number above the critical speed of the inner cylinder. Therefore

$$P \propto K_1 \mu \tag{4.16}$$

where K_1 is a constant.

4.2.2 Frictional Losses

The major part of the power consumption consists of frictional losses. They are the power loss due to (a), (c) and (d) in Section (4.2). No equation, based on theory, has been developed to predict the frictional losses but semi-empirical equations derived from experimentally measured power losses are available in the literature (2,6,16). Unfortunately none of the equations presented distinguish between the power contribution due to (b), (c) or (d) above. For this reason Dykes (2) suggested that the power requirements to overcome all frictions can be combined into one term which is proportional to the speed of rotation of the inner cylinder. That is:-

$$P_{friction} = K_2 N \tag{4.17}$$

where K_2 is a constant that has to be found experimentally.

4.2.3 Empirical Equations for Power Consumption

There are a considerable number of empirical equations in the literature to predict the power consumption for scraped surface heat exchangers "with-leak". However it has been found (17) that the power required for a "no-leak" votator is 30% more than that required for "with-leak" scraped heat exchangers.

Empirical equations presented for power consumption are generally expressed by two types of equations:-

i) Power number is a function of Reynolds number and the number of blades. That is:-

$$P_0 = AN_{Re_R}^{B}(n_B)^{C} \tag{4.18}$$

where $$P_0 = \frac{P}{D_0^5 N^3 \rho} \quad , \quad N_{Re_R} = \frac{D_0^2 N \rho}{\mu}$$

and A, B, C are constants, n_B is the number of blades.

Skelland and Leung (16) proposed the following empirical equations

$$P_0 = 77{,}500 N_{Re_R}^{-1.27}(n_B)^{0.59} \quad \begin{bmatrix}\text{from the graphical}\\ \text{solution of the}\\ \text{equation (4.18)}\end{bmatrix} \tag{4.19}$$

$$P_0 = 38{,}230 N_{Re_R}^{-1.14}(n_B)^{0.64} \quad \begin{bmatrix}\text{from the solution of}\\ \text{equation (4.18) using}\\ \text{the least square method}\end{bmatrix} \tag{4.20}$$

The expressions (4.19) and (4.20) cannot be generalized for all types of scraped surface heat exchangers since they do not include the length of the blades. The effects of the length of the blades are combined with the constant A for particular scraped surface heat exchangers (the length of blades (L_B) = 0.4572m).

Later Leung (18) concluded that for a given scraped surface heat exchanger, the power consumption is directly proportional to the length of blades and modified equations (4.19) and (4.20) to:-

$$\frac{P_0}{L_B} = 169{,}500 N_{Re_R}^{-1.27} (n_B)^{0.59} \qquad (4.21)$$

$$\frac{P_0}{L_B} = 83{,}600 N_{Re_R}^{-1.14} (n_B)^{0.64} \text{ respectively} \qquad (4.22)$$

It will be noticed that the constants 169,500 and 83,600 have units of "length^{-1}" and these expressions do not include the effect of the annulus width.

ii) The second type of empirical equation for power consumption in the scraped surface heat exchanger includes the effect of the annulus width, but they are not explicitly functions of the Reynolds number.

The theory of power consumption was considered in great depth by Trommelen (6) who proposed an empirical equation of the form:-

$$P = \frac{C_0 (ND_0)^{C_1} \mu^{C_2} N_B^{C_3} L_B}{(D_0 - D_i)^{C_4}} \qquad (4.23)$$

where C_0-C_4 are constants and proposed values of them are 251, 1.79, 0.66, 0.68 and 0.31 respectively. Thus equation (4.23) becomes

$$P = \frac{251 (ND_0)^{1.79} \mu^{0.66} n_B^{0.68} L_B}{(D_0 - D_i)^{0.31}} \qquad (4.24)$$

All empirical equations mentioned above are based on experiments carried out using scraped surface heat exchangers

"with-leak". With "no-leak" votator, Westaleken (17) showed that the power consumption was 30% greater than that of a scraped surface heat exchanger "with-leak". Secondly they do not include the friction terms. To find the total power requirement for example, the equations (4.17) and (4.23) can be combined into a single equation:-

$$P_{total} = \frac{C_0(ND_0)^{C_1}\mu^{C_2}n_B^{C_3}L_B}{(D_0-D_i)^{C_4}} + K_2N \qquad (4.25)$$

Since D_0, D_i, n_B and L_B are constants for a given reactor, equation (4.25) can be reduced to:-

$$P_{total} = C_5N^{C_1}\mu^{C_2} + K_2N$$

or in the more usual nomenclature

$$P = AN^B\mu^C + DN \qquad (4.26)$$

This equation has been applied in this study to estimate A, B, C and D.

4.3 EXPERIMENTAL METHOD

To correlate equation (4.26), two quantities namely viscosity of the working liquid and power consumption were measured as accurately as possible, since the speed of rotation of the inner cylinder can easily be monitored by a tachometer, connected into the electronic circuitry.

4.3.1 Viscosity Measurement

Because of viscous dissipation the temperature of the fluid in the annulus increases and consequently the viscosity decreases. From this statement it is necessary to define a mean viscosity and use this in the power consumption calculations.

The mean viscosity can be given by:-

$$\bar{\mu} = \frac{1}{L}\int_0^L \mu_z dz \qquad (4.27)$$

where μ_z is the local viscosity. Provided the temperature range is not too great (not greater than 10°C), the relationship between viscosity and temperature is approximately:-

$$\mu_z = \mu_0 e^{-aT} \qquad (4.28)$$

in which μ_0 and a are constants and their units are N sm^{-2} and deg C^{-1} respectively. If it is assumed that the specific heat and the density of the fluid are only slightly temperature dependent, then the temperature gradient (dT/dz) in the adiabatic votator will be proportional to the viscosity i.e:-

$$\frac{dT}{dz} = C\, e^{-aT} \qquad (4.29)$$

where C is the proportionality constant. Using equation (4.29) with the boundary conditions $T = T_1$ for $z = 0$ and $T = T_2$ for $z = L$, the constant C can be calculated

$$C = \frac{1}{aL}\left(e^{aT_2} - e^{aT_1}\right) \qquad (4.30)$$

From equations (4.27), (4.28) and (4.30) $\bar{\mu}$ can be found as follows:-

$$\bar{\mu} = \frac{a\mu_0(T_2 - T_1)}{e^{a\bar{T}_2} - e^{a\bar{T}_1}} \qquad (4.31)$$

where T_1 and T_2 are inlet and outlet temperatures of the working liquid respectively (deg C°).

Derivation of equation (4.31) and the method of applying it has been demonstrated with an example in the Appendix (A2).

However, such a calculation to find the mean viscosity is rather time consuming. A more rapid and sufficiently accurate method is to measure the viscosity at the arithmetic mean temperature of T_1 and T_2. By this approximation the error will not be greater than 2%, provided the temperature range is not greater than 10°C. Then the experimental viscosity was measured at the arithmetic mean temperature using a U-tube viscometer.

4.3.2 Power Consumption Measurement

It is necessary to give a brief description of the drive unit of the reactor to explain the measurement of the power consumption.

4.3.2.1 Drive Unit

It was mentioned in Chapter (1) that the reactor was inherited from a previous study. A thyristor controlled variable speed unit was chosen to drive the inner cylinder which has many advantages over other forms of a mechanical drive motor and linkage. Apart from the infinitely variable speed between specified limits, it was possible to control the speed of rotation at any predetermined value without further adjustment irrespective of changes in torque requirements. This may occur through variation in fluid viscosity or frictional forces within the reactor.

The chosen unit, a VH041, had a nominal power rating of 7.46 kw (10.06 H.P) and a continuous duty speed range of 90-1460 r.p.m. The VH041 drive consists of an electric motor mounted on top of the eddy-current coupling, belts being employed in conjunction with various pulleys of different diameter to obtain the required range of output speeds, figure (4.1).

Control of the unit was by a control box situated on the

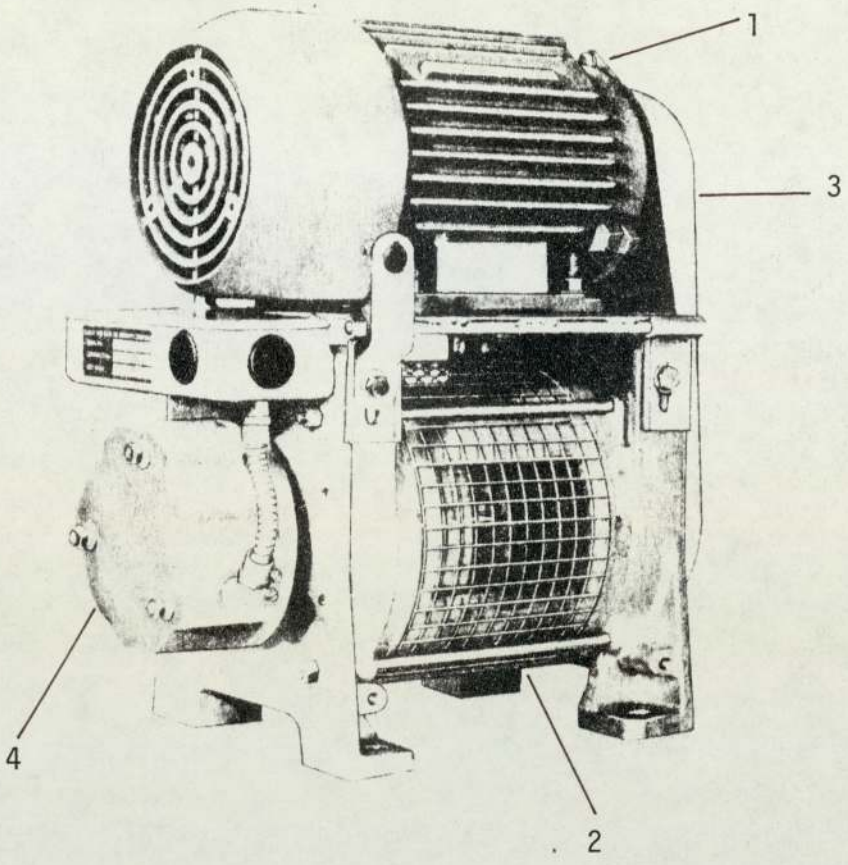

1. Motor
2. Drive Coupling
3. Pulley belt connection
4. Tachogenerator

Figure 4.1 Variable Speed Unit

front panel of the experimental apparatus remote from the unit itself. A tachometer was connected into the electronic circuitry to indicate speed of rotation.

4.3.2.2 Principle of Operation

Power from the motor was transmitted by means of a belt drive to the input member of an eddy-current coupling, the input speed of which was therefore constant (in this case 1460 r.p.m). Torque was transmitted by the coupling to the reactor when an electromagnetic linkage was established between the input and output members. By controlling the strength of this linkage the output speed of the drive could be varied. However, because some slip occurred between the members the maximum obtainable output speed was slightly less than the input speed.

The drive unit was connected to the rotating cylinder (inner cylinder) by means of three wedge pulleys encased in an appropriate guard.

4.3.2.3 Power Measurement

A graph of the torque versus slip speed characteristic of the VH041 coupling had already been obtained from the manufacturers (Appendix B1). This relates the excitation current (the current fed to the field coil from the thyrystor control) and the slip speed (coupling input-output speed) to the torque produced. In this case the coupling input speed was constant and its value was 1460 r.p.m. Then from the relationship:-

Power = Torque x Angular Velocity

the power was calculated.

The excitation current was measured by an ammeter placed

in series with the field coil.

4.3.3 Experimental Procedure

In the power consumption experiments glycerol-water mixtures having viscosities at the operating temperatures of between 30 and 350 cP were used. With the highest viscosities difficulties arose in pumping the liquid into the reactor. The speed of rotation was monitored by means of a tachometer connected into the electronic circuitry. The flow rate was kept constant at 3 litres per minute, since it had been reported that the flow rate had no effect on the power consumption (5).

Experiments were performed at various speeds of rotation and fluid viscosities. The inlet and outlet fluid temperature were measured using thermocouples. The viscosity of the fluid at the mean temperature was measured with a U-tube viscometer. During the experiment the reactor was cooled by water so that temperature differences between inlet and outlet could be kept within 10°C. Without cooling the reactor outlet flow temperature would have increased due to friction in the annulus. At temperature differences greater than 10°C, the mean viscosity cannot be found, since there was not a linear relationship between temperature and viscosity.

Experimental data are tabulated in Appendix B2.

4.4 COMPUTATIONAL ANALYSIS AND RESULTS

The experimental results were analysed by non-linear regression computation using the Nelder Algorithm (19). The mean program was a library package that estimated the minimum of a multivariable, unconstrained, non-linear function:-

$$f(X_1, X_2 \ldots X_N)$$

The master program, which calls this library subroutine also contains the functional form of the equation (4.26)

$$Y_{VAL} = AR^B T^C + DR \qquad (4.32)$$

where A, B, C and D are constants to be found. The designated variables are:-

Y_{VAL} = (P) Power

R = (N) Speed of rotation

T = (μ) Dynamic viscosity of fluid

The numerical data relating to the variables and initial estimations of the magnitude of the constants must be introduced together with scaling factors for each constant. In this computation the initial estimations for A, B, C and D were 0.05, 1.79, 0.66, 0.05 respectively. The initial values for B and C are more common values that appeared in the literature (2,5,6).

Goodness of fit of the resulting equation is usually judged by the optimum value of the objective function. However, as absolute values by which to compare the objective function are not available, judgement can only be made by comparison of experimental points to the computed curves.

Using initial values mentioned above together with experimental results (Appendix B2), the calculated values of the constants of equation (4.26) were:-

A = 34.58

B = 1.928

C = 0.612

D = 35.27

Rounding off the values of the indices to 1.93 and 0.61 respectively and inserting these values into the program, the recalculated constants were:-

$$P = 34.44\ N^{1.93}\ \mu^{0.61} + 34.88N \qquad (4.33)$$

In equation (4.33), keeping the speed of rotation (N) constant and plotting a graph of P versus $\mu^{0.61}$, a straight line was obtained. It can be seen from the figure (4.2) that these lines agree very well with the experimental points. This proved that equation (4.26) represents the power consumption within the annulus and covers both the laminar and the Taylor instability regimes.

Further runs were made with other fixed indices in order to obtain a good comparison of the objective function values. The indices used were those of common occurrence in power consumption models and also those derived by other studies (2,6,16,20). The results are tabulated in Table (4.1).

4.4.1 Discussion of the Results

In Table (4.1) the first four values of the constants represent the second type of empirical equation while the last two values of the constants refer to the first type of empirical equation mentioned in Section (4.2.3). By comparison of the values of the objective function it can be seen that the second type of empirical equation is better than the first to represent the power consumption since the smallest values of the objective function imply smaller deviation from the model.

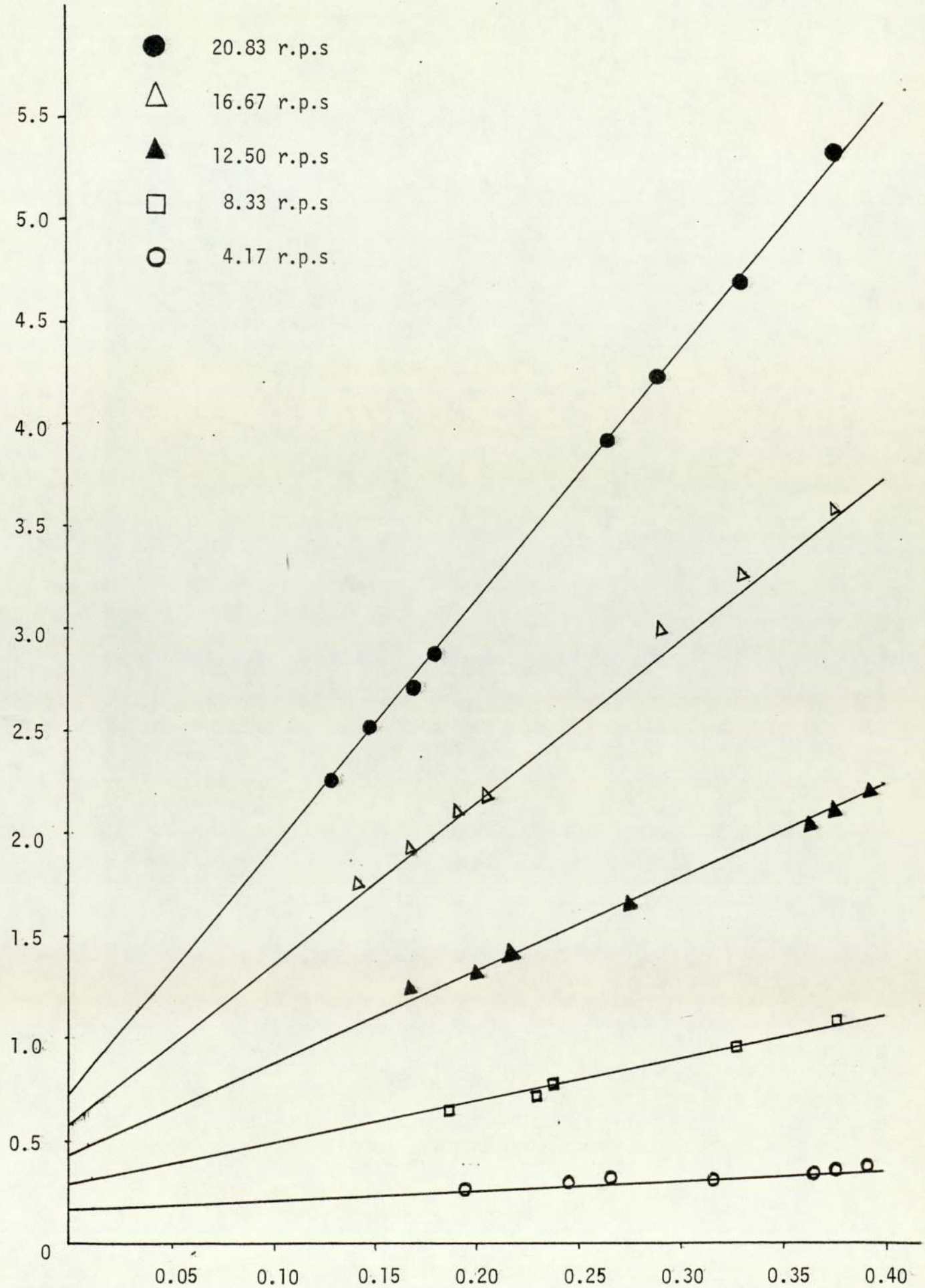

Figure 4.2 Power Consumption (kW) vs $\mu^{0\ 61}$ (M.K.S unit)

A	B	C	D	Objective functions x 10^2	References
34.58	1.928	0.612	35.27	6.39	Present study
34.44	1.93	0.61	34.88	6.40	Present study
29.05	2.00	0.66	43.96	7.29	Dykes (2)
53.40	1.79	0.66	40.41	40.66	Trommelen (6)
39.31	2.00	1.00	79.60	120.24	Froishte (20)
104.50	1.73	1.27	99.21	412.68	Skelland et al. (16)

Table 4.1 The recalculated values of the constants in equation (4.26) using different indices.

If the dimensions of the reactor under consideration are inserted into Trommelen's equation (4.24) the following equation can be obtained

$$P = 34.73\ N^{1.79}\ \mu^{0.66} \qquad (4.34)$$

In obtaining equation (4.34) from equation (4.24), the number of blades was taken to be 6 instead of 3 since the blades of Trommelen's reactor were only half the annular length and were fixed diametrically opposite, so that the whole of the tube surface was scraped.

The expression (4.34) differs from equation (4.33) in two respects; first it does not include a friction term, secondly Trommelen's reactor was a scraped surface heat exchanger "with-leak" while equation (4.33) represents the "no-leak" votator. Westelaken (17) found that the power consumed by "no-leak" reactors is 30% greater than that of the "with-leak" reactor. Therefore, equation (4.34) should be multiplied by 1.30 to apply to the "no-leak" reactor. Thus equation (4.34) becomes:-

$$P = 45.15\ N^{1.79}\ \mu^{0.66} \qquad (4.35)$$

Using Trommelen indices and ignoring the friction term, the first term of equation (4.33) becomes:-

$$P = 53.40\ N^{1.79}\ \mu^{0.66} \qquad (4.36)$$

By comparison of equation (4.35) and (4.36), it can be seen that the power given by equation (4.36) is 18% greater than that given by equation (4.35). It is believed that this difference arose due to experimental error caused by the measurement of the power and fluid viscosity.

With the same reactor as used in the present work, Dykes (2) derived the following expression

$$P = 22.4\ N^2\ \mu^{0.66} + 33.1N \qquad (4.37)$$

It can be seen that frictional terms in both equation (4.33) and (4.37) are in good agreement with each other while the first term in equation (4.37) is considerably smaller than that of the first term of equation (4.33). This error arises from the different viscosity measurements. Dykes measured the viscosity of the fluid using a "Ferranti" viscometer and subsequently corrected his measurement by comparing it to the U-tube viscometer measurement as follows:-

$$\mu_C = \mu_{VHA} - 0.1 \text{ for } \mu_{VHA} > 0.2\ Nsm^{-2} \qquad (4.38a)$$

$$\mu_C = \mu_{VHA} - 0.02 \text{ for } \mu_{VHA} < 0.2\ Nsm^{-2} \qquad (4.38b)$$

where μ_C is the correct viscosity obtained using the U-tube viscometer, while μ_{VHA} is the viscosity of the fluid obtained using the "Ferranti" Viscometer.

An attempt to find a relationship between the U-tube Viscometer and Ferranti Viscometer, in the present work, was not

successful. Assuming that the expressions (4.38) given by Dykes are correct, errors arise at viscosities near 0.2 Nsm^{-2}.

There is no use in conforming equation (4.33) with the first type of empirical equation mentioned in Section (4.2.3) since deviations of the model from experimental results are larger than in the second type of the empirical equation. See Table (4.1).

From this analysis it was concluded that for the scale-up of a pilot plant reactor with "with-leak" for industrial use, Trommelen's equation (equation 4.24) can be used. To apply Trommelen's equation to "no-leak" reactor, Westalken's proposal has to be taken into account to give a power consumption 30% greater than Trommelen's equation.

It was also observed that the indices for speed of rotation and viscosity varied between 1.75-2.00 and 0.60-0.70 respectively which can be used as starting points for further investigations.

CHAPTER 5

CHEMISTRY OF SULPHATION AND EXPERIMENTAL PROGRAM

5.1 INTRODUCTION

In preparation of monalkyl sulphate, sulphation mechanisms may be divided into two classes, addition to alkenes and esterification of alcohols. Alkenes are principally obtained from petroleum while alcohols are often prepared by hydrogenation of fatty esters.

Regents useful for this purpose are:-

Sulphur trioxide	SO_3
Sulphuric acid	$H_2SO_4 = H_2O.SO_3$
Oleum	$H_2SO_4.nSO_3 = H_2O.(n+1)SO_3$
Chlorosulphuric acid	$ClSO_3H = HCl.SO_3$
Sulphamic acid	$H_2NSO_3H = NH_3.SO_3$

The sulphation of an alcohol involves replacement of the O-H bond with an O-S bond (21)

$$R\text{-}OH + H_2SO_4 \longrightarrow RO\text{-}SO_3H + H_2O$$

(MASA)

while the second class of mechanism (addition to alkenes) can be written written as follows:-

$$R\text{-}CH = CH_2 + H_2SO_4 \longrightarrow R\text{-}\overset{\overset{CH_3}{|}}{CH}\text{-}O\text{-}SO_3H$$

(MASA)

In this chapter attention will be focussed on the second class of reaction. Reaction mechanisms and probable side reactions will be discussed.

5.2 REACTION MECHANISM AND KINETICS

The detailed general mechanism of sulphation of olefins using concentrated sulphuric acid is not clear. However, it is believed that an equilibrium formation of a protonated π-complex

followed by a rate-determining transformation to the carbonium ion (22). That is

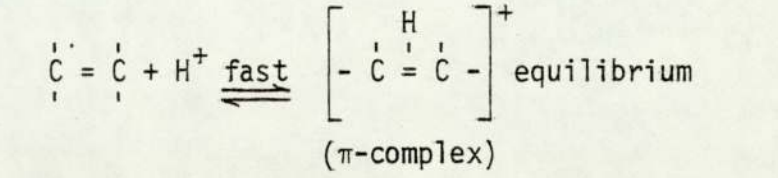

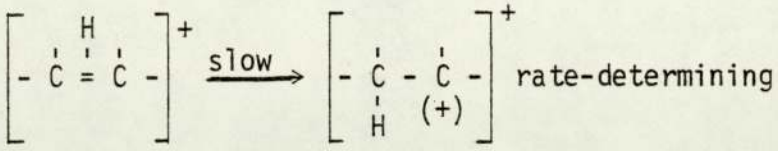

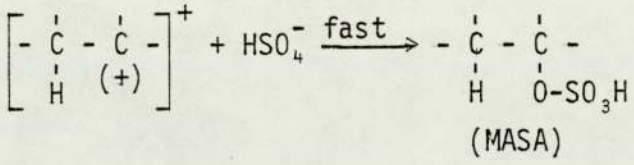

To obtain the "active" sodium mono (sec-alkyl) sulphate (SALS), the monoalkyl sulphuric acid is neutralized with sodium hydroxide

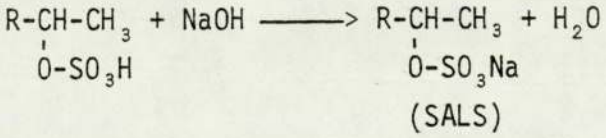

Also it has been reported that dialkyl sulphates are produced after the formation of (MASA). There is no clear mechanistic evidence which explains the formation of these neutral esters. However, it is believed that they may be formed in accordance with the following reaction schemes (23):-

i) 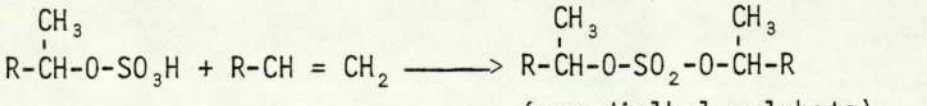

ii) $$2R\text{-}\underset{\displaystyle CH_3}{\underset{|}{CH}}\text{-}O\text{-}SO_3H \longrightarrow R\text{-}\underset{\displaystyle CH_3}{\underset{|}{CH}}\text{-}O\text{-}SO_2\text{-}O\text{-}\underset{\displaystyle CH_3}{\underset{|}{CH}}\text{-}R_2 + H_2SO_4$$

(sec-dialkyl sulphate)

It can be clearly seen that the disadvantage of these reactions is a loss of olefin. This difficulty is partly overcome by hydrolysis or saponification of the dialkyl sulphate in accordance with the following reaction scheme:-

$$R\text{-}\underset{\displaystyle CH_3}{\underset{|}{CH}}\text{-}O\text{-}SO_2\text{-}O\text{-}\underset{\displaystyle CH_3}{\underset{|}{CH}}\text{-}R + H_2O \xrightarrow{NaOH} R\text{-}\underset{\displaystyle CH_3}{\underset{|}{CH}}\text{-}O\text{-}SO_3Na + R\text{-}\underset{\displaystyle CH_3}{\underset{|}{CH}}\text{-}OH$$

(SALS)

However, this is clearly only a partial solution to the problem since the hydrolysis also results in the formation of one mole of secondary alcohol which means a loss of olefin.

It has also been reported (23) that (particularly with low concentrated sulphuric acid) alcohol is formed in a quantity greater than that expected from the hydrolysis of the sec-dialkyl sulphate. This extra quantity may be the result of the hydration of olefins during the sulphation reaction.

The previous studies (24, 25) reveal that the formation of polymer is another important side reaction which has to be reduced as much as possible to achieve a higher yield of monoalkyl sulphuric acid. The reaction between olefin and carbonium ions gives polymer in accordance with the following reaction (26):-

$$R^+ \xrightarrow{\text{C = C}} R\text{-}\underset{|}{C}\text{-}\underset{|}{C}^+ \xrightarrow{\text{C = C}} R\text{-}\underset{|}{C}\text{-}\underset{|}{C}\text{-}\underset{|}{C}\text{-}\underset{|}{C}^+ \xrightarrow{\text{C = C}} \text{polymer}$$

The reactions outlined above are the predominant steps in the process but a number of side reactions may also occur (27).

They are:-

i) With water to give the secondary alcohol (hydration)

ii) Oxidation

iii) Intermolecular 1:2 hydride shift (isomeriation)

iv) The formation of internal olefin

Isomer formation has been studied by several authors (48, 51, 52), since it is believed that secondary-alkyl sulphates with the sulphate ester group in the second position, or localised near the terminal position, have different physical and detergent properties from those isomers having the group located towards the middle of the chain. The experimental findings in the literature contradict each other. Baumgarten (51), adding 100% sulphuric acid at 0°C to dodecene-1 at an acid to olefin mole ratio of 2:1, found that only about 50% of the expected 2-sulphate was formed and the remainder consisted of a mixture of positional isomers with the sulphate group further down the chain. On the other hand, Clippinger (48) observed that, under similar conditions, with a sulphuric acid to olefin mole ratio of 0.5:1, all the isomeric alkyl sulphates were formed; whereas with a 2:1 acid/olefin ratio he found that nearly quantitative yields of the 2-sulphate resulted. Further work by Asinger (52) showed that alkyl sulphate-2 is preferentially formed in the sulphation reaction if excess olefin rather than excess acid is used. These results contradict those of Clippinger. Therefore, the understanding of isomer formation needs further investigation.

The possible reactions between concentrated sulphuric acid and α-olefins are summarized in figure (5.1).

Figure (5.1) shows the complexity of reactions. The kinetics of the formation of the products of olefin sulphation and the

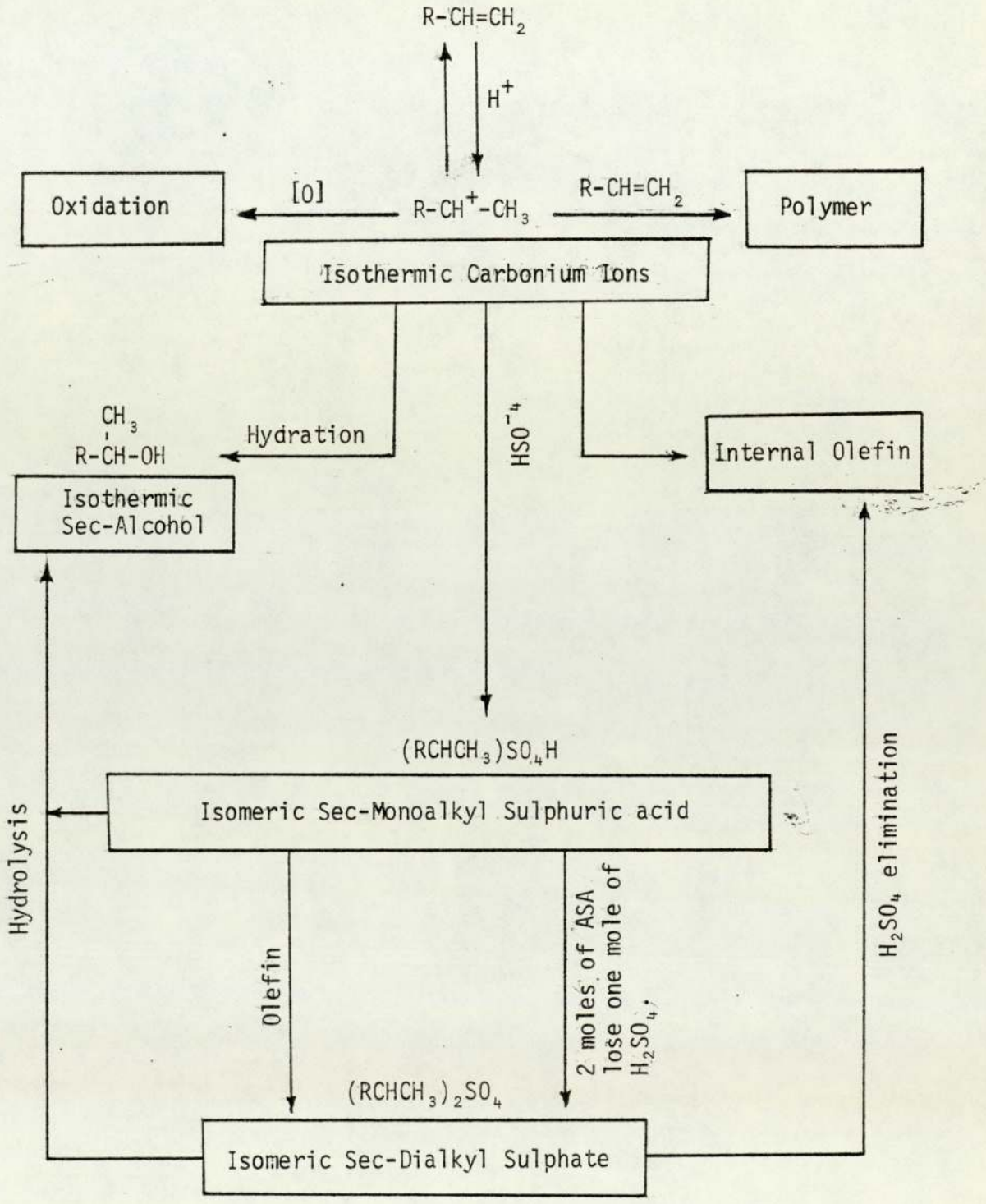

Figure 5.1 Sulphation of α-olefins using concentrated sulphuric acid. (Possible routes by which main and side products can be found.)

reaction mechanism which would explain and relate their formation to the operating parameters are not available in the published literature for those α-olefins with chain lengths of interest to the detergent industry (i.e. more than C_{12}). Some kinetic data and the reaction mechanism fitting these data are however available for the sulphation of non-detergent range α-olefins (i.e. C_6,C_7,C_8) (28,29).

A successful attempt was made by Butcher and Nickson (28) to utilise the concept of the acidity function to relate the rate constants for sulphation of an olefin for a particular chain length (C_6,C_7,C_8). Using this concept, the authors unsuccessfully attempted to extrapolate these data to olefins with longer chains.

5.3 EXPERIMENTAL PROGRAMME

5.3.1 Reactants

The α-olefin, utilized in this study was hexadecene-1 obtained from Unilever Research. The hexadecene-1 was chosen on the grounds of suitability and availability. That is to say, its carbon chain is within the range of lengths of particular interest to the detergent industry and it is also readily available as a petroleum product.

The concentration of sulphuric acid used in this research was 98% (w/w). A preliminary literature survey reveals that 98% (w/w) sulphuric acid is the best for sulphation of α-olefins to prepare detergents (25, 46). However, two samples were also obtained using 95% (w/w) sulphuric acid, because Kooijman (24) achieved the highest yield at the sulphuric acid concentration of 95% (w/w).

Samples obtained after sulphation reaction, were neutralized with 20% (w/w) sodium hydroxide solution.

5.3.2 Reaction Parameters and Flow Rate

Among the many reaction parameters, three were intensively investigated in this study. They are:-

a) Mixing (speed of rotation)

b) Residence time

c) Acid to olefin mole ratio

The effects of the other parameters on the formation of the different reaction products were well established in previous studies (25,28,46). On these grounds they were not investigated.

Predetermined values of residence time and acid/olefin mole ratio were obtained by monitoring the feed rates using rotameters. A list of flow rates of the reactants at the desired acid/olefin mole ratio is tabulated in Appendix (B3).

The reaction temperatures were checked by thermocouples fixed on the outer surface of the outer cylinder. Inlet and outlet temperatures were also recorded. Although it is believed that the reliability of these measured temperatures is questionable since thermocouples were not in direct contact with the reaction mixture.

Samples were obtained for each experiment by changing only one parameter at a time and keeping the others constant. Analysis of these samples enabled the investigation of the effect of a particular parameter on the formation of the different reaction products.

5.3.3 Preliminary Equipment Trials

The feed pumps, reactor and drive unit had already been checked during the flow characteristics and power consumption studies. To gain experience in start-up procedure and overall equipment

operation, runs were made with hot water as a substitute for the reactants in order to provide a heat load for the freon-12 refrigeration unit. For example, under the reaction conditions of 2 minutes residence time and with the acid/olefin mole ratio of 2:1, the flow rate of olefin and acid must be 1.088 and 0.412 litres per min. respectively. The heat of reaction is about 30 kcal. based on per mole olefin (1). Thus under these conditions 1.088 x 3.48 = 3.786 moles olefin take part in reaction per min. In other words 3.786 x 30 = 113.58 kcal energy will be generated within the annulus per minute, so that the refrigeration system must be capable of removing this energy from the reaction zone. This was checked by employing hot water instead of using the reactants.

To enable sampling and the monitoring of the individual items of equipment, as well as to operate safely, it was essential to have an assistant when operating the apparatus under reaction conditions to maintain pre-determined flow rates and note the required readings from the control panel.

It must be emphasised that care was taken during the shut-down operation to bring the temperature of the freon-12 in the cooling annulus up to ambient before removing the heat load. Otherwise, the liquid in the reactor may freeze causing considerable mechanical damage. Similarly the heat load must not be applied if the refrigeration unit was inoperative.

5.3.4 Reaction Procedure

The stock tanks were filled with their respective reactants and the reactor with acid, since acid was to be continuous phase. The reactants were cooled before entering the reactor by circulating the chilled water through the tanks. The air inside the reactor

was released via a small valve in the olefin feed pipe to make sure that the total volume of the reactor was utilised.

The reactor drive unit was rotated at the desired speed for the experiment, the olefin and acid flows were set to the pre-determined values and the refrigeration unit started. Conditions took several minutes to stabilise because the flow rates, in particular, were affected by the increased viscosity in the reactor. When a steady state had been reached the appropriate measurements were recorded (excitation current, temperatures, flow rate). The samples were taken from the reactor outlet. Sampling time interval was 3.5 times the mean residence time. The sample was immediately poured into a stainless steel pot containing an excess of chilled sodium hydroxide solution. The pot was placed in a bucket of ice and stirred vigorously with a flattened steel tube into which a thermocouple had been inserted. The maximum neutralisation temperature was also recorded.

Reactant's flow rates and speed of rotation were adjusted to new values and the procedure was repeated.

It was found that the temperature profile in the reactor as measured by the thermocouples was approximately the same irrespective of the operating conditions. However, at low flow rates of the reactants, the energy generated in the reactor was too small to keep the reaction temperature constant at approximately 15°C, so that in these experiments the refrigerant system was operated discontinuously. The high temperature occurring at the top of the reactor (average 32°C) is believed to be due to poor contact between refrigerant and reaction zone. The average temperature at the reactor outlet was about 10°C. However, from the measurements

recorded it is evident that the method used is not sufficiently sensitive to control the temperature within the desired range since thermocouples are not in direct contact with the reaction mixture.

5.4 CHEMICAL ANALYSIS

The samples obtained at the different reaction conditions were analysed to establish a relationship between the reaction parameters and the conversion of olefin to the products. The analysed quantities were:-

i) NDOM (non-detergent organic matters)

ii) AD (Active detergent)

iii) Olefin

iv) Secondary alcohol

v) Polymer

The method used to analyse the non-detergent organic matters and active detergent were obtained from Unilever Research Laboratory. The analysis of olefin and secondary alcohol was carried out using GLC method. Finally, the amount of polymer was found from a material balance.

The author is most grateful to Unilever Research for providing training in their laboratories so that he would be more confident of the analytical techniques.

5.4.1 Determination of the Non-Detergent Organic Matter (NDOM)

Non-detergent organic matter consisting principally of unreacted hydrocarbons, alcohols and polymer was extracted with petroleum spirit from an aqueous/alcohol medium. The method is as follows:-

Approximately 10 gms of sample was accurately weighed and placed in a 250 ml beaker. Then it was dissolved in 100 mls of

50% industrial methylated spirit (IMS) by warming in a water bath. The dissolved sample was then transferred to a 500 ml separatory funnel containing 100 mls of petroleum ether (40° - 60°C boiling range). After shaking gently it was left to settle for about 10 minutes and then the bottom layer was separated from the petroleum ether phase and transferred into the second separating funnel containing 75 mls of petroleum ether. The same procedure was repeated once more in the third separating funnel. Then all the petroleum ether phase was collected in the first funnel and poured into a tared flask containing anti-bubling granule and subsequently evaporated in the water bath. Five mls of dry acetone were added and the liquid was subjected to a gentle stream of air until no odour of acetone could be detected. Then the flask was placed in a desiccator for about 15 minutes so that the water-free non-detergent organic matter could be obtained by weighing.

The percentage of the non-detergent organic matter in the reaction mixture after neutralization was estimated by the following calculation:-

$$\% \text{ (NDOM)} = \frac{w_2 \times 100}{w_1}$$

where w_1 is the weight or original sample and w_2 the weight of NDOM.

5.4.2 Determination of the Active Detergent

An aqueous solution of the sample was titrated with a standard cationic active solution (Hyamine 1622) in a two phase water-chloroform system using a mixture of a cationic dye (dimidium bromide) and an anionic dye (disulphone blue V) as indicator. The anionic surfactant forms a salt with cationic dye which dissolves in the chloroform layer and colours it red-pink. The end point

was observed when the hyamine cation displaces the dimidium cation from chloroform soluble salt and pink colour leaves the chloroform layer as the dye passes to the aqueous phase. Hyamine added in excess forms a salt with the anionic dye disulphone blue V which dissolves in the chloroform layer and colours it blue.

Hyamine 1622 solution (0.004M) and mixed indicator stock solution were obtained from Unilever Research Laboratory. Acid indicator solution was prepared from the mixed indicator stock solution (200 mls water and 20 mls mixed indicator stock solution were mixed in a 500 ml graduated flask. After adding 20 mls 5N sulphuric acid the mixture was diluted with distilled water to 500 ml. Then it was stored in an amber bottle).

The procedure is as follows:-

Approximately 10 gms of sample were weighed and placed in a 250 ml beaker. Then the sample was dissolved in 150 mls of distilled water by warming in a water bath. This dissolved sample was transferred to a 1000 ml graduated flask and diluted up to the level with distilled water. Then 10 mls. of this solution was transferred to a 100 ml titration vessel with stopper. After adding 10 mls of acid indicator solution and 15 mls of chloroform the mixture was titrated with 0.004M Hyamine 1622 solution until a blue colour was obtained in the chloroform phase. The titration was performed by shaking the titration vessel vigorously each time after adding 0.5 ml of hyamine 1622 solution.

The calculation to find the percentage of active detergent was made as follows:-

Let: Weight (gm) of the sample W

Molarity of Hyamine 1622 solution M

Molecular weight of anionic-active matter MW

Volume (ml) of Hyamine 1622 used for titration V

Then: $$\text{Anionic-active matter (\%)} = \frac{10 \times V \times MW \times M}{W}$$

where the values of M and MW are known (0.004, 344.5 respectively). Thus % AD becomes,

$$\% \text{ AD} = \frac{13.78 \times V}{W}$$

5.4.3 Determination of Olefin, Secondary Alcohol and Polymer

It is believed that non-detergent organic matter consists of olefin (unreacted or formed during the sulphation reaction), secondary alcohol (formed after hydrolysis of dialkyl sulphate) and polymer. It is also assumed that the formation of secondary alcohol due to hydration of carbonium ion is negligible. At low acid concentrations it cannot be neglected, since acid at low concentrations contains more water.

The non-detergent organic matter extracted (described in Section 5.4.1) was redissolved in 100 mls of petroleum ether and analysed using the GLC method. To prepare a standard solution, the required secondary alcohol (2-Hexadecanol) was obtained from Aldrich Chemical Co. Ltd. The analysis of olefin and secondary alcohol was performed under the following conditions using a PYE Unicam series 204 chromatograph.

Column	10% SE 30 ON DIATOMITE C
Gas flowrate	40 mls/min
Maximum operating temperature	250°C
Detector temperature	300°C
Injector temperature	300°C
Range of recorder	20 mm V FSD
Range and attenuation of FID	32 x 10

The amount of olefin and secondary alcohol was found from the graph obtained using the results of the standard solutions. The amount of polymer was also calculated from the mass balance equation; that is:-

Polymer = NDOM - (olefin + secondary alcohol)

The percentage of each species was obtained as follows:-

$$\%(\text{Species}) = \frac{\text{the amount of species}}{\text{the original weight of sample}} \times 100$$

5.5 DETERMINATION OF CONVERSION OF OLEFIN TO THE REACTION PRODUCTS

After hydrolysis of the dialkyl sulphate which preceded neutralisation of the reaction mixture the olefin will be in the form of monoalkyl sulphate, secondary alcohol, polymer and free olefin. Therefore the total number of mole olefin can be expressed by:-

$$M_{total} = \frac{\%\ AD}{344.5} + \frac{\%\ Alcohol}{242.44} + \frac{\%\ Polymer + \%\ Olefin}{224.44}$$

where 344.5, 242.44, and 224.44 are the molecular weights of the sodium monalkyl sulphate, 2-hexadecanol and hexadecene-1 respectively.

The conversion of olefin to the reaction products was calculated as follows:-

i) To total monoalkyl sulphate (after hydrolysis of dialkyl sulfate)

$$X_{TMAS} = \frac{\frac{\%\ AD}{344.5}}{M_{total}}$$

ii) To polymer

$$X_{p} = \frac{\frac{\%\ Polymer}{224.44}}{M_{total}}$$

iii) To dialkyl sulphate

$$X_{DAS} = \frac{2X\ \frac{\%\ Alcohol}{242.44}}{M_{total}}$$

Assuming that the total amount of the secondary alcohol formed as a result of hydrolysis of the dialkyl sulphate. In fact, some of it formed during the sulphation reaction by hydration of the carbonium ion. However, this can be neglected at high (98% w/w) acid concentrations.

iv) To monoalkyl sulphuric acid

$$X_{MAS} = \frac{\frac{\%\ AD}{344.5} - \frac{\%\ Alcohol}{242.44}}{M_{total}}$$

v) Free olefin

$$X_O = \frac{\frac{\%\ \text{olefin}}{224.44}}{M_{total}}$$

The results of these calculations are tabulated in Appendix B4.

The conversion of olefin to total monoalkyl sulphate for some of the samples, was approximated by:-

$$X_{TMAS} = \frac{\frac{\%\ AD}{344.5}}{\frac{\%\ AD}{344.5} + \frac{\%\ NDOM}{224.44}}$$

where the error is not greater than (-1%).

CHAPTER 6

MATHEMATICAL MODEL OF THE REACTOR

6.1 INTRODUCTION

From the study of residence time distributions it was concluded that the reactor consists of two parallel plug-flow reactors. These have been named "inner" and "outer" branch and their volumes were found to be one and two litres respectively. The study of residence time distributionshas also revealed that the fraction of volumetric feed to each branch is 0.5 (f=0.5), so that the reactor model is illustrated in figure (6.1)

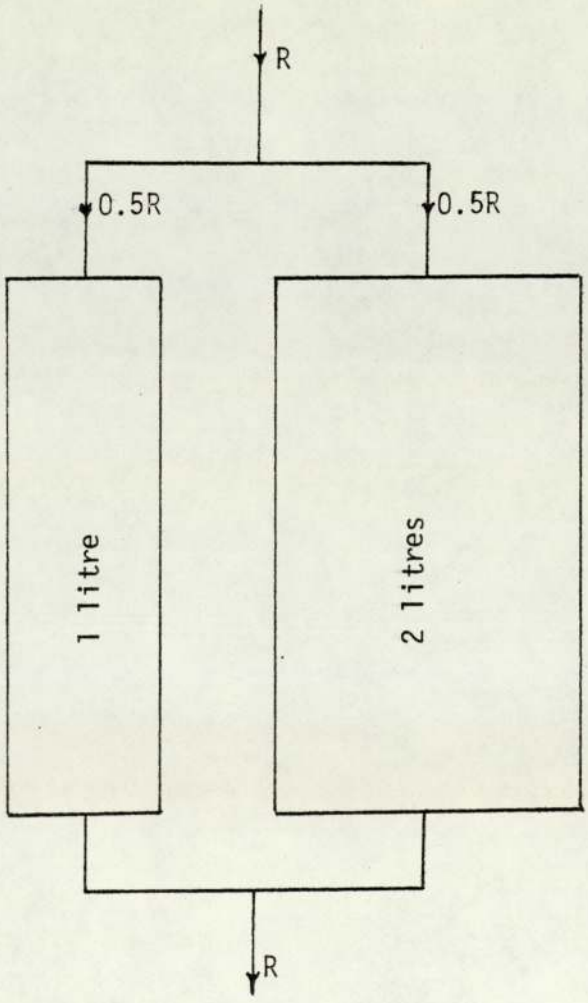

Figure 6.1 Reactor model (Two parallel plug-flow reactor.)

In this study, the dispersed phase was olefin (C_{16} chain α-olefin) and the continuous phase 98% (w/w) sulphuric acid. The reason for choosing olefin as the dispersed phase is the solubility of the reaction products in the continuous (acid) phase. Since the products are soluble in the acid phase but not in the dispersed phase the dispersed phase remains as pure olefin and reduces the diffusional resistance within the droplets (30). The effect of the products on the diffusional mass transfer in the continuous phase is relatively small.

To develop a mathematical model for the reactor, several assumptions have been made. These are:-

i) It is known from Section (6.2) that the droplets are very small (diameters are smaller than 0.5 mm) so that circulations within the droplets are negligible. Thus, the droplets may be regarded as rigid solid particles (31). From this it can be concluded that the dispersed phase (olefin) droplets are surrounded by a liquid film and chemical reactions take place on the surface of the droplets. This implies that the acid molecules have to travel through the film to reach the droplet surface (32). The reaction scheme is shown in figure (6.2).

ii) The chemical reaction is very fast compared with the mass transfer from the acid to the droplets. This means that the reaction rate is controlled by the mass transfer rate rather than by the rate of chemical reaction. In the literature, this type of reaction is known as a film controlled reaction. This assumption is based on the fact that highly exothermic reactions are also very fast and mass diffusion very slow in viscous media (the viscosity of the reaction mixture is as high as $\sim$ 350 cP). However, this

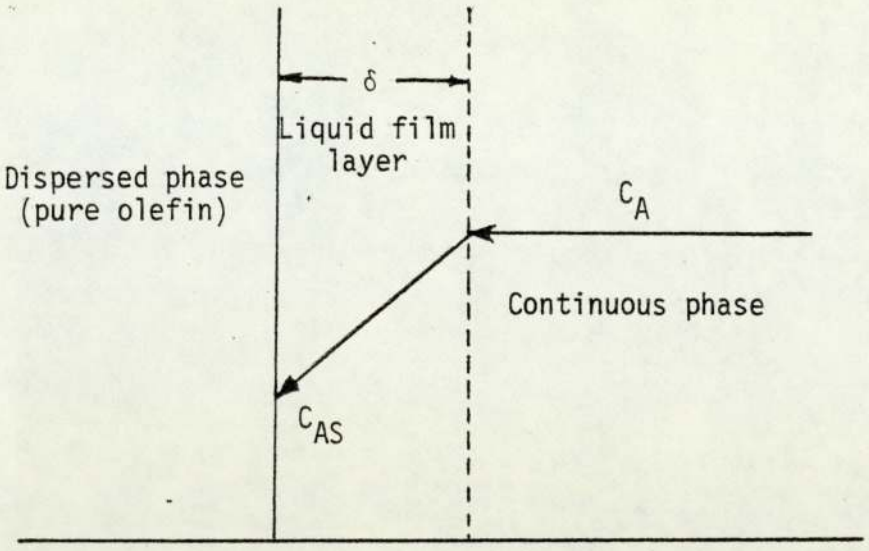

Figure 6.2 Reaction scheme

should be investigated in future work to show whether the reaction rate is very sensitive to variations in temperature. Generally, the rate constants of chemical reactions are far more temperature dependent than the mass transfer coefficients (Arrhenius' law, $k = k_0 \exp(-E/RT)$). The present apparatus is not suitable for such a study.

iii) The formation of by-products at the droplet surface is negligible compared to the formation of monalkyl sulphuric acid.

iv) Olefin entering the reactor forms droplets instantaneously.

Thus a mathematical model can be established, based on the above assumptions. For this purpose the initial size of the droplets is required.

6.2 DROP SIZE

As the reaction progresses the size of the droplets gets smaller and inevitably the droplets will eventually disappear. As a result of this phenomenon the volumetric fraction of the continuous phase increases while that of the dispersed phase decreases.

The volumetric increment in the continuous phase is equal to the volumetric reduction in the dispersed phase because it was assumed that volume changes due to the liquid - liquid reactions are negligible.

Although the drop size is not constant it is possible to calculate its initial size using one of the correlation formulas from the literature.

It has long been established that mechanical energy supplied at a sufficient rate to a mixture of two liquids of mutually limited solubility causes one of the phases (usually that in the smaller amount) to disperse in droplet form within the other, the continuous phase. It is possible, however, to obtain a heterogeneous mixture in which the dispersed phase is greater than 70% of the total volume (33). This is achieved by introducing the dispersed phase reactant after filling the reactor with the continuous phase reactant.

Droplets in an agitated vessel cannot exceed a certain size, because the fluid circulation within the drop increases as its size increases and this liquid motion exerts pressure on the interfacial surface. There is also a shear force caused by the liquid motion outside the droplets. As the droplets size increase, the intensity of these forces also increases and the droplets break-up. The maximum drop size at which droplet break-up occurs has been investigated by many research workers (34,35,36). Because of its extreme complexity it is very difficult to obtain a theoretical model from which drop size can be predicted. All available drop size correlations in agitated systems are of a semi-empirical nature. However, their common conclusion is that the critical drop size mainly depends on the properties of the two liquids (density, interfacial tension, viscosity) and the rate of energy supply.

Kolmogoroff (37) investigated droplet break-up phenomena in great detail and proposed an expression for the maximum drop diameter. His equation is based on a theoretical analysis given by:-

$$\frac{\phi_{max}}{2} = \sqrt{2}\left(\frac{\sigma}{k_f \rho_c}\right)^{3/5} \varepsilon^{-2/5} \qquad (6.1)$$

in which k_f = 0.5 (Kolmogoroff dimensionless constant).

Later Baird (38) and McManamey (39) showed that droplets in agitated vessels have smaller diameters than those predicted by equation (6.1).

In his early work Clay (34) investigated droplet break-up phenomena within the rotating cylinders. Later Hinze (35) using Clay's date proposed the following semi-empirical equation:-

$$\phi_{max} = K\left(\frac{\sigma}{\rho_c}\right)^{3/5} \varepsilon^{-2/5} \qquad (6.2)$$

where K is a dimensionless constant and its value, given by Hinze, is 0.725. J. Kubie and Gardner (36) subsequently found a similar value for the constant K.

In the present work Hinze's expression was chosen to determine the initial drop size since his correlation is based on data obtained with rotating cylinders. A modified form of equation (6.2) is illustrated in figure (6.3).

From the study of the power requirement of votator, it was found that power consumption can be expressed in terms of the viscosity of the working liquid and the rotation of the inner cylinder. It is given in Section (4.4) by expression (4.33)

$$P = 34.44\ N^{1.93}\ \mu^{0.61} + 34.88\ N \qquad (4.33)$$

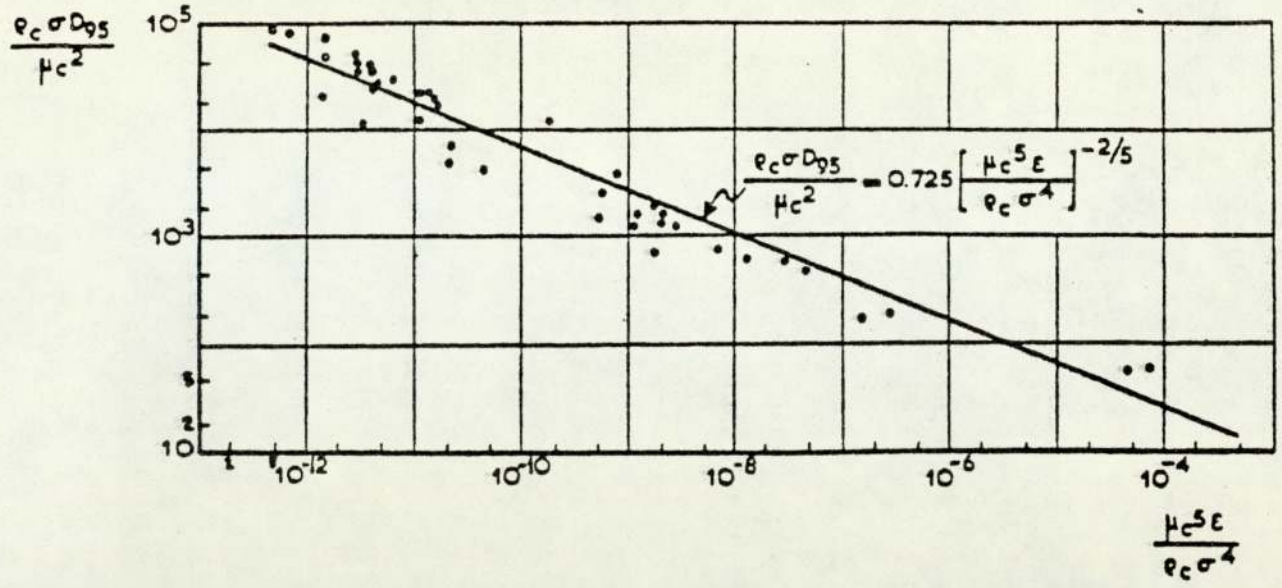

Figure 6.3 Maximum drop size as a function of the energy input according to experimental data by Clay, where D_{95} is maximum drop diameter.

The second term of expression (4.33) is the frictional loss by the scraping action of the blades against the wall together with the other losses caused by mechanical frictions (bearing, mechanical seals etc.). Thus, the second term of the equation has no effect on the determination of drop size. The energy responsible for droplet break-up is the first term of equation (4.33). That is

$$P' = 34.44\ N^{1.93}\ \mu^{0.61} \qquad (6.3)$$

The average density of the reaction mixture is 1070 kg m^{-3} (the molar ratio of acid to olefin is 2:1). Therefore, the total mass in the reactor is $1070 \times 3 \times 10^{-3} = 3.21$ kg. The viscosity of acid (continuous phase) at the reaction temperature of 15°C is 0.036 kg m^{-1} sec^{-1}. (μ=0.036 kg m^{-1} s^{-1}) assuming that initially the continuous phase consists of pure acid, otherwise the viscosity of sulphuric acid containing monalkyl sulphuric acid is much higher. N in equation (6.3) is the revolution of the inner cylinder per second. Putting this value into equation (6.3) and dividing by the total mass

in the reactor, the energy dissipation per unit mass can be obtained:-

$$\varepsilon = 1.413\ N^{1.93}\ W/kg \qquad (6.4)$$

σ (interfacial tension) can be roughly approximated by taking the difference between the surface tension of acid and olefin (40). The surface tension of 98% (w/w) sulphuric acid is given approximately as 0.050 Nm^{-1} (41) and the surface tension of olefin is 0.025 Nm^{-1} (experimentally determined). Thus:-

$$\sigma = \sigma_{acid} - \sigma_{olefin} = 0.050 - 0.025 = 0.025\ Nm^{-1}$$

ρ_c (density of 98% (w/w) sulphuric acid) is 1840 kg m^{-3}. Replacing these values in equation (6.2) the initial diameter of the droplets becomes:-

$$\phi_0 = 7.59 \times 10^{-4}\ N^{-0.77} m$$

The initial diameters of the droplets are tabulated in table (6.1)

N(r.p.s)	ϕ_0(m)
4.17	2.53×10^{-4}
8.33	1.48×10^{-4}
16.67	0.87×10^{-4}

Table 6.1 The Initial Diameters of Droplets for Different Speed of Rotation of the Inner Cylinder.

6.3 COALESCENCE OF THE DROPLETS

The forces responsible for coalescence of the droplets are:-

i) The centrifugal force - trying to move the drop towards the outer stationary cylinder.

ii) The drag force - trying to oppose the movement of the drop towards the outer cylinder.

If the centrifugal force is greater than the drag force, coalescence will occur at the region near the outer cylinder. Otherwise, the separation of phases will not be possible and the drop should follow the flow pattern within the annulus.

These forces were calculated on a drop in two places, one in the middle of the inner section ($r = 5.82 \times 10^{-2}$m) and the other in the middle of the reverse flow section ($r = 6.62 \times 10^{-2}$m).

The centrifugal and drag forces acting on a drop of diameter ϕ are given by the following equations (45)

$$F_C = \frac{\pi\phi^3(\rho_s - \rho_c)}{6} \frac{V_\theta^2}{r} \qquad (6.5)$$

$$F_D = \frac{\pi\phi^2 \rho_c V_\theta^2}{8} \times C \quad \text{respectively} \qquad (6.6)$$

where ρ_s and ρ_c are the density of the drop and continuous phase respectively. C is the drag coefficient which is given in reference (53) as a function of the drop Reynolds number.

These two forces are in opposite directions. The resultant force on a drop is:-

$$F_R = F_C - F_D \qquad (6.7)$$

The other terms involving the calculation of the centrifugal and drag forces are:-

i) $$V_\theta = V_i \left(715.34r \ln r + 1584.91r + \frac{1.545}{r}\right) \qquad (3.4)$$

where $V_i = 2\pi N r_i$

ii) Drop Reynolds number $(N_{Re_\phi}) = \frac{\phi V_\theta \rho_c}{\mu_c}$

iii) Drag Coefficient $(C) = \frac{24}{N_{Re_\phi}}$ for $N_{Re_\phi} < 0.3$

$$C = \frac{18.5}{N_{Re_\phi}^{0.6}} \quad \text{for } 0.3 < N_{Re_\phi} < 1000$$

$$C = 0.44 \quad \text{for } 1000 < N_{Re_\phi} < 200{,}000$$

(These values of drag coefficient were obtained from Perry's Handbook 5th edition P 5.61).

The calculated values are tabulated in table (6.2)

N (r.p.s)	ϕ(m)	r(m)	V_θ (ms^{-1})	N_{Re_ϕ}	C	F_C(N)	F_D(N)	F_R(N)
4.17	2.53×10^{-4}	5.82×10^{-2}	0.568	7.35	5.59	-4.98×10^{-8}	8.34×10^{-5}	-8.34×10^{-5}
		6.62×10^{-2}	-0.457	5.91	6.37	-2.83×10^{-8}	6.15×10^{-5}	-6.15×10^{-5}
8.33	1.48×10^{-4}	5.82×10^{-2}	1.134	8.58	5.09	-3.95×10^{-8}	1.04×10^{-4}	-1.04×10^{-4}
		6.62×10^{-2}	-0.914	6.91	5.80	-2.26×10^{-8}	7.67×10^{-5}	-7.67×10^{-5}
16.67	0.87×10^{-4}	5.82×10^{-2}	2.268	10.08	4.62	-3.23×10^{-8}	1.30×10^{-4}	-1.30×10^{-4}
		6.62×10^{-2}	-1.828	8.13	5.26	-1.84×10^{-8}	9.61×10^{-5}	-9.61×10^{-5}

Table 6.2 The centrifugal and drag forces acting on a drop at the different conditions.

It can be seen from the table (6.2) that, the resultant force (F_R) is negative under any circumstances. This shows that the force acting against the centrifugal force is greater. This should prevent the separation of the phases and the drop should follow the flow

pattern within the annulus (see figure 3.1).

These calculations hold only for the laminar flow regime, because in this case, the velocity profile is known. It has also been assumed that the centrifugal force is smaller than the drag force, in the unstable flow regime, since $\rho_c > \rho_s$.

6.4 RATE EXPRESSION FOR THE REACTOR

Under the assumption that chemical reaction is faster than diffusion, there will be no acid molecules at the surface of the droplets, because at the surface acid consumption is greater than its supply. This is illustrated in figure (6.2). Therefore, the reaction rate can be expressed as follows:-

$$-\frac{1}{S}\frac{dn}{dt} = -\frac{1}{\pi\phi^2}\frac{dn_0}{dt} = k_c\,(C_A - C_{AS}) \qquad (6.8)$$

where C_{AS} is the acid concentration at the surface of the droplets and as has already been mentioned its value is zero. Thus, the rate expression becomes:-

$$-\frac{1}{\pi\phi^2}\frac{dn_0}{dt} = k_c\,C_A \qquad (6.9)$$

n_0 (the molecular number of olefin) can be expressed in terms of the droplet diameter.

$n_0 = \rho_0 V \;\therefore\; dn_0 = \rho_0 dV$ and leads to

$$dn_0 = \rho_0 \frac{\pi}{2}\phi^2\, d\phi \qquad (6.10)$$

Combining this equation with the expression (6.9), the reaction rate becomes:-

$$-\frac{d\phi}{dt} = \frac{2k_c}{\rho_0}\,C_A \qquad (6.11)$$

To solve this differential equation C_A must also be written in terms of the droplet diameter. For this purpose the following approach can be followed (see figure 6.4).

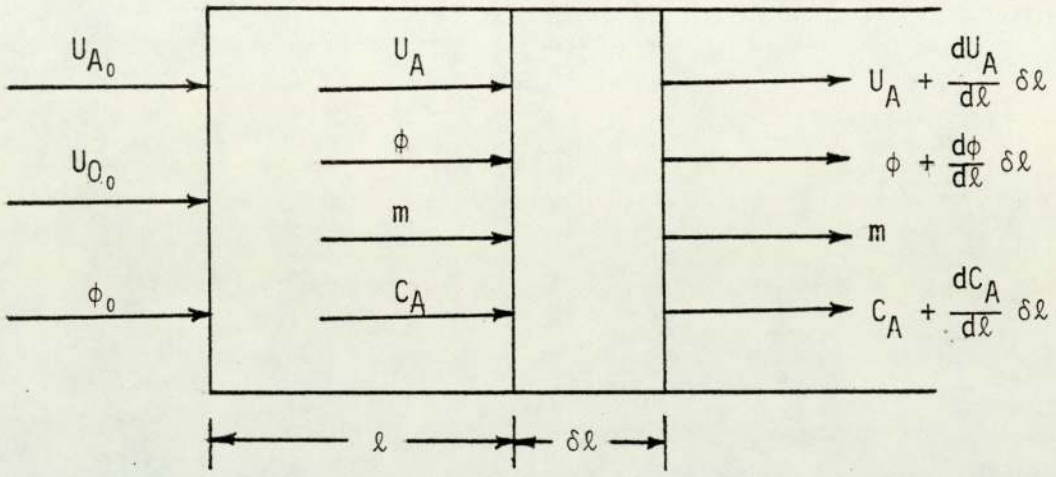

Figure 6.4 Plug-flow reactor with heterogeneous reaction.

Volume of the element = $A\delta\ell$

Number of droplets within the element = $\frac{mA\delta\ell}{U_{O_0} + U_{A_0}}$

Volume of the dispersed phase = $\frac{mA\delta\ell}{U_{O_0} + U_{A_0}} \frac{\pi}{6} \left(\phi^3 + \frac{3}{2}\phi^2 \frac{d\phi}{d\ell}\delta\ell\right)$

Acid concentration in the continuous phase = $C_A + \frac{1}{2}\frac{dC_A}{d\ell}\delta\ell$

Reaction rate = $-\frac{1}{S}\frac{dn_o}{dt} = k_c C_A$.

Mass balance of acid over the element:-

Input = $U_A C_A$

$$\text{Output} = \left(U_A + \frac{dU_A}{d\ell}\,\delta\ell\right)\left(C_A + \frac{dC_A}{d\ell}\,\delta\ell\right)$$

Disappearance by chemical reaction = $k_c S C_A$ =

$$\frac{k_c m A \delta\ell}{U_{O_0} + U_{A_0}}\,\pi\left(\phi^2 + \phi\,\frac{d\phi}{d\ell}\,\delta\ell\right)\left(C_A + \frac{1}{2}\,\frac{dC_A}{d\ell}\,\delta\ell\right)$$

Using the unsteady-state mass balance equation, that is,

input = output + disappearance by reaction

and making the necessary simplifications (and ignoring terms involving powers of $\delta\ell$ higher than 1) one obtains:-

$$\frac{d}{d\ell}\left(U_A C_A\right) = -\frac{\pi k_c m A \phi^2 C_A}{U_{O_0} + U_{A_0}}$$

where $U_A C_A = F_A$ and therefore

$$\frac{dF_A}{d\ell} = -\frac{\pi k_c m A \phi^2 C_A}{U_{O_0} + U_{A_0}} \qquad (6.12)$$

Mass balance of olefin over the element:-

$$\text{Input} = m\,\frac{\pi}{6}\,\rho_0 \phi^3$$

$$\text{Output} = m\,\frac{\pi}{6}\,\rho_0\left(\phi^3 + 3\phi^2\,\frac{d\phi}{d\ell}\,\delta\ell\right)$$

Disappearance by chemical reaction is the same as that of acid, that is:-

$$\frac{\pi k_c m A \phi^2 C_A}{U_{O_0} + U_{A_0}}\,\delta\ell$$

Applying the mass balance over the element one obtains:-

$$\frac{d\phi}{d\ell} = - \frac{2k_c A C_A}{\rho_0 \left[U_{O_0} + U_{A_0}\right]} \tag{6.13}$$

From equation (6.12) and (6.13), the following equation was obtained

$$\frac{dF_A}{d\phi} = \frac{\pi \rho_0 m \phi^2}{2} \tag{6.14}$$

The solution of equation (6.14) with the initial values of $F_A = F_{A_0}$ and $\phi = \phi_0$ gives:-

$$F_A = F_{A_0} - \frac{\pi \rho_0 m}{6} \left(\phi_0^3 - \phi^3\right) \tag{6.15}$$

where $\frac{\pi \rho_0 m}{6} \phi_0^3 = F_{O_0}$. Therefore equation (6.15) becomes

$$F_A = F_{A_0} - F_{O_0} + \frac{\pi \rho_0 m}{6} \phi^3 \tag{6.16}$$

The variation of the volume of continuous phase can also be calculated as follows:-

$$\text{Input} = U_A$$

$$\text{Output} = U_A + \frac{dU_A}{d\ell} \delta\ell$$

$$\text{Generation within the element} = m \frac{\pi}{6} \phi^3 - m \frac{\pi}{6} \left(\phi^3 + 3\phi^2 \frac{d\phi}{d\ell} \delta\ell\right)$$

$$= - m \frac{\pi}{2} \phi^2 \frac{d\phi}{d\ell} \delta\ell$$

From the unsteady-state mass balance equation, that is

$$\text{Input} + \text{Generation} = \text{Output}$$

one obtains

$$\frac{dU_A}{d\phi} = - \frac{m\pi}{2} \phi^2 \tag{6.17}$$

The solution of equation (6.17) with the initial values of $U_A = U_{A_0}$ and $\phi = \phi_0$ gives:-

$$U_A = U_{A_0} + \frac{m\pi}{6} (\phi_0^3 - \phi^3) \tag{6.18}$$

where $\frac{m\pi}{6} \phi_0^3 = U_{O_0}$, and thus equation (6.18) becomes

$$U_A = U_{A_0} + U_{O_0} - \frac{m\pi}{6} \phi^3 \tag{6.19}$$

From equations (6.16) and (6.19) the acid concentration in the continuous phase can be found as follows:-

$$C_A = \frac{F_A}{U_A} = \frac{F_{A_0} - F_{O_0} + \frac{m\pi\rho_0}{6} \phi^3}{U_{A_0} + U_{O_0} - \frac{m\pi}{6} \phi^3} \tag{6.20}$$

Inserting C_A from equation (6.20) into equation (6.13) the following equation can be obtained:-

$$\frac{d\phi}{d\ell} = - \frac{2k_c A}{\rho_0 (U_{A_0} + U_{O_0})} \frac{F_{A_0} - F_{O_0} + \frac{m\pi\rho_0}{6} \phi^3}{U_{A_0} + U_{O_0} - \frac{m\pi}{6} \phi^3} \tag{6.21}$$

The analytical solution of equation (6.21) is possible, but before doing this the drop size at which the olefin becomes soluble must be found. Work in the chemical process Section (1) showed that olefin is completely soluble in sulphuric acid when the monoalkyl sulphuric acid mole fraction reaches 0.20. It is also known that one molecule of olefin reacts with one molecule of sulphuric acid and produces one molecule of monoalkyl sulphuric acid. From this, the following calculation can be made:-

$$M = F_{O_0} - F_O \; ; \quad F_A = F_{A_0} - M$$

$$X_M = \frac{M}{M + F_A} = \frac{F_{O_0} - F_O}{F_{A_0}} \qquad (6.22)$$

where $\frac{F_{A_0}}{F_{O_0}} = p$ (Initial mole ratio of acid to olefin), therefore

equation (6.22) becomes:-

$$X_M = \frac{1 - \frac{F_O}{F_{O_0}}}{p} \qquad (6.23)$$

Since it is known that the olefin is soluble in continuous phase when $X_M = 0.20$, so then

$$\frac{F_O}{F_{O_0}} = \frac{m\rho_0 \frac{\pi}{6} \phi^3}{m\rho_0 \frac{\pi}{6} \phi_0^3} = 1 - 0.2p$$

and finally

$$\phi = \phi_0 \, (1\text{-}0.2p)^{1/3} \qquad (6.24)$$

Equation (6.24) means that when $\phi = \phi_0 \, (1\text{-}0.2p)^{1/3}$ the olefin becomes soluble in the continuous phase and the drops disappear. From this point onwards the reaction takes place in a homogeneous medium.

To find the length of the reactor at which the reaction becomes homogeneous, equation (6.21) has to be integrated between ϕ_0 and $\phi_0 \, (1\text{-}0.2p)^{1/3}$. It is known that the reactor consists of two parallel plug-flow reactors and the feed fraction to each branch is 0.5, (see Section 3.3.4). Therefore, ℓ, has to be calculated separately for the inner and outer branches.

i) Inner Section;

$$\frac{d\phi}{d\ell} = - \frac{2k_c A_{inner}}{\rho_0 \left(\frac{U_{A_0} + U_{O_0}}{2} \right)} \; \frac{\frac{F_{A_0} - F_{O_0}}{2} + \frac{m\pi\rho_0}{12} \phi^3}{\frac{U_{A_0} + U_{O_0}}{2} - \frac{m\pi}{12} \phi^3} \qquad (6.25)$$

Replacing m by $\frac{6U_{O_0}}{\pi\phi_0^3}$ and making the necessary simplifications

equation (6.25) becomes:-

$$\frac{d\phi}{d\ell} = -\frac{4k_c A_{inner}}{\rho_0\left(U_{A_0}+U_{O_0}\right)} \frac{\phi_0^3\left(F_{A_0}-F_{O_0}\right) + \rho_0 U_{O_0}\,\phi^3}{\phi_0^3\left(U_{A_0}+U_{O_0}\right) - U_{O_0}\,\phi^3} \qquad (6.26)$$

The final solution of equation (6.26) is

$$\ell = \frac{Q}{6S^2} \ln \frac{(S+\phi_0)^3(S^3+\phi^3)}{(S^3+\phi_0^3)(S+\phi)^3} + \frac{Q}{S^2\sqrt{3}}\left[\tan^{-1}\frac{2\phi_0-S}{S\sqrt{3}} - \tan^{-1}\frac{2\phi-S}{S\sqrt{3}}\right] - T(\phi_0-\phi) \qquad (6.27)$$

where $\phi = \phi_0\,(1-0.2p)^{1/3}$

$$Q = \frac{\phi_0^3\,\rho_0\left(U_{A_0}+U_{O_0}\right)^2 + \phi_0^3\left(F_{A_0}-F_{O_0}\right)\left(U_{A_0}+U_{O_0}\right)}{4k_c A_{inner}\rho_0 U_{O_0}}$$

$$S = \phi_0\left[\frac{\left(F_{A_0}-F_{O_0}\right)}{\rho_0 U_{O_0}}\right]^{1/3}$$

$$T = \frac{U_{A_0} + U_{O_0}}{4k_c A_{inner}}$$

ii) Outer Branch;

To find ℓ for the outer branch, expression (6.27) can be used, replacing A_{inner} by A_{outer} which can be calculated from the reactor dimensions. The calculated values of A_{inner} and A_{outer} are 19.36 cm^2 and 44.06 cm^2 respectively. The full solution of equation (6.26) is available in Appendix A3.

6.4.1 Determination of Mass Transfer Coefficient (k_c)

In equation (6.27) k_c is the only unknown. Numerous experiments have already been performed to investigate mass transfer coefficients for particles suspended in agitated vessels. Among them Hales' (42) graphical correlation has been recommended by many authors (43, 44). Later Levins and Glastonbury (44) reported similar results. Hales showed the mass transfer coefficient to be a function of energy dissipation per unit mass in the vessel (see figure 6.5).

Hales' graphical presentation in figure (6.5) is based on the c.g.s unit system so the same unit system will be used here. Correlation can be expressed as follows:-

$$\frac{k_c \phi}{D} N_{sc}^{-1/3} = f\left[\left(\frac{\varepsilon \phi^4}{\nu^3}\right)^{1/3}\right] \qquad (6.28)$$

Since ϕ is not constant it is necessary to use the average diameter of droplets which can be found as follows:-

$$\phi_{av} = \frac{\phi_0 + \phi_0 (1-0.2p)^{1/3}}{2} \qquad (6.29)$$

In table (6.3) the calculated average diameter of the droplets has been tabulated.

6.4.1.1 Determination of Diffusion Coefficient (D)

The diffusion coefficients for dilute solutions are available in literature. Unfortunately, there is no information about the diffusion coefficient for 98% (w/w) sulphuric acid. However, in "International Critical Tables" the diffusion coefficient and viscosity are given 2.7×10^{-5} $cm^2 s^{-1}$ and 3.75 c.P respectively

for 10N (38% w/w) sulphuric acid at 20°C

N(r.p.s)	p(acid/olefin)	ϕ_0(cm)	ϕ_{av}(cm)	$\overline{\phi}_{av}$(sm)
	1.0		0.0244	
4.17	1.5	0.0253	0.0239	0.0234
	2.0		0.0233	
	3.0		0.0220	
	1.0		0.0143	
8.33	1.5	0.0148	0.0140	0.0137
	2.0		0.0136	
	3.0		0.0129	
	1.0		0.0084	
16.67	1.5	0.0087	0.0082	0.0081
	2.0		0.0080	
	3.0		0.0076	

Table 6.3 The average diameter of the droplets at the different speed of rotation and acid to olefin mole ratio.

It is also known from the Stokes-Einstein equation that diffusion coefficients are inversely proportional to the viscosity of the medium. That is:-

$$D = \frac{kT}{6\pi\mu r}$$

where T and μ are the temperature and viscosity of the liquid respectively and r is the radius of the ion. Therefore, for the same ion and at the same temperature, but for different concentration (different viscosity), the following holds:-

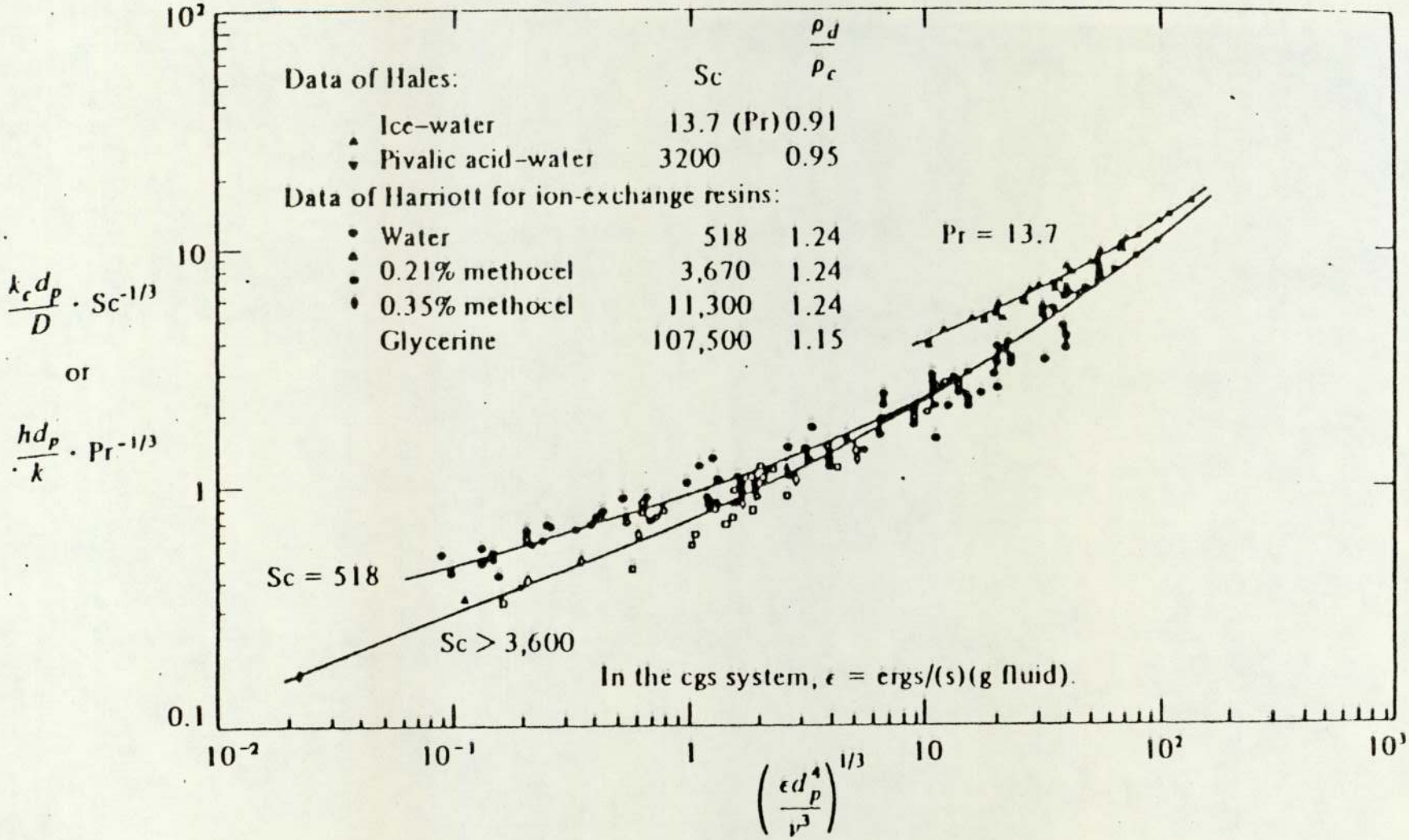

Figure 6.5 Heat - and -mass transfer data for particles suspended in agitated vessels, where d_p is the diameter of the particle.

$$\frac{D_1}{D_2} = \frac{\mu_2}{\mu_1} \quad \text{or} \quad D_2 = D_1 \frac{\mu_1}{\mu_2} \tag{6.30}$$

where $D_1 = 2.7 \times 10^{-5}$ cm^2 sec^{-1} (diffusion coefficient for 38% w/w sulphuric acid), $\mu_1 = 3.75$ c.P (viscosity of 38% w/w sulphuric acid) $\mu_2 = 36$ c.P (viscosity of 98% w/w sulphuric acid). Inserting these values into equation (6.30) D_2 (diffusion coefficient for 98% w/w sulphuric acid) was calculated. That is:-

$$D_2 = 2.8 \times 10^{-6} \text{ cm}^2 \text{ sec}^{-1}$$

From the known quantities, the terms involving Hales' graphical correlation have been calculated and tabulated in table (6.4).

N(r.p.s)	$\overline{\Phi}_{av}$(cm)	$\left(\frac{\varepsilon \overline{\Phi}_{av}^4}{\nu^3}\right)^{1/3}$	$\frac{k_c \overline{\Phi}_{av}}{D} N_{sc}^{-1/3}$	k_c(cm sec^{-1})
4.17	0.0234	2.03	0.97	4.78×10^{-3}
8.33	0.0137	1.55	0.87	7.32×10^{-3}
16.67	0.0081	1.20	0.76	10.82×10^{-3}

Table 6.4 The values of k_c for different parameters.

In table (6.4) $N_{sc} = \frac{\nu}{D} = \frac{0.36/1.84}{2.8 \times 10^{-6}} \cong 70{,}000$. Therefore, the third column has been obtained from Hales' graphical correlation for $N_{sc} > 3600$ and k_c calculated from it.

Now we are ready to calculate ℓ in equation (6.27). For different parameters the calculated value of ℓ has been tabulated in Appendix B5.

6.5 DISCUSSION OF THE RESULTS

It can be seen from the results tabulated in Appendix B5 that the length of the reactor at which drops disappear is very small (approximately 0.5 cm). Therefore, it was concluded that the reaction can be regarded as a homogeneous liquid reaction. Even in the case of 1000% error in the calculation of mass transfer coefficient, the greatest value of ℓ at which the drops disappear is not greater than 3 cm (sample IE-1 in Appendix B5) which does not violate the concept of homogeneous reactions.

In Appendix (B4) it can also be seen that the conversion of olefin is independent of the speed of rotation of the inner cylinder (over the range 4-16 revolutions per second). This result is consistent with the model proposed above which predicts that conversion in the (homogeneous plug-flow) reactor should be independent of mixing.

CHAPTER 7

REACTION PARAMETERS

7.1 INTRODUCTION

In Section (5.2) the main and possible side reactions between the concentrated sulphuric acid and α-olefins were discussed in detail. To achieve a high percentage conversion of olefin to monoalkyl sulphuric acid and to minimize the side reactions, the right reaction parameters must be chosen, since conversion of olefins to the different reaction products is very sensitive to the reaction parameters.

The most important reaction parameters are:-

i) Mixing (speed of rotation of the inner cylinder)

ii) Residence time

iii) Mole ratio of reactants

iv) Acid concentration

v) Temperature of reaction and neutralization

vi) Order of dispersion of the reactants

vii) Chain length of olefins

The effects of the first three reaction parameters on olefin conversion have been investigated in great detail. The effects of the other parameters were not examined, since their effects on conversion are well documented in the literature (25, 28, 46). However, two samples designated IH-1 and IH-2 in Appendix B4 were obtained using sulphuric acid concentrations of 95% (w/w) which differ from the rest of the samples obtained using 98% (w/w) sulphuric acid.

In this chapter, the experimental findings obtained in this research, together with the result of the previous studies, will be discussed.

7.2 MIXING (SPEED OF ROTATION)

A literature survey (25, 28) reveals that if the olefin and acid are well mixed in the reactor, relatively high percent conversions and high yield of monoalkyl sulphuric acid can be achieved. Using hexene-1 with 7.5:1 acid to olefin molar ratio and 79.6% (w/w) sulphuric acid, Butcher and Nickson (28) were able to increase the conversion of olefin to monohexyl sulphuric acid from 89.2% to 92.1% by increasing the speed of rotation from 2800 r.p.m. to 5600 r.p.m. in a batch reactor.

In the present study, the speed of rotation of the inner cylinder was varied in a series of runs between 250 and 1000 r.p.m. It was shown in Section (6.2) that the droplets in the dispersed phase, at these speeds, disappear in a very short time so that the reactor almost behaves as a homogeneous plug-flow reactor. Therefore, the speed of rotation has no great effect on the conversion of the reactants.

The experimental results are tabulated in Appendix B4. From these results it can be seen that it is not possible to identify any specific conclusion about the effect of speed of rotation on the conversion of the reactants. If the other parameters are kept constant, the differences in conversion of olefin, at the different speeds of rotation, are within experimental error. Nevertheless, it is necessary to keep the speed of rotation above a certain level so that the olefin can be dispersed in acid phase and thereafter the reactants are intimately mixed. This minimum level of rotation was found to be 250 r.p.m.

7.3 RESIDENCE TIME

Usually increasing the contact time promotes side reactions

at the expense of the formation of monoalkyl sulphuric acid. Grant (25) showed that at high acid concentrations (97.3 - 99.2% w/w) the conversion of olefins to monoalkyl sulphuric acid increased with decreasing residence time (down to 2 minutes) in a continuous reactor. He also reported that the formation of dialkyl sulphate decreased with decreasing contact time. Kooijman (24) obtained similar results by showing that at acid concentrations over 90% (w/w) the formation of monoalkyl sulphuric acid and dialkyl sulphate reached a maximum after approximately 3 and 10 minutes respectively. Following this, the proportion of both products in the reaction mixture decreased with increasing contact time in favour of polymer. Kooijman carried out his experiments at a mole ratio of 3:1 (acid to hexadecene-1) and at 20°C in a batch reactor.

In unpublished work Malhotra (46), using a static mixer reactor, achieved a relatively high conversion of olefins to monoalkyl sulphate in a very short residence time. At an acid to olefin molar ratio of 1:1 with 98% (w/w) sulphuric acid he was able to obtain 52.3% conversion of olefin to monoalkyl sulphate in 6 seconds time. With the same conditions, by decreasing the residence time to 2.5 seconds, he observed that conversion of olefin decreased to 40.6%. Keeping the other conditions constant and using $\sim$ 100% sulphuric acid, Malhotra achieved higher conversion of olefin at 2.5 seconds than at 6 seconds (73.4% and 53.0% respectively). He did not analyse the monoalkyl sulphuric acid and dialkyl sulphate separately and his results were obtained after the hydrolisis of the dialkyl sulphate.

In this study, the residence times were chosen to be 1.5, 2.0, 2.5 minutes initially, when it was found that if all the other conditions were kept constant, the conversion of olefin to

monoalkyl sulphuric acid was almost the same irrespective of the residence times. To obtain additional information of the effect of residence time, three more runs were made at residence times of 0.5, 5.0 and 10.0 minutes; and by designing two further reactors (continuous and batch), two more samples were also obtained at residence times of 5 seconds and 280 minutes respectively, because the original reactor was not suitable for operation at these residence times. In both cases the temperature of reaction was kept constant at $\sim$ 15°C by cooling with solid carbon dioxide.

The experimental results have been tabulated in table (7.1) and a plot of conversion of olefin to the different products is illustrated in figure (7.1).

7.3.1 Discussion of Results

From the table (7.1) it can be seen that, at a residence time of 5 seconds, the conversion of olefin to monoalkyl sulphate (after hydrolisis) is only 5%. This result contradicts Malhotra's, where probably the discrepancy may be attributed to the difference in reaction temperatures. Malhotra carried out his experiments at 80°C whereas in this study the temperature was kept constant as 15°C. Assuming the Arrhenius law [$k = A \exp(-E/RT)$] the reaction rate would be much higher at high temperatures.

From the figure (7.1) it was concluded that the highest conversion of olefin to monoalkyl sulphate was achieved at the residence time of approximately 3 minutes. The formation of dialkyl sulphate reached a maximum after monoalkyl sulphuric acid ($\sim$ 5 minutes) and the conversion of olefin to polymer increased as the reactants contact time was further increased. An important conclusion is that the decomposition of monoalkyl sulphuric acid

Sample No.	Speed of rotation (r.p.m)	Malar ratio (acid/olefin)	Residence time (min)	X_{MAS}	X_{DAS}	X_{p}	X_{TMAS}
IJ-1	500	1.5:1	5*	-	-	-	0.050
IG-1	500	1.5:1	0.5	0.452	0.122	0.072	0.513
IB-2	500	1.5:1	1.5	0.537	0.210	0.112	0.642
IIB-3	1000	1.5:1	2.0	0.527	0.187	0.143	0.621
IIIB-3	1000	1.5:1	2.5	0.551	0.204	0.139	0.653
IF-1	500	1.5:1	5.0	0.499	0.242	0.154	0.620
IF-2	500	1.5:1	10.0	0.478	0.220	0.201	0.588
IF-3	Batch with stirrer	3:1	280.0	0.122	0.095	0.721	0.170

Table 7.1 Conversion of hexadecene-1 to the reaction products at the different residence times and constant temperature of 15°C.

Where:-

* : Seconds

MAS : Monoalkyl sulphuric acid

DAS : Dialkyl sulphate

P : Polymer

TMAS : Total monoalkyl sulphate (obtained after hydrolysis of the dialkyl sulphate).

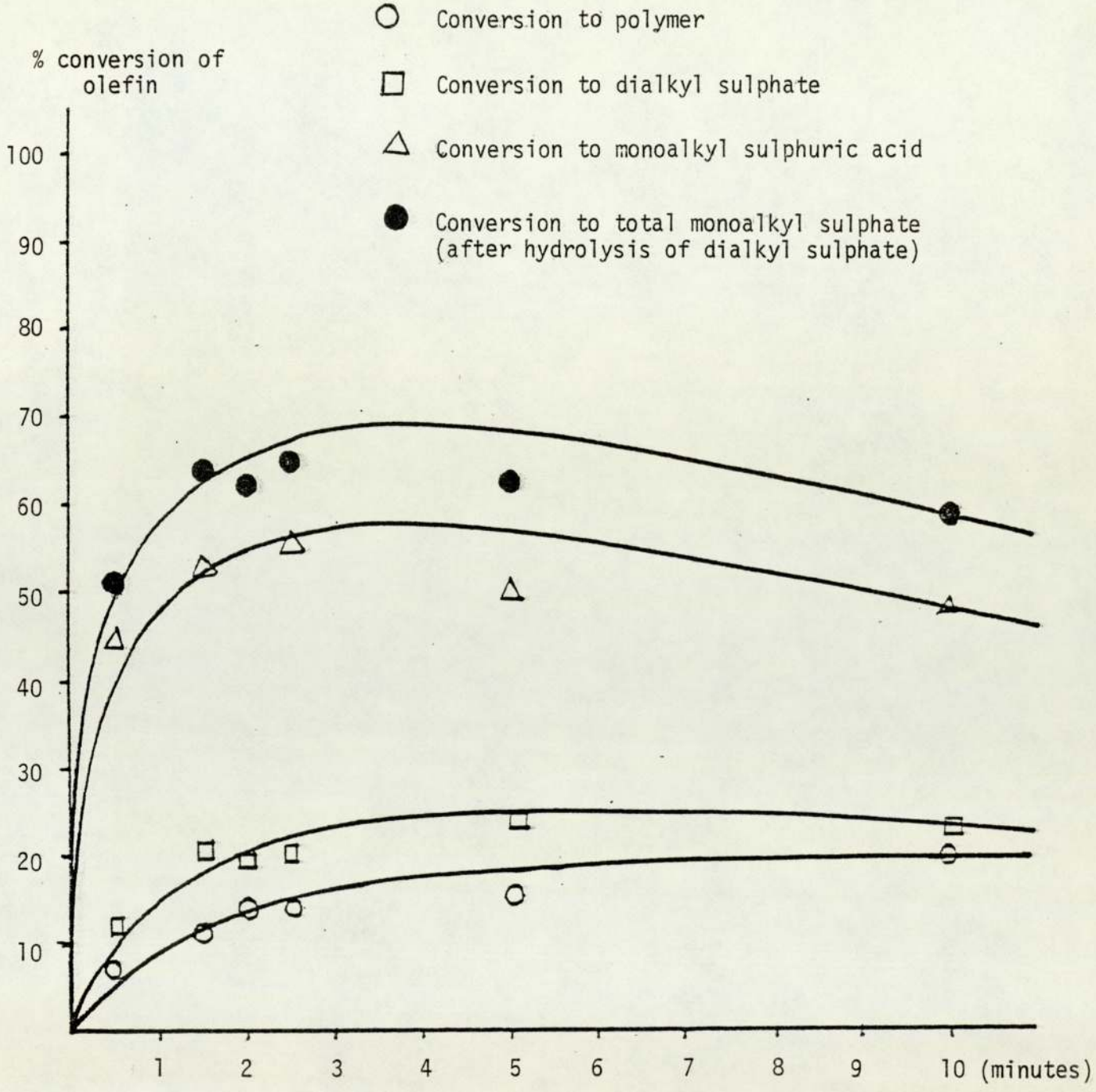

Figure 7.1 Conversion of olefin to the different reaction products as a function of reaction time

Where:-

Reaction temperature is 15°C

Acid to olefin mole ratio is 1.5:1

Acid concentration is 98% (w/w)

and dialkyl sulphate is not very sensitive to time, because it was found that in a vigorously mixed batch reactor olefin conversion to monoalkyl sulphate was 17%, even after 280 minutes. This is attributed to a probable chemical equilibrium between products and reactants (47). These results are consistent with the experimental results of Grant (25) and Kooijman (24), so that 3.0 minutes can be safely chosen as the best residence time to achieve the highest yield at the reaction temperature of 15°C.

The highest conversion of olefin to total monoalkyl sulphate (after hydrolisis of the dialkyl sulphate) was 71.6% which was obtained at the residence time of 2 minutes with acid to olefin mole ratio 1.5:1.

7.4 MOLE RATIO OF REACTANTS

Another important parameter which affects the conversion of olefin to different reaction products is the mole ratio of the reactants. Its effect upon product composition is very complex. It has been found (25, 28, 46) that the optimum value of the ratio is dependent on the acid concentration, the temperature and residence time.

Clippinger (48) reported that the first, H_2SO_4 added to α-olefin combined almost exclusively to form dialkyl sulphate. As the addition of acid was continued, the amount of monoalkyl sulphuric acid in equilibrium increased gradually. When about 1 mole of acid had been added, a rapid shift in equilibrium favouring monoalkyl sulphuric acid occurred. This did not continue indefinitely, and a large excess of sulphuric acid decreased the fraction of dialkyl sulphate only slightly. Clippinger had carried out his experiment using 96% (w/w) sulphuric acid and

dodecene-1 at the temperature of 0°C.

Grant (25) found that, at fixed residence times for sulphation with 99.2% (w/w) and 97.3% (w/w) sulphuric acid, the polymerization increases with increasing ratio of acid to olefin and the formation of dialkyl sulphate decreases as acid to olefin mole ratio increases. However, at a short residence time (2 minutes) with 97% (w/w) sulphuric acid, he showed that the monoalkyl sulphate reached a maximum of 69% at 3:1 acid to olefin mole ratio.

Kooijman (24) found, at a reaction temperature of 20°C and reaction time 5 minutes, that the formation of monoalkyl sulphuric acid, dialkyl sulphate and polymer are a function of the sulphuric acid concentration and the sulphuric acid to olefin mole ratio. He used dodecene-1 as an α-olefin. Kooijman's experimental results are presented in figure (7.2), (7.3) and (7.4).

Figure (7.2) shows that the optimum formation of dialkyl sulphate (over 50% based on dodecene-1) takes place at sulphuric acid concentrations greater than 90% (w/w) and a sulphuric acid to dodecene-1 ratio of about 2:1. From figure (7.3) it can be seen that the optimum formation of monoalkyl sulphuric acid (over 70%) also takes place at a sulphuric acid concentration of greater than 90% (w/w), the appropriate molecular sulphuric and/dodecene-1 ratio is about 3.4:1. Figure (7.4) reveals that the formation of polymer increases with increasing sulphuric acid/dodecene-1 ratio and with increasing sulphuric acid concentration. Malhotra (46) found that the best acid/hexadecene-1 mole ratio was 1:1 at an acid strength of 100% with 15 seconds residence time and at a reaction temperature of 80°C. Using 98% (w/w) sulphuric acid, at the same reaction temperature, he achieved the highest conversion of hexadecene-1

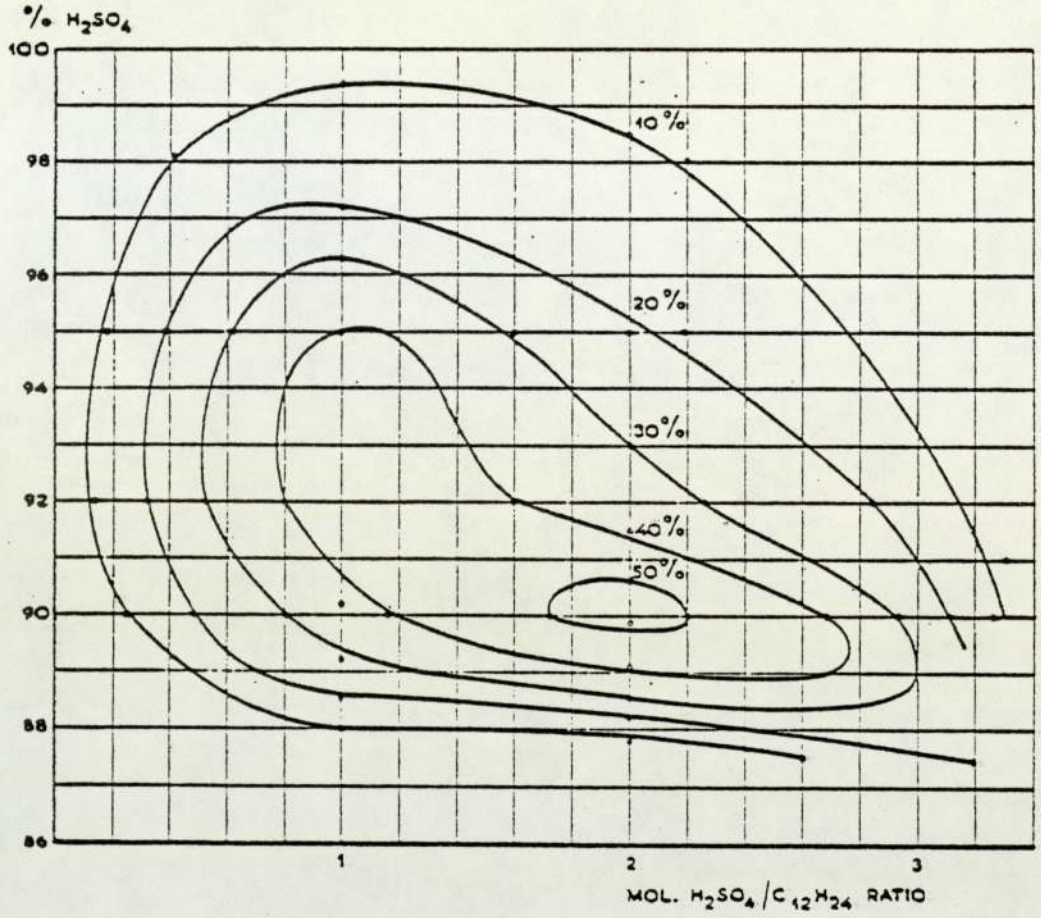

Figure 7.2 The formation of didocyl sulphate in % of dodecene-1 as a function of the sulphuric acid concentration and the sulphuric acid/dodecene-1 mole ratio (Reaction time 5 min.; reaction temp. 20°C).

to hexadecyl sulphate (75%, after hydrolysis of dialkyl sulphate) at the mole ratio of acid to olefin 3:1.

In this study, using 98% (w/w) sulphuric acid and the reaction temperature of ∿15°C, samples were obtained at the acid/olefin mole ratios of 1:1, 1.5:1, 2:1 and 3:1. In Section (7.2) it was shown that the speed of rotation had no significant effect on the conversion of olefin and from Section (7.3) it was also concluded that the variation of conversion of olefin between 1.5 - 2.5 minutes time period was negligible. Thus, in table (7.2) the variation of olefin conversion to the different reaction products can only be attributed to the differences in the acid/olefin mole ratio.

Molar ratio (acid/olefin)	$\overline{X}_p$	$\overline{X}_{MAS}$	$\overline{X}_{DAS}$	$\overline{X}_{TMAS}$
1:1	0.123 s:0.023	0.485 s:0.068	0.239 s:0.028	0.604 s:0.054
1.5:1	0.122 s:0.024	0.545 s:0.016	0.203 s:0.011	0.651 s:0.031
2:1	0.196 s:0.022	0.518 s:0.025	0.135 s:0.004	0.583 s:0.024
3:1	0.278 s:0.019	0.460 s:0.018	0.117 s:0.010	0.519 s:0.024

Table 7.2 The effect of acid/olefin mole ratio on the conversion of olefin to the different reaction products with 98% w/w sulphuric acid at ∿ 15°C.

where:-

s : Standard deviation

$\overline{X}_p$: Average conversion to polymer

$\overline{X}_{MAS}$: Average conversion to monoalkyl sulphuric acid

$\overline{X}_{DAS}$: Average conversion to dialkyl sulphate

$\overline{X}_{TMAS}$: Average conversion to total monoalkyl sulphate (after hydrolysis of the dialkyl sulphate)

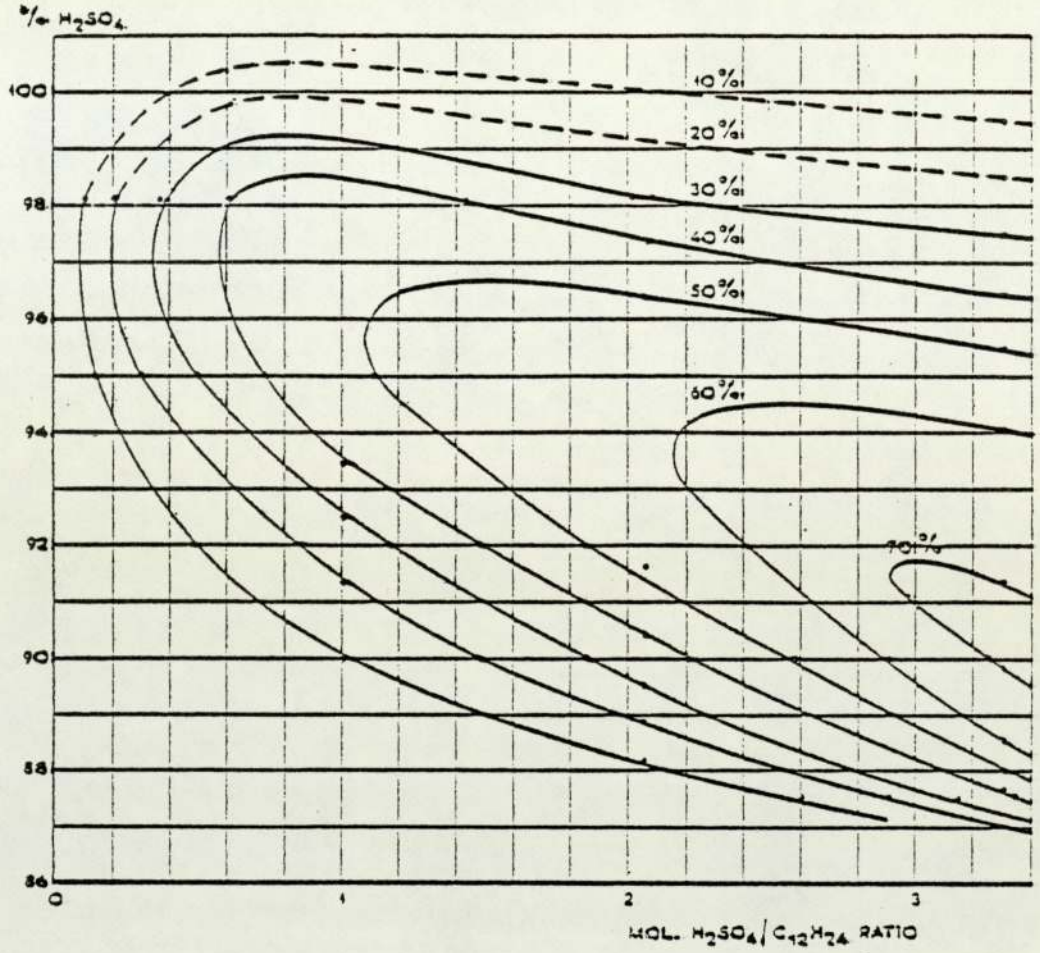

Figure 7.3 The formation of monododecyl sulphuric acid in % of dodecene-1 as a function of the sulphuric acid concentration and the sulphuric acid/dodecene-1 mole ratio (Reaction time 5 min.; reaction temp. 20°C).

In table (7.2), the first figures in columns 2, 3, 4 and 5 indicate the average conversion of olefin to the corresponding reaction products at different acid/olefin mole ratios. The second figures give the standard deviations for each set of experimental results obtained at the same acid/olefin mole ratio. These values were obtained from the table in Appendix B4. They are also represented graphically in figure (7.5), in which the formation of monoalkyl sulphuric acid, dialkyl sulphate and polymer have been plotted as a function of the sulphuric acid/olefin mole ratio at the constant acid concentration of 98% (w/w).

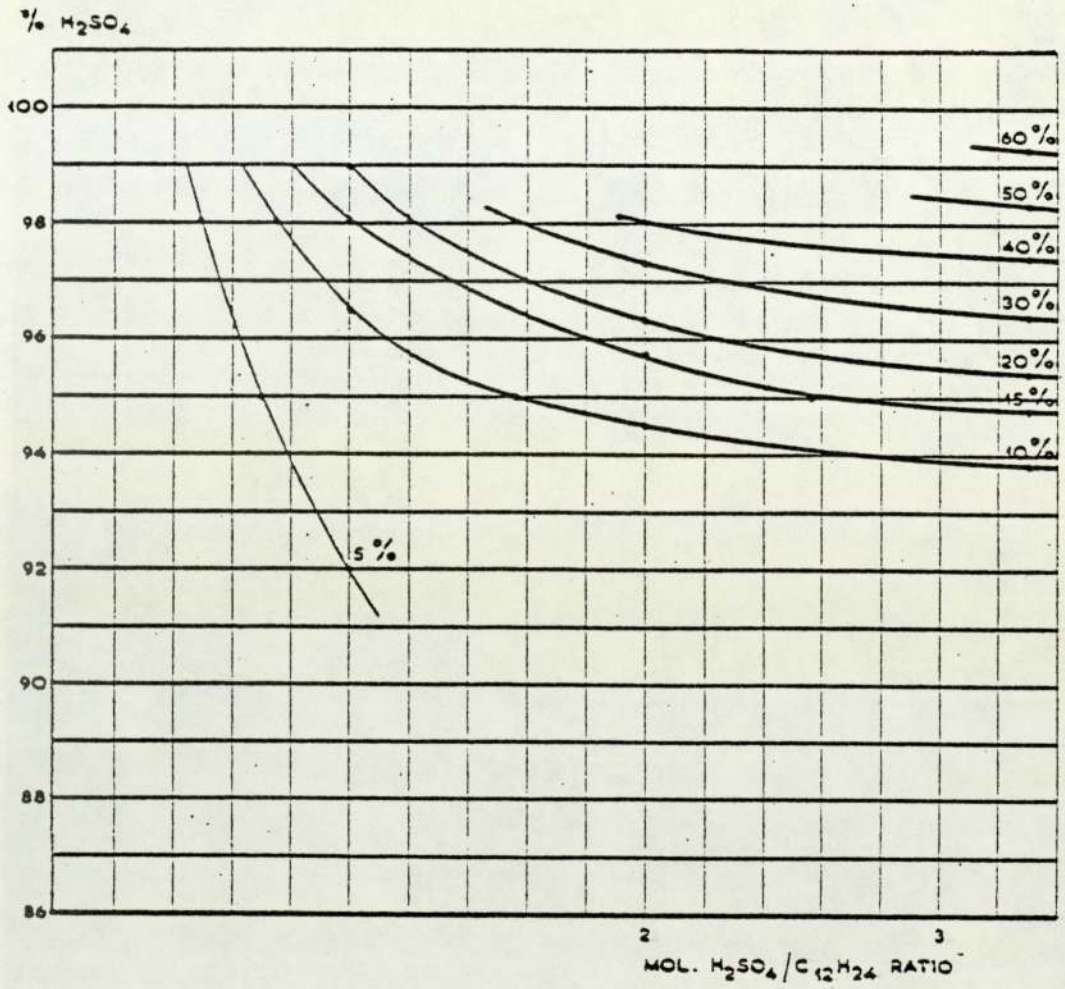

Figure 7.4 The formation of polymer in % of dodecene-1 as a function of the sulphuric acid concentration and the sulphuric acid/dodecene-1 mole ratio (Reaction time 5 min.; reaction temp. 20°C).

Table (7.2) and figure (7.5) show that the formation of polymer increases (almost linearly) while the conversion of the dialkyl sulphate decreases with increasing acid/olefin mole ratio within the range of 1:1 to 3:1. The formation of monoalkyl sulphate reaches a maximum at the acid/olefin mole ratio 1.5:1, then starts to decrease with increasing the acid/olefin mole ratio. With the acid/olefin mole ratio less than 1.5:1 a relatively higher percentage of converted olefin was detected. (See table in Appendix B4). Figure (7.5) also shows that the highest conversion of olefin to total monoalkyl sulphate (after hydrolysis of dialkyl sulphate)

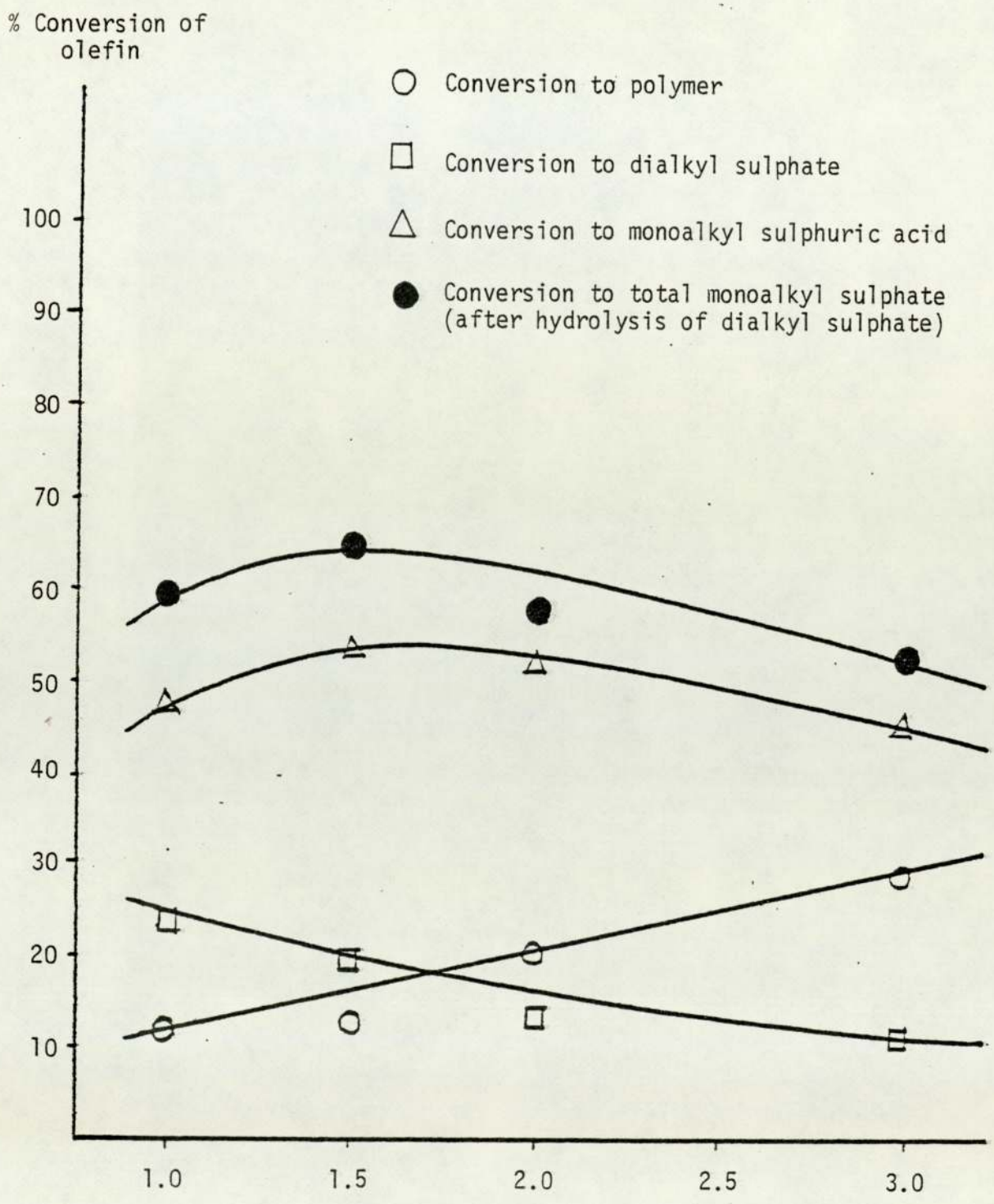

Figure 7.5 The conversion of olefin to the different reaction products as a function of acid/olefin mole ratio (Acid concentration 98% w/w; reaction temp. 15°.)

were obtained at the acid/olefin mole ratio 1.5:1. These results are similar to those of Kooijman.

From this analysis it was concluded that the best acid/olefin mole ratio is 1.5:1 at the residence time of three minutes and with the acid strength of 98% (w/w) at ∿ 15°C.

7.4.1 Discussion of Results

The literature on the sulphation of olefins reveals that:-

i) Experimental design and the approach of different workers are not consistent and consequently have led to apparent contradictions of the proposed reaction mechanism for reported conversion/yields and product compositions.

ii) The chemistry of olefin sulphation suggests that very high yields of monoalkyl sulphate is possible. However, it is not known whether (or how) these high yields can be achieved on a large scale under industrially realistic conditions. Conversions greater than 75% of olefin to total monoalkyl sulphate have not been reported in the literature.

The highest yield achieved by different researchers are as follows:-

1. Malhotra (46) 75%
2. Grant (25) 74%
3. Dykes (2) 73%
4. Present work 72%

The differences in these results can be considered to be within experimental error. In a private discussion, Fairclough (47) suggested that these results are equilibrium positions of composition. The reaction conditions which cause equilibrium to move in favour of monoalkyl sulphate must be investigated in future work, i.e. using an inert solvent process at very low (down to -15°C) temperature.

The conversions mentioned above were achieved using C_{16} chain length α-olefin (hexadecene-1). Butcher and Nickson (28) obtained much higher conversions (up to 92%) using hexene-1 as an α-olefin which is not the detergent range of olefin.

iii) The kinetics of the sulphation reaction for the detergent range of olefins, and a reaction mechanism fitting the experimental data, are not available.

iv) There are some problems outstanding in the analysis of the products of sulphation due to the lack of quantification and superimposition of the responses of more than one compound, e.g. internal olefin and parafins in G.L.C. Nevertheless, a common conclusion reached by different workers is that acid concentrations lower than 90% (w/w) are not suitable to achieve good conversion of the olefins to the monoalkyl sulphate. Furthermore, it is frequently reported that the higher acid concentration and high acid/olefin mole ratios promote the formation of polymer and reduce the formation of dialkyl sulphate. There is no explanation for this phenomena in the literature, therefore the following mechanism is proposed.

It is believed that olefins are protonated by acid to form carbonium ions which are in equilibrium with the olefins. These carbonium ions react with HSO_4^- ion forming monoalkyl sulphate. The reactions of carbonium ions are very complex and give many products. One important product is the polymer which is the result of the reaction between the carbonium ion and olefin itself. After formation of monoalkyl sulphuric acid, this product either reacting with olefin or eliminating one mole sulphuric acid from two moles itself, gives dialkyl sulphate. Later, monoalkyl sulphuric acid

and dialkyl sulphate decompose in a very complex manner to form polymer in a long contact reaction time. These reactions have already been discussed in detail in Section (5.2). However, to explain the effects of the parameters on the conversion of olefins to the different reaction products, it will be useful to summarize here, as follows:-

$$\text{Olefin} + H^+ \rightleftharpoons [\text{carbonium ion}]^+ \qquad (7.1)$$

$$[\text{Carbonium ion}]^+ + HSO_4^- \longrightarrow \text{MASA} \qquad (7.2)$$

$$[\text{Carbonium ion}]^+ + \text{Olefin} \longrightarrow \text{Polymer} \qquad (7.3)$$

$$\text{MASA} + \text{Olefin} \longrightarrow \text{DAS} \qquad (7.4)$$

$$2\text{MASA} \longrightarrow \text{DAS} + H_2SO_4 \qquad (7.5)$$

$$\text{MASA} \longrightarrow \text{Polymer} \qquad (7.6)$$

$$\text{DAS} \longrightarrow \text{Polymer} \qquad (7.7)$$

$$[\text{Carbonium ion}]^+ \longrightarrow \text{Internal olefin} \qquad (7.8)$$

where MASA and DAS are monoalkyl sulphuric acid and dialkyl sulphate respectively.

Reactions (7.6) and (7.7) take place after a long reaction time and probably only after some intermediate stages are monoalkyl sulphuric acid and dialkyl sulphate transformed into polymer. These processes are very low. In a stirred batch reactor with a reaction time of 280 minutes 17% of the original olefin was still in the form of the monoalkyl sulphate (Sample IF-3 in table 7.1).

Wyatt (49) reported that the mole fraction of the most probable species in sulphuric acid depended on the concentration of sulphuric acid. For acid concentrations between 80% and 98% (w/w) he proposed the following reaction schemes:-

$$H_2SO_4 + H_2O \longrightarrow H_3O^+ + HSO_4^- \qquad (7.9)$$

$$H_3O^+ + H_2SO_4 \rightleftharpoons H_3O^+(H_2SO_4) \qquad (7.10)$$

$$2H_3O^+ + HSO_4^- \rightleftharpoons H_3O^+(H_2O) + H_2SO_4 \qquad (7.11)$$

Wyatt also calculated the mole fraction of each species at different acid concentrations. These are tabulated in table (7.3).

$\%H_2SO_4$	H_2SO_4	H_3O^+	HSO_4^-	$H_3O^+(H_2SO_4)$	$H_3O^+(H_2O)$
79.7	0.0103	0.2850	0.4948	0.0027	0.2071
85.7	0.0721	0.3880	0.4639	0.0278	0.0481
89.5	0.1876	0.3322	0.4062	0.0619	0.0121
93.2	0.3828	0.2214	0.3086	0.0851	0.0020
94.5	0.6437	0.1083	0.1782	0.0697	0.0002
98.2	0.8104	0.0521	0.0948	0.0427	0.0000

Table 7.3 The most probable species present in different sulphuric acid concentrations.

It is believed that all positive ions in table (7.3) accelerate the formation of carbonium ions and these carbonium ions are consumed by HSO_4^- ions and olefin to form monoalkyl sulphuric acid and polymer respectively. Furthermore, it has been proposed (27) that the rate of formation of carbonium ions is higher, due to the high acidity function at high concentrations of sulphuric acid than at low concentrations. Therefore, at sulphuric acid concentrations over 95% (w/w) there will be a high concentration of carbonium ions and a low concentration of HSO_4^- ions (see table 7.3). That is to say, the concentration of HSO_4^- ions is too low to consume all carbonium ions. These excess carbonium ions react with olefin in accordance with reaction (7.3), forming polymer. On the other hand,

it can be seen from the reactions (7.4) and (7.5) that the formation of dialkyl sulphate is proportional to the concentrations of monoalkyl sulphuric acid and olefin which, at high concentrations of acid are low due to formation of polymer. Therefore, the formation of dialkyl sulphate decreases with increasing acid concentration. Similarly it can be argued that, with a high acid to olefin mole ratio there will be a high concentration of carbonium ions and consequently, the formation of polymer increases while the formation of dialkyl sulphate decreases. This explanation is consistent with experimental findings both in the literature and in this study. On the other hand, use of a low sulphuric acid concentrations and a low acid to olefin mole ratios has some negative effects. That is, with low concentrations of sulphuric acid, the formation of secondary alcohol increases due to the hydrogenation of carbonium ions and at low acid to olefin mole ratios (smaller than 1.0) acid combined almost exclusively to form dialkyl sulphate (48).

In the literature the proposed acid concentration required to achieve a high conversion of olefin to monoalkyl sulphuric acid is 98% (w/w) (25, 46). However, Kooijman (24) obtained the highest yield at a sulphuric acid concentration of 95% (w/w). In this study, experiments were carried out at acid concentrations of 98% (w/w). However, two analyses were obtained using 95% (w/w) sulphuric acid which were not significantly different from the others (see Appendix B4). As a result it was concluded that the best acid/olefin mole ratio is 1.5:1 with an acid concentration of 98% (w/w). It is also believed that further investigations are needed to assess the effect of acid concentration on the conversion of olefin to monoalkyl sulphuric acid.

7.5 THE OTHER REACTION PARAMETERS

Apart from the parameters investigated in Sections (7.2), (7.3) and (7.4) it was mentioned in Section (7.1) that there are a number of other parameters which affect the conversion of olefins to the desired product (monoalkyl sulphuric acid). They were not examined in this study, since their effects on conversion were well documented in the literature (25, 28, 46). However, it is believed that brif discussion of these parameters will be useful to achieve further understanding of the phenomena.

7.5.1 Temperature of Reaction and Neutralization

It has been reported (27, 28, 29) that by reducing the temperature of reaction, the conversion of olefins to monoalkyl sulphuric acid increases and formation of dialkyl sulphate and polymer decreases. This is due to the fact that the rate of hydrolysis and polymerization decreases more rapidly than the rate of sulphation reaction with temperature.

Butcher and Nickson (28) observed that, with 7.5:1 acid to olefin (hexene-1) molar ratio and 79.6% (w/w) sulphuric acid in a stirred batch reactor the conversion of olefin to monohexyl sulphate was higher at 0°C than at 25°C and 10°C. In this study, the reaction temperature was kept constant at approximately 15°C, because at lower temperatures the power consumption increased beyond the power of the driving unit, due to the increase of viscosity of the reaction mixture.

In the literature (48) inert-solvent processes have been proposed to lower the freezing point of olefin to -15°C. Hexadecene-1 freezes at 4°C, but when dissolved in an inert solvent, it will remain in solution at -15°C. Using these inert-solvent

processes Clippinger (48) was able to increase the conversion of olefin to monoalkyl sulphuric acid by 10% at -15°C compared to results at 0°C. This is because by the lowering of temperature the equilibrium was disturbed resulting in material being precipitated away from the "sphere of reaction", thereby inhibiting side reactions. The only disadvantage is that this process is more hazardous than non-solvent processes, since inert solvents (40/60 petroleum ether or pentane) have very low flash points.

Malhotra (46) reported that at neutralization temperatures, higher than 50°C monoalkyl sulphate undergoes thermal breakdown in accordance with the reaction

$$R - \underset{\underset{OSO_3Na}{|}}{CH} - CH_3 \xrightarrow[\text{breakdown}]{\text{Thermal}} R' - CH = CH_2 - CH_3 + NaHSO_4$$

Internal Olefin

This was checked, at the neutralization temperature both above and below 50°C, but no significant differences were observed. Nevertheless, the neutralization temperature was kept below 50°C using precooled 20% (w/w) NaOH solution.

7.5.2 Order of Dispersion of the Reactants

Malhotra (46) found that olefins dispersed in the acid increase the percent conversion of olefins to monoalkyl sulphuric acid by 3-8 percent. This may be explained if we assume that the reaction takes place within the acid phase, as follows:-

Olefin drops are protonated at the olefin/acid interface. The protonated olefin reacts with acid and the product dissolves in the continuous (acid) phase. The olefins are extremely soluble in monoalkyl sulphuric acid. Hence the continuous phase contining monoalkyl sulphuric acid dissolves tiny olefin droplets

at a much faster rate. This high rate of solubilisation helps to homogenise the reactants and is believed to slow the degradative reactions. When acid is the dispersed phase the transfer of monoalkyl sulphuric acid and olefin into the acid drops is likely to be slow. This would reduce solubilisation of the reactants and hence promote degradative reactions i.e. reduce percent conversion to monoalkyl sulphuric acid.

For these reasons, olefin was chosen as the dispersed phase throughout the experimental work.

7.5.3 Chain length of Olefin

A qualitative relationship has been found between the sulphation reactivity and the chain length of the olefin, such that an increase in the carbon number of the olefin produces a strong drop in reaction rate. Butcher and Nickson (28) showed that an 80% yield of monohexyl sulphuric acid occurred with 80% (w/w) sulphuric acid, whereas decene-1, at the same acid concentration and with the same reaction time gave only a 1% yield of monodecyl sulphuric acid. The observed decrease in reactivity from C_6 to C_{10} was explained by a change in steric hindrance in either the olefin molecule or the solvated olefin. Additionally, the formation of the side products increases at the expense of monoalkyl sulphuric acid with increasing chain length of the olefins. Butcher and Nickson (28) were able to achieve 92% conversion of hexene-1 to monohexyl sulphuric acid, whereas conversions of C_{16} olefins (hexadecene-1) of greater than 75% have not been reported in the literature even after the hydrolysis of dialkyl sulphate.

CHAPTER 8

CONCLUSION AND

RECOMMENDATIONS FOR FURTHER WORK

8.1 INTRODUCTION

In this study, the performance of a reactor, termed a "no-leak" votator was investigated. Flow patterns within the annulus were examined and an expression for the velocity profile derived. A model was also developed describing the axial flow characteristics, in the form of residence time distribution curves, by tracer analysis using a coloured dye. Power consumption, one of the important criteria for scaling-up a pilot plant reactor, was investigated and an empirical equation for the power consumption found.

The reaction between α-olefins (hexadecene-1) and 98% (w/w) sulphuric acid has been investigated for different reaction and reactor parameters and the optimum conditions necessary to obtain the highest yield found.

In this chapter, conclusions drawn from the results of this study will be summarized and recommendations for future work will be made.

8.2 MIXING AND FLOW CHARACTERISTICS OF THE REACTOR

8.2.1 Tangential Flow

In the absence of Taylor vortices tangential flow is stable. A theoretical investigation using the principles of fluid dynamics shows that the flow direction is altered at an annulus width of d/3. The expressions for the velocity profile are:-

i) In rectangular co-ordinate systems

$$\frac{V_x}{V_i} = \frac{d - y}{d} - \frac{3(d-y)y^2}{d^2}$$

ii) In cylindrical co-ordinate systems

$$\frac{V_\theta}{V_i} = Ar\ell nr + Br + Cr^{-1}$$

where A, B and C are constants that can be determined using the boundary conditions shown in Section (3.2:1) for given reactor dimensions.

The tangential velocity profile divides the annulus into two sections. These are:-

i) Inner section: Between r_i and $(r_i+d/3)$

ii) Outer section: Between $(r_i+d/3)$ and r_0

The inner section behaves like an inner cylinder of radius r_i, rotating inside a stationary outer cylinder of radius $(r_i+d/3)$. Therefore the critical velocity for instability is given by the Taylor number;

$$T_a = \frac{V_c d_0}{\nu}\sqrt{\frac{d_0}{r_i}} \geq 41.3$$

in which $d_0 = d/3$. However, it was shown that (4) the critical velocity in the inner section is 0.54 times smaller than the critical velocity calculated from the Taylor number because of the effects of the outer section on the instability in the inner section.

The outer section is bounded by two curved planes, both of which are at rest. The radius of the inner plane is $(r_i+d/3)$, while that of the outer is r_0. This section has a parabolic velocity distribution, therefore the Dean number can be used to find the critical velocity for stability. That is:-

$$D_a = \frac{V_c d'}{\nu}\sqrt{\frac{d'}{r_i}} \geq 36$$

where d' = 2d/3.

From this analysis it was found that instability occurs first in the inner section as the speed of rotation increases.

8.2.2 Axial Flow

It was expected that below the critical velocities (stable flow regime) mixing in the radial direction is likely to flatten the parabolic velocity profile in the annulus in the axial direction, thus helping to create plug-flow. Furthermore, at the onset of flow instability the Taylor vortices would act as a series of stirred tanks and again plug-flow would be approached.

From a study of the axial flow characteristics, in which residence time distribution curves were produced using a dye, slow speed photography and spectrophotometrical colour analysis, it was found that the reactor consisted of two series of C.S.T.R's approximating to two parallel plug-flow reactors having the volumes of $(V_{total}/3)$ and $(2V_{total}/3)$ which are approximately the volumes of the inner and outer sections respectively.

8.3 POWER CONSUMPTION

Power consumption is an important factor in scale-up considerations. In scraped surface heat exchangers, unlike most agitators, the power number is not a unique function of the rational Reynold's number. Therefore, it was necessary to find an empirical equation based on experimental results. In previous work Trommelen proposed the following expression for scraped surface heat exchangers with "with-leak":-

$$P = \frac{251(ND_o)^{1.79}\ \mu^{0.66}\ n_B^{0.68}\ L_B}{(D_o - D_i)^{0.31}}$$

Later Westaleken showed that the power consumption is 30% greater for a scraped surface heat exchanger with "no-leak" than for one "with-leak".

In this study, using the pilot plant reactor dimensions, it was found that power consumption could be expressed as follows:-

$$P = 34.44N^{1.93}\,\mu^{0.61} + 34.88N$$

where the last term is the total frictional loss. This power Consumption is 18% greater than the calculated power from the Westaleken correlation. The difference can be considered only within experimental error. Therefore, it was concluded that, for scraped surface heat exchangers "with-leak", power requirements can be found from Trommelen's equation. On the other hand, to find the power consumption for scraped surface heat exchangers with "no-leak" the Westaleken correlation can be used giving a result which is 1.30 times greater than the power consumption calculated from Trommelen's equation.

8.4 SULPHATION REACTION

The sulphation of hexadecene-1, using 98% (w/w) sulphuric acid was investigated in this study. Olefin was dispersed in the acid phase in the form of droplets and the reaction temperature was kept constant at approximately 15°C. It was found that, the reaction products were mainly monoalkyl sulphuric acid, dialkyl sulphate and polymer. Internal olefin and probably unreacted olefin were also detected in G.L.C. analysis. To obtain a high conversion of olefin to monoalkyl sulphuric acid, which is the desired product, it is necessary to satisfy the reaction parameters mentioned in Section (7.1). The effects of the three reaction

parameters, namely mixing, residence time and acid to olefin mole ratio were investigated in great detail, since the effects of other parameters on olefin conversion were well established in the literature (see Section 7.5).

Olefin was dispersed in the acid phase in the form of droplets and it may be assumed that each droplet was surrounded by a liquid film. Therefore, the acid molecules have to travel through this liquid film to reach the droplets and react with olefin at the surface of the droplet. The reaction products (mainly monoalkyl sulphuric acid) are soluble in the acid phase; olefin is also soluble in sulphuric acid when the mole fraction of monoalkyl sulphuric acid in the acid phase reaches 0.20. Therefore, the reaction is initially heterogeneous, but when the mole fraction of monoalkyl sulphuric acid in the acid phase reaches 0.20 it becomes homogeneous. It was proved in chapter (6) that a heterogeneous reaction takes place at the top of the reactor within a reactor length of approximately 0.5 cm. This is negligible, compared to the total length of the reactor of 45.72 cm so that the reaction can be considered a homogeneous liquid reaction. The residence time distribution in Section (3.3) also reveals that the reactor consists of two series of C.S.T.R's approximating to two parallel plug-flow reactors. Therefore, conversion of reactants should be independent of mixing in a plug-flow reactor with heterogeneous reactions. It can be seen clearly from the experimental results tabulated in Appendix B4 that the conversion of olefin was not affected by increasing or reducing the speed of rotation of the inner cylinder between 250-1000 r.p.m. However, it is necessary to keep the speed of rotation above a certain level to disperse the olefin within the acid phase. This minimum speed of rotation

was found to be 250 r.p.m.

The effects of the residence time on olefin conversion were investigated. It was concluded that the highest conversion of olefin to monoalkyl sulphate was achieved at a residence time of approximately 3.0 minutes. The formation of dialkyl sulphate reached a maximum after about five minutes (later than monoalkyl sulphuric acid) and the conversion of olefin to polymer increased as the reactant's contact time increased further. An important conclusion is that the decomposition of monoalkyl sulphuric acid and dialkyl sulphate is not very time dependent. This is attributed to a probable chemical equilibrium between products and reactants, so that it would be possible to achieve a higher conversion if the products could be removed from the reaction mixture. This can be performed using an inert solvent process at very low temperatures ($\sim$ -15°C).

Another important parameter which affects the conversion of olefin to different reaction products is the mole ratio of the reactants. At high acid concentrations and acid to olefin mole ratios, the formation of the carbonium ion intermediate is high due to the high acidity function of the sulphuric acid. On the other hand, the concentration of bisulphate ion is low at high acid concentrations. Therefore, all carbonium ions formed cannot be consumed by the bisulphate ions and the excess of carbonium ions react with the olefin to promote the formation of polymer and other side reactions. This was proved in this study, i.e. the yield was higher at the acid/olefin mole ratio of 1.5:1 than at the acid/olefin mole ratio of 3:1 with an acid concentration of 98% (w/w). Using low sulphuric acid concentrations promotes the formation of secondary alcohol and dialkyl sulphate, so that the optimum acid

concentration must be found experimentally. A literature survey shows that acid concentrations below 90% (w/w) are not suitable for the sulphation of α-olefins with carbon chain lengths of particular interest to the detergent industry. Thus, the effects of acid concentration between 90% (w/w) and 100% should be investigated in future work.

In this study, using 95% to 98% (w/w) sulphuric acid at 15°C, it was found that the best acid/olefin mole ratio was 1.5:1 with a residence time of three minutes.

8.5 RECOMMENDATIONS FOR FURTHER WORK

The majority of the equipment used in this study was considered to operate satisfactorily. However, there were some areas which require further consideration and improvement. These are:-

i) The viscosity of the reaction mixture increases to 350 cP during the sulphation reaction (at 15°C). Therefore it was necessary to investigate the power consumption and flow patterns using viscous liquids (glycerol-water mixture). The existing pumps (0.21 kW centrifuge pump) were not powerful enough to pump these viscous solutions into the reactor. Therefore, during the experiments to investigate the power requirements and flow patterns they were replaced by more powerful pumps. However, the existing pumps were capable of pumping the acid and olefin into the reactor during the sulphation reaction.

ii) At low feed rates of reactants (mean residence times greater than 5 minutes), the heat generated in the reactor due to reaction was less than the heat removed by the refrigeration system and a steady-state temperature of $\sim$ 5°C was reached. Because of this, the power consumption increased beyond the power of the

drive unit due to the increased viscosity at the low temperature. Therefore, it is recommended that a by-pass system should be introduced with the refrigerant system or the existing drive unit should be replaced by a more powerful drive unit.

iii) Another problem is the inability of the thermocouples placed in the outer annular wall to determine the reaction temperature. Since these thermocouples were not in contact with the reaction mixture, it was not possible to obtain a reliable temperature profile. It is suggested that the problem may be overcome by placing "fine" tube thermocouples into holes that are precision drilled tangentially into the cylinder and thereafter sealed. This method would however measure the temperature adjacent to the wall. Alternatively, thermocouples could be attached to the baffles vertically and connected to the recorder by a commutator ring arrangement.

iv) It was also noticed that the refrigerant vapour locked at the top of the cooling annulus thereby preventing cooling of the upper section of the reactor. This problem can only be overcome by a re-design of the vapour outlet tube.

v) Finally, the reported effects of the acid concentration on olefin conversion are inconsistent in the literature, consequently, it is recommended that the effects of acid concentrations over 90% (w/w) should be investigated in future work.

8.6 GENERAL CONCLUSION

It is concluded from this research that the type of reactor used in this study (scraped surface heat exchanger with "no-leak" votator) is ideal for reactions between α-olefins and concentrated

sulphuric acid, because it has been proved that:-

i) It provides good heat transfer and vigorous mixing.

ii) It approaches plug-flow in the axial direction so that all segments of the fluid undergo the same reaction history.

iii) It is mechanically simple.

iv) It is simple to control.

Since the reactor is capable of satisfying the necessary requirements high conversion of olefins to monoalkyl sulphuric acids depends on reaction parameters rather than reactor parameters. Therefore, further pilot scale investigations are required before a satisfactory reactor design and scale-up criteria can be developed for commercial use.

APPENDICES

A1 Residence Time Distribution Function for Laminar Flow Between Two Flat Plates

The velocity profile for the laminar flow between two flat plates is given by (3)

$$U_z = \frac{3}{2}\bar{U}_z\left(1 - \frac{x^2}{B^2}\right) \tag{A1.1}$$

where 2B: the thickness of the annulus

X: the distance from the centre of the annulus

U_z: velocity of axial flow at the distance x

$\bar{U}_z$: average velocity of axial flow

Let the length of the reactor be L, it follow that

$$t = \frac{L}{U_z}, \quad \bar{t} = \frac{L}{\bar{U}_z}$$

and from the definition

$$\theta = \frac{t}{\bar{t}} = \frac{\bar{U}_z}{U_z} \tag{A1.2}$$

From equations (A1.1) and (A1.2) x can be expressed in term of dimensionless time unit,

$$X = B\left(1 - \frac{2}{3\theta}\right)^{\frac{1}{2}} \tag{A1.3}$$

From the definition $F(\theta)$ is given by

$$F(\theta) = \frac{C}{C_0} = \frac{\int_0^X U_z CW dx}{\int_0^B \bar{U}_z CW dx} \tag{A1.4}$$

where C_0 and C are tracer concentrations at the inlet and outlet

respectively. W is the width of each plate.

The solution of equation (A1.4) can be obtained from (A1.1) and (A1.3). That is:-

$$F(\theta) = \left(1 - \frac{2}{3\theta}\right)^{\frac{1}{2}} \left(1 + \frac{1}{3\theta}\right) \qquad \text{(A1.5)}$$

and

$$E(\theta) = \frac{dF(\theta)}{d\theta} = \frac{1}{3\theta^3} \frac{1}{\left(1 - \frac{2}{3\theta}\right)^{\frac{1}{2}}}$$

thus

$$E(\theta) = 0 \quad \text{for} \quad 0<\theta<\tfrac{2}{3}$$

$$E(\theta) = \frac{1}{3\theta^3} \frac{1}{\left(1 - \frac{2}{3\theta}\right)^{\frac{1}{2}}} \quad \text{for} \quad \theta>\tfrac{2}{3} \qquad \text{(A1.6)}$$

A2 Derivation of Equation (4.31)

From equation (4.29) and (4.30) it can be shown that,

$$dz = \frac{aLe^{aT}}{e^{aT_2} - e^{aT_1}}\, dT \qquad \text{(A2.1)}$$

Using equations (A2.1) and (4.28) with the boundary conditions $T = T_1$ at $z = 0$ and $T = T_2$ at $z = L$, equation (4.27) becomes

$$\bar{\mu} = \frac{a\mu_0}{e^{aT_2} - e^{aT_1}} \int_{T_1}^{T_2} dT \qquad \text{(A2.2)}$$

and

$$\mu = \frac{a\mu_0(T_2 - T_1)}{e^{aT_2} - e^{aT_1}} \qquad \text{(A2.3)}$$

Example: Let T_1 and T_2 be 20°C and 30°C respectively and let the working liquid be 90% (w/w) glycerol-water mixture. Its viscosities at 20°C and 30°C are 0.2346 Nsm^{-2} and 0.1153 Nsm^{-2} respectively (54).

From equation (4.28)

$$\mu_{T_1} = \mu_0^{-20a}$$

$$\mu_{T_2} = \mu_0^{-30a}$$

and

$$\frac{\mu_{T_1}}{\mu_{T_2}} = e^{10a} = \frac{0.2346}{0.1153} \therefore a = 0.071$$

$$\mu_0 = \mu_{T_1} e^{20a} = \mu_{T_2} e^{30a} = 0.971$$

Inserting the values of a and μ_0 into equation (4.31)

$$\bar{\mu} = \frac{0.071 \times 0.971 \times 10}{e^{2 \cdot 13} - e^{1 \cdot 42}} = 0.161 \text{ Nsm}^{-2}$$

The viscosity of 90% (w/w) glycerol-water mixture of the mean temperature (25°C) is given (54) 0.164 Nsm^{-2}. It can be seen that an error not greater than 2% arises by using the simple viscosity measurement. Therefore the viscosity measurement can be carried out at the mean temperature without making any significant error.

A3 Solution of Equation (6.26)

Equation (6.26) is given by

$$\frac{d\phi}{d\ell} = -\frac{4k_c A_{inner}}{\rho_0 \left(U_{A_0}+U_{O_0}\right)} \quad \frac{\phi_0^3 \left(F_{A_0}-F_{O_0}\right) + \rho_0 U_{O_0} \phi^3}{\phi_0^3 \left(U_{A_0}+U_{O_0}\right) - U_{O_0}\phi^3} \tag{A3.1}$$

Let:

$$a = \frac{4k_c A_{inner}}{\rho_0 \left(U_{A_0}+U_{O_0}\right)}$$

$$b = \phi_0^3 \left(F_{A_0}-F_{O_0}\right)$$

$$c = \rho_0 U_{O_0}$$

$$d = \phi_0^3 \left(U_{A_0}+U_{O_0}\right)$$

$$e = U_{O_0}$$

Equation (A3.1) becomes

$$\frac{d\phi}{d\ell} = a \frac{c\phi^3 + b}{e\phi^3 - d}$$

and it follows

$$\ell = \frac{1}{a} \int_{\phi_0}^{\phi} \frac{e\phi^3 - d}{c\phi^3 + b} \, d\phi \tag{A3.2}$$

$$\frac{e\phi^3 - d}{c\phi^3 + b} = \frac{e}{c} - \frac{cd + be}{c^2 \left(\phi^3 + \frac{b}{c}\right)}$$

Equation (A3.2) becomes

$$\ell = -\frac{e}{ac}(\phi_0-\phi) - \frac{cd+be}{ac^2}\int_{\phi_0}^{\phi}\frac{d\phi}{\phi^3+\frac{b}{c}} \qquad (A3.3)$$

Further simplifications

$$T = \frac{e}{ac}$$

$$Q = \frac{cd+be}{ac^2}$$

$$s^3 = \frac{b}{c}$$

Thus equation (A3.3) becomes

$$\ell = -T(\phi_0-\phi) - Q\int_{\phi_0}^{\phi}\frac{d\phi}{\phi^3+S^3} \qquad (A3.4)$$

The solution of the second term of equation (A3.2) is readily available in mathematical tables. The final expression becomes

$$\ell = \frac{Q}{6S^2}\ln\frac{(S+\phi_0)^3(S^3+\phi^3)}{(S^3+\phi_0^3)(S+\phi)^3} + \frac{Q}{S^2\sqrt{3}}\left[\tan^{-1}\frac{2\phi_0-S}{S\sqrt{3}} - \tan^{-1}\frac{2\phi-S}{S\sqrt{3}}\right] - T(\phi_0-\phi)$$

B1 Torque/Slip Chacteristics of VH041 Coupling.

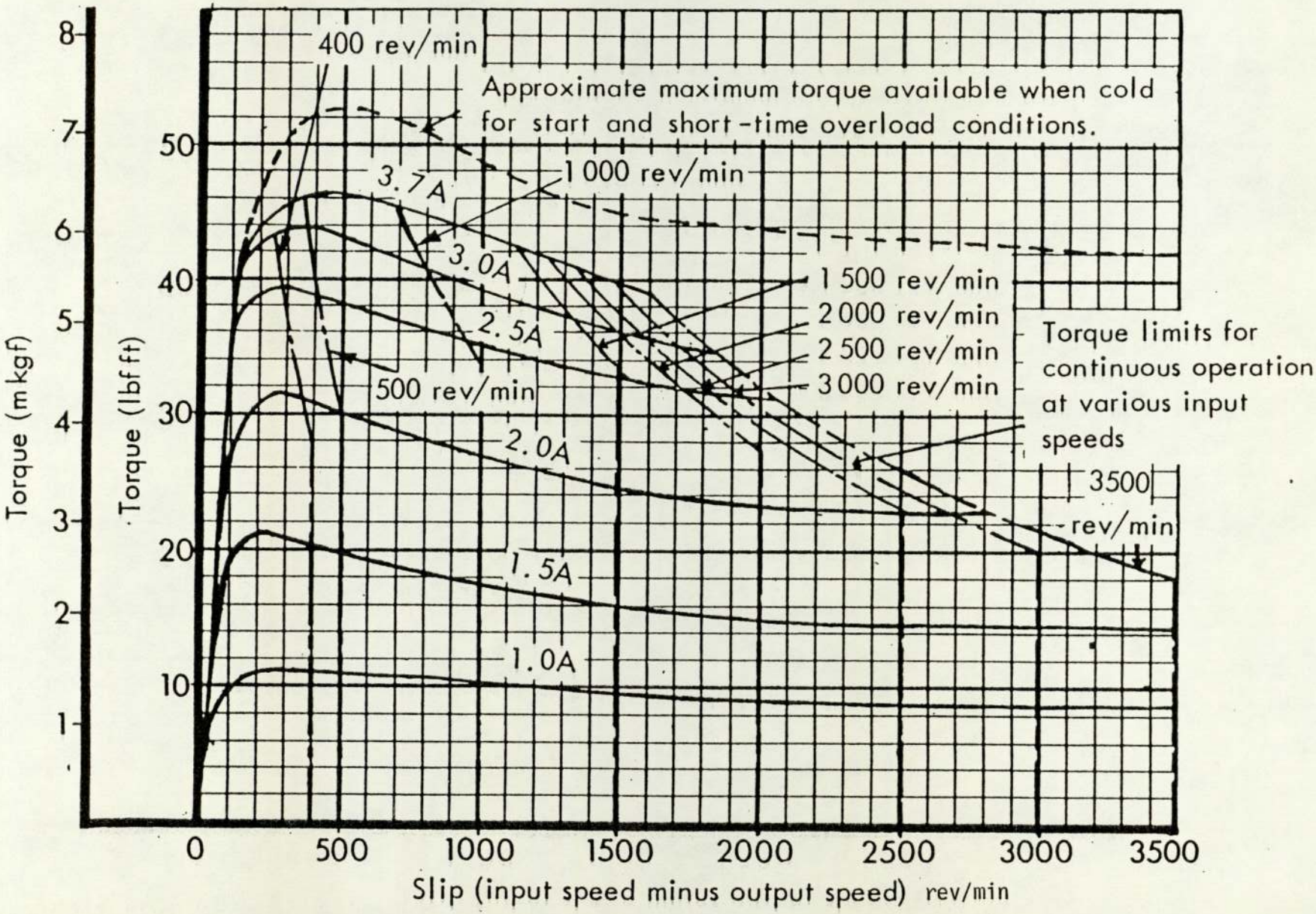

B2 Results from Power Consumption Experiments

N = 20,83 r.p.s		N = 16.67 r.p.s		N = 12.50 r.p.s		N = 8.33 r.p.s		N = 4.17 r.p.s	
$\mu(Nsm^{-2})$	P(watt)	$\mu(Nsm^{-2})$	P(watt)	$\mu(Nsm^{-2})$	P(watt)	$\mu(Nsm^{-2})$	P(watt)	$\mu(Nsm^{-2})$	P(watt)
0.035	2263	0.041	1765	0.054	1234	0.064	665	0.068	251
0.044	2520	0.054	1920	0.072	1320	0.090	723	0.099	289
0.055	2711	0.066	2098	0.082	1426	0.095	780	0.115	295
0.060	2873	0.075	2174	0.120	1652	0.160	955	0.150	300
0.114	3902	0.132	2988	0.190	2022	0.200	1085	0.190	340
0.132	4222	0.162	3256	0.200	2108	0.230	1156	0.192	338
0.162	4682	0.200	3584	0.215	2193	0.272	1234	0.200	350
0.200	3521	0.247	3912	0.230	2278	0.317	1326	0.215	355
		0.317	4384	0.247	2363	0.364	1404	0.230	365
				0.272	2490				

B3 Flow and total heats of reaction of a given molar ratio and residence time

Molar ratio acid/olefin	Flows	Residence time (min.) 1.5 L/min	1.5 Mol/min	2.0 L/min	2.0 Mol/min	2.5 L/min	2.5 Mol/min	5.0 L/min	5.0 Mol/min
1:1	Acid	0.318	5.851	0.239	4.398	0.191	3.514	0.095	1.748
	Olefin	1.682	5.853	1.261	4.388	1.009	3.511	0.505	1.757
	HR(kcal/min)	175.59		131.64		105.33		52.72	
1.5:1	Acid	0.442	8.133	0.331	6.090	0.265	4.876	0.133	2.447
	Olefin	1.558	5.412	1.169	4.068	0.935	3.254	0.467	1.625
	HR(kcal/min)	162.36		122.04		97.62		48.75	
2:1	Acid	0.549	10.102	0.412	7.581	0.329	6.054	0.165	3.036
	Olefin	1.451	5.050	1.088	3.786	0.871	0.030	0.435	1.514
	HR(kcal/min)	151.50		113.58		90.90		45.42	
3:1	Acid	0.724	13.322	0.543	9.990	0.434	7.986	0.217	3.993
	Olefin	1.276	4.441	0.957	3.330	0.766	2.666	0.383	1.333
	HR(kcal/min)	133.23		99.91		79.98		39.99	

B4 Conversion of the olefin to the different reaction products at different conditions

SAMPLE NO	SPEED OF ROTATION N(rps)	MOLAR RATIO p(acid/olefin)	RESIDENCE TIME $\bar{t}$(min)	% NDOM	% OLEFIN	% ALCOHOL	% POLYMER	% AD	X_{OLEFIN}	X_p	X_{MAS}	X_{DAS}	X_{TMAS}
IA-1	4.17	1:1	1.5	5.92	2.13	1.94	1.85	15.93	0.132	0.115	0.531	0.222	0.642
IA-2	8.33	1:1	1.5	7.68	2.98	2.43	2.27	14.58	0.175	0.134	0.426	0.265	0.559
IIA-1	4.17	1:1	2.0	7.10	2.76	2.26	2.07	15.00	0.165	0.124	0.460	0.251	0.585
IIA-2	8.33	1:1	2.0	5.16	2.06	1.68	1.42	16.34	0.131	0.091	0.580	0.198	0.679
IIIA-2	8.33	1:1	2.5	5.14	1.84	1.58	1.72	9.63	0.163	0.152	0.426	0.259	0.555
IB-1	4.17	1.5:1	1.5	3.42	-	-	-	8.96	-	-	-	-	0.635
IB-2	8.33	1.5:1	1.5	2.88	1.11	0.89	0.88	7.74	0.141	0.112	0.537	0.210	0.642
IB-3	16.67	1.5:1	1.5	3.95	-	-	-	9.59	-	-	-	-	0.619
IIB-1	4.17	1.5:1	2.0	2.79	-	-	-	10.42	-	-	-	-	0.716
IIB-2	8.33	1.5:1	2.0	2.89	-	-	-	7.41	-	-	-	-	0.632
IIB-3	16.67	1.5:1	2.0	3.37	1.25	0.88	1.2	8.30	0.143	0.143	0.527	0.187	0.621
IIIB-1	4.17	1.5:1	2.5	2.37	0.93	0.80	0.64	7.17	0.133	0.092	0.563	0.212	0.669
IIIB-2	8.33	1.5:1	2.5	2.60	-	-	-	7.97	-	-	-	-	0.673
IIIB-3	16.67	1.5:1	2.5	3.70	1.10	1.15	1.45	10.43	0.106	0.139	0.551	0.204	0.653
IC-1	4.17	2:1	1.5	5.99	1.96	1.04	2.69	12.00	0.143	0.218	0.499	0.140	0.569
IC-2	8.33	2:1	1.5	7.42	-	-	-	15.86	-	-	-	-	0.589
IC-3	16.67	2:1	1.5	8.67	3.16	1.35	4.16	16.12	0.166	0.218	0.485	0.131	0.551
IIC-1	4.17	2:1	2.0	5.62	-	-	-	13.02	-	-	-	-	0.608
IIC-2	8.33	2:1	2.0	4.92	1.81	0.94	2.17	11.83	0.144	0.174	0.544	0.138	0.613
IIC-3	16.67	2:1	2.0	7.86	2.79	1.35	3.72	17.30	0.147	0.195	0.527	0.131	0.592
IIIC-1	4.17	2:1	2.5	6.86	2.61	1.26	2.99	15.64	0.155	0.176	0.533	0.136	0.601
IIIC-2	8.33	2:1	2.5	6.87	-	-	-	13.74	-	-	-	-	0.571
IIIC-3	16.67	2:1	2.5	10.16	-	-	-	18.67	-	-	-	-	0.550
IE-1	4.17	3:1	1.5	6.17	1.86	0.77	3.54	10.21	0.146	0.277	0.465	0.112	0.521
IE-2	8.33	3:1	1.5	5.07	1.59	0.69	2.79	8.40	0.152	0.266	0.461	0.121	0.522
IIE-1	4.17	3:1	2.0	4.14	1.15	0.65	2.34	7.74	0.126	0.256	0.486	0.132	0.552
IIE-2	8.33	3:1	2.0	5.89	1.75	0.67	3.47	8.68	0.152	0.302	0.438	0.108	0.492
IIIE-2	8.33	3:1	2.5	5.95	1.75	0.72	3.48	9.27	0.147	0.291	0.450	0.112	0.506
IF-1	8.33	1.5:1	5.0	6.75	1.82	2.26	2.67	16.48	0.105	0.154	0.499	0.242	0.620
IF-2	8.33	1.5:1	10.0	6.50	1.56	1.84	3.10	13.94	0.101	0.201	0.478	0.220	0.588
IF-3**	8.33	3:1	280.0	13.52	1.01	0.83	11.68	4.22	0.062	0.721	0.122	0.095	0.170
IG-1	8.33	1.5:1	0.5	7.85	5.65	1.05	1.15	12.56	0.354	0.072	0.452	0.122	0.513
IG-2	8.33	2.5:1	0.5	5.27	3.49	0.58	1.20	7.60	0.343	0.118	0.433	0.106	0.486
IH-1*	8.33	1.5:1	2.0	5.47	-	-	-	15.67	-	-	-	-	0.658
IH-2*	8.33	2.5:1	2.0	4.52	-	-	-	7.69	-	-	-	-	0.531

* acid concentration is 95% w/w
** stirred batch reactor

B5 Length of reactor at which the reaction becomes homogeneous

SAMPLE NO.	SPEED OF ROTATION N(rps)	FLOW RATE OF ACID U_{A_0} (cm^3s^{-1})	FLOW RATE OF OLEFIN U_{O_0} (cm^3s^{-1})	MOLAR RATIO P(acid/olefin)	RESIDENCE TIME t(min)	INITIAL DIAMETER OF DROPS ϕ_0(cm)	MASS TRANSFER COEFFICIENT $k_c x10^3$($cm\,s^{-1}$)	LENGTH OF REACTOR AT WHICH DROPS DISAPPEAR $\ell x10^2$(cm) Inner branch	outer branch
IA-1	4.17	5.37	27.97	1.01:1	1.5	0.0253	4.78	5.47	2.40
IA-2	8.33	5.37	27.97	1.01:1	1.5	0.0148	7.32	2.09	0.92
IIA-1	4.17	4.02	20.98	1.01:1	2.0	0.0253	4.78	4.10	1.80
IIA-2	8.33	4.02	20.98	1.01:1	2.0	0.0148	7.32	1.56	0.69
IIIA-2	8.33	3.22	16.78	1.01:1	2.5	0.0148	7.32	1.25	0.55
IB-1	4.17	7.43	25.90	1.52:1	1.5	0.0253	4.78	8.44	3.71
IB-2	8.33	7.43	25.90	1.52:1	1.5	0.0148	7.32	3.21	1.41
IB-3	16.67	7.43	25.90	1.52:1	1.5	0.0087	10.82	1.27	0.56
IIB-1	4.17	5.58	19.42	1.52:1	2.0	0.0253	4.78	6.34	2.79
IIB-2	8.33	5.58	19.42	1.52:1	2.0	0.0148	7.32	2.42	1.06
IIB-3	16.67	5.58	19.42	1.52:1	2.0	0.0087	10.82	0.96	0.42
IIIB-1	4.17	4.47	15.53	1.52:1	2.5	0.0253	4.78	5.08	2.23
IIIB-2	8.33	4.47	15.53	1.52:1	2.5	0.0148	7.32	1.94	0.85
IIIB-3	16.67	4.47	15.53	1.52:1	2.5	0.0087	10.82	0.77	0.34
IC-1	4.17	9.23	24.10	2.02:1	1.5	0.0253	4.78	11.82	5.19
IC-2	8.33	9.23	24.10	2.02:1	1.5	0.0148	7.32	4.50	1.98
IC-3	16.67	9.23	24.10	2.02:1	1.5	0.0087	10.82	1.78	0.78
IIC-1	4.17	6.93	18.07	2.02:1	2.0	0.0253	4.78	8.88	3.90
IIC-2	8.33	6.93	18.07	2.02:1	2.0	0.0148	7.32	3.38	1.49
IIC-3	16.67	6.93	18.07	2.02:1	2.0	0.0087	10.82	1.34	0.59
IIIC-1	4.17	5.53	14.47	2.02:1	2.5	0.0253	4.78	7.07	3.11
IIIC-2	8.33	5.53	14.47	2.02:1	2.5	0.0148	7.32	2.69	1.18
IIIC-3	16.67	5.53	14.47	2.02:1	2.5	0.0087	10.82	1.07	0.47
IE-1	4.17	18.25	31.75	3.04:1	1.0	0.0253	4.78	30.34	13.33
IE-2	8.33	18.25	31.75	3.04:1	1.0	0.0148	7.32	11.53	5.07
IIE-1	4.17	12.17	21.17	3.04:1	1.5	0.0253	4.78	20.23	8.89
IIE-2	8.33	12.17	21.17	3.04:1	1.5	0.0148	7.32	7.32	3.38
IIIE-2	8.33	7.30	12.70	3.04:1	2.5	0.0148	7.32	4.61	2.03
IF-1	4.17	2.75	7.25	2.01:1	5.0	0.0253	4.78	3.51	1.54
IF-3	4.17	1.38	3.50	2.01:1	10.0	0.0253	4.78	1.79	0.79

SYMBOLS*

A	Cross sectional area of the reactor	L^2
C_{exit}	Outlet tracer concentration	ML^{-3}
C_A	Acid concentration in continuous phase	ML^{-3}
C_{AS}	Acid concentration at the surface of the doplets	ML^{-3}
C_o	Inlet trace concentration	ML^{-3}
D	Diffusion coefficient	L^2T^{-1}
D_i	Rotating cylinder diameter	L
D_o	Outer cylinder diameter	L
d	Annular width	L
$d_o = d/3$	Annular width at which flow changes its direction	L
F_A	Molar feed rate of acid at length of reactor ℓ	MT^{-1}
F_{A_o}	Initial molar feed rate of acid	MT^{-1}
f	Fraction of feed	-
F_o	Molar feed rate of olefin at length of reactor ℓ	MT^{-1}
F_{O_o}	Initial molar feed rate of olefin	MT^{-1}
k_c	Mass transfer coefficient	LT^{-1}
ℓ	Length of reactor section	L
L	Total length of the reactor	L
M	Number of moles of monoalkyl sulphuric acid	-
m	Number of drops in dispersed phase	-
N	Speed of rotation of inner cylinder	T^{-1}
n_B	Number of blades	-
n_o	Number of moles of olefin	-
P	Power consumption	ML^2T^{-3}
p	Initial molar ratio (acid to olefin)	-
R	Volumetric feed rate	L^3T^{-1}
r_i	Radius of the inner cylinder	L
r_o	Radius of the outer cylinder	L

t	Time	T
$\bar{t}$	Mean residence time	T
U_A	Volumetric flow rate of acid at a given reactor length ℓ	L^3T^{-1}
U_{A_0}	Initial volumetric flow rate of acid	L^3T^{-1}
U_{O_0}	Initial volumetric flow rate of olefin	L^3T^{-1}
$\bar{v}$	Average velocity of liquid in the outer section	LT^{-1}
V_c	Critical linear velocity of the inner cylinder	LT^{-1}
$\bar{V}_c$	Average critical velocity of liquid in the outer section	LT^{-1}
V_i	Linear velocity of the inner cylinder	LT^{-1}
V_m	Volume of the inner branch of the reactor	L^3
V_n	Volume of the outer branch of the reactor	L^3
V_x	Tangential velocity of liquid in reactangular co-ordinates	LT^{-1}
V_θ	Tangential velocity of liquid in cylindrical co-ordinates	LT^{-1}
X_M	Mole fraction of monoalkyl sulphuric acid in continuous phase	-

Greek Letters

μ	Viscosity of working liquid	$ML^{-1}T^{-1}$
μ_c	Viscosity of continuous phase	$ML^{-1}T^{-1}$
ν	Kinematic viscosity	L^2T^{-1}
ρ	Density of working liquid	ML^{-3}
ρ_c	Density of continuous phase	ML^{-3}
ρ_s	Density of dispersed phase	ML^{-3}
ρ_0	Pure olefin concentration	ML^{-3}
ε	Power dissipation per unit mass	L^2T^{-3}
Ω_c	Critical angular velocity of inner cylinder	Rads T^{-1}
ϕ	Diameter of drops	L

ϕ_0	Initial diameter of drops	L

* Symbols (and their units) not shown above have been appropriately explained in the text.

REFERENCES

1. Malhotra, V. N. and Jeffreys, G. V., Proposed Design for a Reactor to Study Fast and Exothermic Liquid/ Liquid Reactions (unpublished paper).

2. Dykes, D. J., Studies of The Sulphation of α-olefins, Ph.D Thesis, Aston University, October 1980.

3. Bird, R. B., Stewart, W. E., and Lightfoot, E. N., Transport Phenomena, John Wiley and Sons, 1960.

4. Brewster, D. B., and Nissan, A. H., The Hydrodynamics of Flow Between Horizontal Concentric Cylinders-I, Chem. Eng. Sci. 7, 215-211, 1958.

5. Trommelen, A. M., and Boerema, S., Power Consumption in a Scraped Surface Heat Exchanger, Trans. Inst. Chem. Engrs. 44, 329-334, 1966.

6. Trommelen, A. M., Physical Aspects of Scraped Surface Heat Exchanger, Thesis Delft, February 1970.

7. Taylor, G. I., Stability of a Viscous Fluid Contained Between two Rotating Cylinders, Phil. Trans. Royal. Soc. Series A 223, 289-343, 1923.

8. Lewis, J. W., An Experimental Study of the Motion of a Viscous Liquid Contained Between Two Coaxial Cylinders, Proc. Roy. Soc. Series A. 117, 388-407, 1928.

9. Dean, W. R., Fluid Motion in a Curved Channel, Proc. Roy. Soc. Series A 121, 402-420, 1928.

10. Di Prima, R. C., Application of the Galerkin Method to Problems in Hydrodinamic Stability, Quart. Appl. Math. XIII, 55-62, 1955.

11. N.van Lookeren Campagne, Longitudinale Dispersie in de Stroming Door Een Ringspleet met Draaiende Binnencilinder, Thesis Groningen, 1966, Cited in Trommelen, A. M., Physical Aspects of Scraped Surface Heat Exchanger, Thesis Delft, February 1970.

12. Bott, T. R., Azoory, S. and Porter, K. E., Scraped Surface Heat Exchanger - Part I, Hold up and Residence Time Studies, Trans. Inst. Chem. Engrs., 66, 33-36, 1968.

13. Goldstein, S., The Stability of Viscous Fluid Flow Between Rotating Cylinders, Proceeding of the Cambridge Philosophical Society, 33, 41-61, 1937.

14. Cornish, R. J., Flow of Water Through Fine Clearances with Relative Motion of the Boundaries, Proceedings of Royal Society of London, Series A 140, 227-240, 1933.

15. Himmelblau, D. M., and Bischoff, K. B., Process Analysis and Simulation Deterministics System, John Wiley and Sons, 59-88, (Chapter 4), 1968.

16. Skelland, A. H. P., and Leung, L. S., Power Consumption in a Scraped Surface Heat Exchanger, Brit. Chem. Eng. 7, 264-267, 1962.

17. van de Westelaken, H. C., Trommelen, A. M. and Lansbergen, N. A. M., Votator Performance 12, Heat Transfer and Power Consumption Measurements with Plastic Scraper Blades, Cited in Malhotra, V. N., and Jeffreys, G. V., Proposed Design for a Reactor to Study Fast and Exothermic Liquid/Liquid Reactions (unpublished paper).

18. Leung, L. S., Power Consumption in a Scraped Surface Heat Exchanger, Trans. Inst. Chem. Eng., 45, 179-181, 1967.

19. Bates, H. T., Computer Code Developed at Kansas State University, U.S.A., Cited in Dykes, D. J., Studies of the Sulphation of α-Olefins, Ph.D Thesis, Aston University, October, 1980.

20. Froishteter, G. B., et al Relationships of Laminar Flow and Power Consumption in Scraped Surface Equipment, J. Appl. Chem. USSR, 51 (1), 100-105, 1978, Cited in Dykes, D. J., Studies of the Sulphation of α-Olefins, Ph.D Thesis, Aston University, October, 1980.

21. Shore, S., and Berger, D. R., Anionic Surfactants, 7, 137 Part-1, Edited by Warner M. Linfield, Marcel Dekker, 1976.

22. Taft, R. W., The Dependence of the Rate of Hydation of Isobutene on the Acidity Function, H_0, and the Mechanism for Olefin Hydration in Aqueous Acids, J. Am. Chem. Soc. 74, 5372-5376, 1952.

23. Netherlands Patent Application No. 77, 13058, By Shell Internationale Research, November 1977, Process for the Production of Monoalkyl Sulphates.

24. Kooijman, P. L., Investigation into the Reactions Between Concentrated Sulphuric Acid an Hexadecene-1 and Dodecene-1, Proc. Int. Congr., Pure and Appl. Chem. (LONDON) 11, 499-507, 1947.

25. Grant, P. E., Some Aspects of the Manufacture of Secondary Mono-Alkyl Sulphates, Ph.D Thesis, University of Birmingham, November 1970.

26. Bethell, D and Gold, V., "Carbonium Ions an Introduction" Academic Press, 186/187, 1967.

27. Fairclough, C. S., and Malhotra, V. N., Secondary Alkyl Sulphates - A Literature Review (unpublished paper).

28. Butcher, K. L. and Nickson, G. M., The Sulphation Reaction Between Aqueous Sulphuric Acid and α-Olefins. J. Appl. Chem., 10, 65-73, 1960.

29. Nickson, G. M., A Study of the Reaction Between Sulphuric Acid and Olefins, Ph.D Thesis, University of Leeds, 1957.

30. Horak, J. and Pasek, J., "Design of Industrial Chemical Reactors from Laboratory Data". Translated by Stanek, V., Heydene 374-386, 1978.

31. McCabe, W. L., and Smith, J. C., "Unit Operation of Chemical Engineering", Third Edition, McGraw-Hill, 697/698, 1976.

32. Levenspiel, O., "Chemical Reaction Engineering", John Wiley and Sons, Second edition, Chapter 12, 1972.

33. Perry, R. H., and Chilton, C. H., Chemical Engineers' Handbook, Fifth edition, McGraw-Hill, 21-7,

34. Clay, P. H., Proc. Roy. Acad. Sci. (Amsterdam) 43, 852, 972, 1940.

35. Hinze, J. O., Fundamentals of the Hydrodynamic Mechanism of Splitting in Dispersion Processes, AIChE. J., 1, 289-295, 1955.

36. Kubie, J., and Gardner, G. C., Drop Size and Drop Dispersion in Straight Horizontal Tubes and in Helical Coils, Chem. Eng. Sci. 32, 195, 1977.

37. Levich, V. G., "Physicochemical Hydrodynamics, Prentice-Hall, 458, 1962.

38. Baird, M.H.I., Droplet Diameters in Agitated Liquid-Liquid System, Chem. Eng. Sci., 34, 1362, 1979.

39. McManamey, W. J., Sauter Mean and Maximum Drop Diameters of Liquid-Liquid Dispersions in Turbulent Agitated Vessels at Low Dispersed Phase Hold-up Chem. Eng. Sci. 34, 432, 1979.

40. Antonow, G. N., Sur la Tension Superficiele a la Limite de Deux Couches, J. Chim. Phys. 372-385, 1907.

41. Wyatt, P. A. H., et al, Surface Tension Measurements in Solvent Sulphuric Acid, J. Chem. Soc. (A), 304-306, 1969.

42. Brian, P. L. T. and Hales, H. B., Effects of Transpiration and Changing Diameter on Heat and Mass Transfer to Spheres, AICHE, J., 15, 419-425, 1969.

43. Sherwood, T. K., Pigford, R. L. and Wilke, C. R., "Mass Transfer", McGraw-Hill, 1975, 220-224.

44. Levins, D. M. and Glastonbury, J. R., Application at Kolmogoroff's Theory to Particle-Liquid Mass Transfer in Agitated Vessels, Chem. Eng. Sci. 27, 537-543, 1972.

45. Badger and Banchero, "Introduction to Chemical Engineering" McGraw-Hill, 638, 1955.

46. Malhotra, V. N., Experimental Study of the Preparation of Secondary Alkyl Sulphate in a Short Residence Time Reactor (unpublished paper).

47. Fairclough, C. S., Private Communication.

48. Clippinger, E., Reaction of α-Olefins, Industr. Eng. Chem. Product Research and Development, 3, (1) 3-7, 1964.

49. Wyatt, P. A. H., The Constitution of 80-100% Aqueous Sulphuric Acid: A Case of Overlapping Equilibria, Trans. Faraday. Soc., 56, 490-497, 1960.

50. Jenson, V. G. and Jeffreys, G. V., "Mathematical Methods in Chemical Engineering", Second edition, Academic Press, 339, 1977.

51. Baumgarten, P., Ber. Dtsch. Chem, Ges., 75, 977, 1942, cited by Fairclough (27).

52. Asinger, F., Chem. Ber., 100, 448, 1967, cited by Fairclough (27).

53. Perry, R. H., and Chilton, C. H., "Chemical Engineer Handbook" Fifth edition, McGraw-Hill, 5-61/62.

54. Sheeley, M. L., Glycerol Viscosity Table, Ind. Eng. Chem. 24, 1060-1064, 1932.